

**ESTABLISHING THE KINETICS OF ESCHERICHIA BACTERIOPHAGE T4 AND ITS
TARGET BACTERIUM WITHIN THE INTESTINAL MUCOSA OF A GNOTOBIOTIC
MOUSE MODEL**

by

Nicola Jacqueline Pett

B.Sc., The University of Queensland, 2016

A THESIS SUBMITTED IN PARTIAL FULFILLMENT OF
THE REQUIREMENTS FOR THE DEGREE OF

MASTER OF SCIENCE

in

THE FACULTY OF GRADUATE AND POSTDOCTORAL STUDIES
(Microbiology and Immunology)

THE UNIVERSITY OF BRITISH COLUMBIA
(Vancouver)

December 2023

© Nicola Jacqueline Pett, 2023

The following individuals certify that they have read, and recommend to the Faculty of Graduate and Postdoctoral Studies for acceptance, the thesis entitled:

Establishing the kinetics of *Escherichia* bacteriophage T4 and its target bacterium within the intestinal mucosa of a gnotobiotic mouse model

submitted by Nicola Jacqueline Pett in partial fulfilment of the requirements for

the degree of Master of Science

in Immunology and Microbiology

Examining Committee:

Dr. Lisa Osborne, Associate Professor, Microbiology and Immunology, UBC
Supervisor

Dr. Carolina Tropini, Assistant Professor, Microbiology and Immunology, School of Biomedical Engineering, UBC
Co-supervisor

Dr. Kirk Bergstrom, Assistant Professor, Biology, UBC
Supervisory Committee Member

Dr. Marc Horwitz, Professor, Microbiology and Immunology, UBC
Additional Examiner

Additional Supervisory Committee Members:

Dr. Curtis Suttle, Professor, Botany, Earth, Ocean & Atmospheric Sciences, Microbiology and Immunology, UBC
Supervisory Committee Member

Abstract

Bacteriophages (phages) are viruses that infect bacteria with species- and strain-level specificity and are the most abundant biological entities across all known ecosystems. Within bacterial communities, such as those found in the gut microbiota, phages are implicated in regulating microbiota population dynamics and driving bacterial evolution. The specificity of phage-bacterial interactions has generated renewed interest in phage research as a potential alternative strategy to counter the increasing threat of antimicrobial resistant bacteria. While there has been some success in using phage therapy to combat bacterial septic infections, we still do not have the foundational understanding of phage-bacteria-host dynamics within our gut ecosystems that is needed for their safe development.

Recent studies demonstrating that phages adhere to intestinal mucus through specific capsid proteins (Hoc) have suggested that phages may protect the underlying epithelium from bacterial invasion, providing a host-extrinsic mechanism to maintain intestinal homeostasis. Here, I build upon these findings to investigate the kinetics between *Escherichia* bacteriophage T4 (containing a Hoc domain) and its target bacterium, *Escherichia coli*, within the intestinal tract of a gnotobiotic mouse model. I determined that T4 phage and *E. coli* can stably coexist within the murine gastrointestinal tract in the absence of other microbes, despite continual phage predation. However, I was unable to conclude that T4 phage retention within the murine gut requires Hoc protein-mediated mucus adhesion. Further, my data suggest that gut-colonising T4 phage elicit a type 1 immune response in the gut-draining lymph nodes, without causing inflammatory disease. Together, these results suggest that T4 phage is well tolerated in the gastrointestinal tract of gnotobiotic mice by the bacterial and metazoan hosts and may contribute to immune system priming.

Lay Summary

Bacteriophages (phages) are viruses that infect and kill bacteria with a high degree of specificity. They are the most abundant organisms on Earth and are active members of our gut microbial communities. Because phages target specific bacteria, they can be leveraged against invading human pathogens, a much-needed approach given the rising inefficacy of antibiotic-based therapies against multi-drug resistant pathogens. The overarching goal of this work is to determine how phage interactions with the gut environment influence bacterial abundance and the immune system of the mammalian gut. I found that T4 phage was able to stably reside within the mouse gut in the presence of its target bacteria, without apparent reduction of the total bacterial population. This coincided with local increases in the production of inflammatory cytokines without causing clinical signs of disease, which indicates that phages may have a role in immune system education. These results further our understanding of phage-bacteria-immune system interactions in the gut, which may be applied to the development of anti-bacterial phage therapies.

Preface

I was responsible for the experimental design, investigation, and analysis of data for all experiments performed in this thesis, under the co-supervision of Dr. Carolina Tropini and Dr. Lisa Osborne.

The manuscript accepted to the Journal of Visualised Experiments (JoVE) (Pett et al., 2023. In-press) was a combination of efforts by all authors. Dr. Michael Hunter assisted with *in vitro* phage optimisation experiments. Dr. Jung Hee Seo helped with optimising ELISAs and qPCRs. Dr. Jung Hee Seo, Natalia Carranza García and Dr. Samuel Collins provided support and animal care. Dr. Lisa Osborne, Dr. Carolina Tropini and I conceived the rationale for the manuscript, wrote and edited the manuscript.

The wild type and Δ Hoc T4 phage were kindly provided by our collaborator Dr. Forest Rohwer (Department of Biology, San Diego State University).

The figure in Chapter 1 (**Figure 1.1**) was adapted with the authors' permission from a recent literature review: *The gut microbiota and its biogeography*. McCallum & Tropini (2023).

A version of **Figures 3.2 and 3.3** in Chapter 3 have been submitted for publication: *T4 Bacteriophage and E. coli Interaction in the Murine Intestine: A Prototypical Model for Studying Host-Bacteriophage Dynamics in vivo* by N Pett, M Hunter, NA Carranza García, JH Seo, SR Collins, F Rohwer, LC Osborne, C Tropini.

The excel files and R scripts used to calculate DNA quantities for qPCR standard curves, and calculate gene copies from the standard curve, respectively, were created by Juan Burckhardt.

Histology slides were prepared by Dr. Olena Mayden at the BC Children's Hospital Research Institute Histology Core facility.

The set up and maintenance of a sterile gnotobiotic isolator for the generation and breeding of *E. coli* monoclonised mice was performed by Dr. Samuel Collins and Natalia Carranza García. Natalia Carranza García and Dr. Jung Hee Seo provided animal husbandry, colony management expertise, and maintained the sterility of gnotobiotic animals.

Dissection and tissue harvesting from phage-inoculated mice for phage enumeration was performed with the help of Dr. Leah Hohman, Juan Burckhardt, Charlotte Clayton, Naomi Fettig and Andrew Sharon.

The piloting and analysis of multianalyte flow assays was conducted in collaboration with Andrew Sharon.

Dissection of animals for immunophenotyping experiments was dependent on help offered by Dr. Leah Hohman and Blair Hardman. Cell isolation from tissues was performed with the help of Dr. Leah Hohman. Dr. Leah Hohman and Naomi Fettig were crucial educators during the process of immunostaining, flow cytometry and data analysis.

This project required animal ethics approval for inoculation of *E. coli* monoclonised mice with T4 phage. All experiments were performed in accordance with recommendations from the Canadian Council for Animal Care. The Animal Care Committee of the University of British Columbia approved all protocols (A23-0113, A19-0332, A23-0012, B19-0038).

Table of Contents

Abstract.....	iii
Lay Summary	iv
Preface.....	v
Table of Contents	vii
List of Tables	xi
List of Figures.....	xii
List of Symbols	xiv
List of Abbreviations	xv
Glossary	xix
Acknowledgements	xx
Chapter 1: Introduction	1
1.1 Bacteriophages in the mammalian microbiome.....	1
1.2 The human gut phageome.....	2
1.3 Bacteriophage adaptation to the intestinal mucosa.....	4
1.3.1 The gut mucosa.....	4
1.3.2 T4 phage adherence to mucus.....	6
1.4 Phage interactions with eukaryotic cells.....	7
1.5 Interrogation of the microbiome using gnotobiotic mouse models	8
1.6 Phage-specific immune responses	9
1.7 Phages in health and disease	11
1.7.1 The gut phageome is associated with IBD.....	11

1.7.2	Faecal filtrate transplants in the treatment of disease	12
1.8	Phage therapy	12
1.9	Hypothesis.....	15
Chapter 2: Methods		16
2.1	Mouse strains, housing and diets	16
2.2	Bacteria and phage strains	16
2.3	Phage propagation, cleaning, and purification.....	17
2.4	<i>E. coli</i> monocolonization of germ-free mice and breeding.....	18
2.5	Inoculation of monocolonised mice with phage	18
2.6	Quantification of phage and bacteria by spot plating assays	19
2.7	Quantification of phage and bacteria by quantitative PCR (qPCR)	19
2.7.1	Phage DNA extraction from faeces and caecal contents	19
2.7.2	Generation of T4 phage DNA standards.....	19
2.7.3	Measurement of phage loads by qPCR.....	20
2.8	Detection of T4 phage DNA by PCR and gel electrophoresis.....	21
2.9	Histology and immunofluorescence	21
2.9.1	Fixation and processing	21
2.9.2	Immunostaining	22
2.9.3	Confocal microscopy	23
2.10	Cytokine detection in mouse spleens and mLN's	23
2.10.1	Cytokine bead arrays.....	23
2.10.2	Flow cytometry acquisition and analysis	24
2.11	Immune cell isolation from spleens and mLN's	25

2.12	<i>Ex vivo</i> lymphocyte stimulation.....	25
2.13	Immunostaining of isolated cells for flow cytometry.....	26
2.14	Cell detection by flow cytometry.....	26
2.15	Statistical analysis.....	27
Chapter 3: Results.....		29
3.1	Wildtype T4 phages are retained in the intestines of bi-colonised mice	29
3.1.1	T4 phage can be visualised by immunofluorescence imaging of mouse intestinal sections and localises within the mucus layer.....	29
3.1.2	T4 phage cohabitate alongside their target bacteria, <i>E. coli</i> , in the intestine of bi-colonised mice.	32
3.1.3	Inter-mouse variation in T4 phage colonisation is evident post-inoculation.	36
3.1.4	The T4 phage Hoc protein may be required for T4 phage habitation of the bi-colonised mouse intestine.	38
3.1.5	T4 phage can be transferred between mice by co-housing.....	42
3.2	T4 Phages introduced to the intestine of <i>E. coli</i> monocolonised mice induce a weak, Th1 skewing immune response.....	45
3.2.1	T4 phage do not translocate across the intestinal epithelium of bi-colonised mice <i>in vivo</i>	45
3.2.2	T4 phage inoculation of <i>E. coli</i> monocolonised mice leads to local increases in pro-inflammatory cytokine production.....	47
3.2.3	T4 phage inoculation of <i>E. coli</i> monocolonised mice leads to elevated numbers of activated CD4+ Th1 cells and CD8+ T cells in the mLN.....	51

3.2.4 T4 phage inoculation of <i>E. coli</i> monocolonised mice does not significantly increase the cytokine-production capacity of T cells within mLNs and spleens	55
Chapter 4: Discussion	59
4.1 Discussion	59
4.2 Applications	64
4.3 Future directions	65
4.4 Conclusion	66
References	67
Appendices	76
Appendix A Cross-reactivity of T4 phage anti-Gp23 antibody with <i>E. coli</i>	76
Appendix B DNA gel of extracted phage DNA from faecal pellets from the experiments discussed in Chapter 3.1.4	77
Appendix C <i>E. coli</i> appeared to translocate across the intestinal epithelium both with and without T4 phage inoculation	78
Appendix D Oral inoculation of T4 phage into <i>E. coli</i> monocolonised mice did not stimulate chemokine production or increase levels of IFN β or IL-6.....	79
Appendix E Representative flow cytometry gating strategy for immunophenotyping of cells isolated from T4 phage-inoculated mouse mLN and spleens.....	81
Appendix F Total lymphocyte numbers in mLNs and spleens were not significantly different between vehicle, T4 phage and MNV-inoculated mice.....	82
Appendix G Representative flow cytometry gating strategy for PMA/ionomycin stimulation controls.....	83

List of Tables

Table 2.1	Recipes for commonly used buffers in phage preparation and visualisation	17
Table 2.2	Antibodies	23
Table 2.3	Cytokines examined in the LEGENDPlex Mouse Anti-Virus Response Panel (BioLegend)	24
Table 2.4	Lymphocyte isolation buffers.....	27

List of Figures

Figure 1.1	Mucus, oxygen, antimicrobial peptides and other immune factors drive bacterial colonization and organization near the epithelium	6
Figure 3.1	T4 phages appear to localise to the ileum (distal SI) and colon more densely than in the duodenum and jejunum	32
Figure 3.2	T4 phage and <i>E. coli</i> levels in faecal pellets of C57BL/6 <i>E. coli</i> monocolonised mice, over 29 days post- WT T4 phage inoculation by oral gavage.	36
Figure 3.3	T4 phage unable to be detected in mouse caecal contents by plaque assay was detected by qPCR	37
Figure 3.4	First trial – Δ Hoc T4 phage and <i>E. coli</i> levels in bi-colonised mice following inoculation with WT or Δ Hoc T4 phage	39
Figure 3.5	Second trial - Δ Hoc T4 phage and <i>E. coli</i> levels in bi-colonised mice following inoculation with WT or Δ Hoc T4 phage	40
Figure 3.6	Co-housing of <i>E. coli</i> monocolonised, phage-naïve mice with WT T4 phage-inoculated mice	43
Figure 3.7	T4 phage were unable to translocate across the intestinal epithelium after inoculation into <i>E. coli</i> monocolonised mice	46
Figure 3.8	Oral inoculation of T4 phage into <i>E. coli</i> monocolonised mice resulted in modest but significant increases in cytokine levels in the MLN and spleen	50
Figure 3.9	T4 phage inoculation of <i>E. coli</i> monocolonised mice leads to elevated numbers of B cells, CD4+ and CD8+ T cells in the mLN	53

Figure 3.10 T4 phage inoculation of *E. coli* monoclonised mice leads to elevated numbers of CD4+, CD8+ and CD4+ Tbet+ Th1 cells in mLN's 55

Figure 3.11 T4 phage inoculation of *E. coli* monoclonised mice leads to small, non-significant increases in proportions and numbers of IFN γ and TNF α producing CD4+ T cells upon *in vitro* stimulation..... 57

List of Symbols

α	Alpha
β	Beta
Δ	Delta/change
γ	Gamma
μ	Micron
%	Percent

List of Abbreviations

ACK	Ammonium-Chloride-Potassium
AIM2	Absent in melanoma 2
AMR	Antimicrobial resistance
ANOVA	Analysis of variance
APC	Antigen presenting cell
BCR	B cell receptor
BSC	Biological safety cabinet
CCL	Chemokine (C-C motif) ligand
CD	Crohn's disease
CDM	Centre for disease modelling
Cfu	Colony forming units
CTCM	Complete tissue culture media
CXCL	Chemokine (C-X-C motif) ligand
DC	Dendritic cell
DNA	Deoxyribonucleic acid
ds	Double-stranded
EDTA	Ethylenediaminetetraacetic acid
ELISA	Enzyme-linked immunosorbent assay
EU	Endotoxin units
FACS	Fluorescence-activated cell sorting
FBS	Fetal bovine serum

FFT	Faecal filtrate transplant
FMT	Faecal microbiota transplant
GALT	Gut-associated lymphoid tissue
GF	Germ-free
GI	Gastrointestinal
GIT	Gastrointestinal tract
GM-CSF	Granulocyte-macrophage colony-stimulating factor
Gp23	Gene product 23
Hoc	Highly antigenic outer capsid
IBD	Inflammatory bowel disease
IEC	Intestinal epithelial cell
IFN	Interferon
Ig	Immunoglobulin
IL	Interleukin
JoVE	Journal of visualised experiments
LB	Luria broth/lysogeny broth
LP	Lamina propria
LPL	Lamina propria lymphocyte
LPS	Lipopolysaccharides
mLN	Mesenteric lymph node
MNV	Murine norovirus
NCS	Newborn calf serum
NK	Natural killer

PAA	Peracetic acid
PAMP	Pathogen-associated molecular pattern
PBS	Phosphate buffered saline
PCR	Polymerase chain reaction
Pfu	Plaque forming units
PMA	Phorbol 12-myristate 13-acetate
PRR	Pattern recognition receptor
qPCR	Quantitative polymerase chain reaction
rCDI	Recurrent <i>Clostridioides difficile</i> infection
RM	Repeated measures
RNA	Ribonucleic acid
RPMI	Roswell Park Memorial Institute
RT	Room temperature
SD	Standard deviation
SEM	Standard error of the mean
SFB	Segmented filamentous bacteria
SI	Small intestine
SM	Saline magnesium
Soc	Small outer capsid
SPF	Specific pathogen-free
ss	Single-stranded
TCR	T cell receptor
Th	T helper

TLR	Toll-like receptor
TNF α	Tumour necrosis factor alpha
Treg	T regulatory cell
UBC	University of British Columbia
UC	Ulcerative colitis
UEA-1	Ulex-Europaeus agglutinin-1
VLP	Viral-like particle
WGA	Wheat germ agglutinin
WT	Wild Type

Glossary

Bi-colonised:	Colonised with two microorganisms.
Conventional:	Containing a complete “conventional” laboratory microbiome.
Germ-free:	Devoid of all microorganisms.
Gnotobiotic:	Containing known or defined microorganisms.
Lysogen:	A bacterial cell containing a prophage.
Lysogenic:	A phage lifecycle facilitating the integration of phage genetic material into the genome of its target bacterium upon infection.
Lytic:	A phage lifecycle resulting in phage replication within a bacterium, lysis of the bacterial cell and release of progeny virions.
Monocolonised:	Colonised with a single microorganism.
Phage-naïve:	Mice that have never encountered bacteriophages.
Prophage:	The genetic material of a lysogenic phage when integrated into the bacterial genome.
Pseudolysogeny:	Lytic phage conversion to a pseudo-lysogenic state, causing phage replication to stall within a host cell.
Specific pathogen-free:	Free of a defined list of pathogens.

Acknowledgements

First and foremost, I would like to thank my family for their unwavering love and support. Especially, I thank my grandma, Jean, for encouraging me to take this step in furthering my education. I am so thankful that we are close, and cherish our conversations, even more so on the rare occasions that our conversations can be in person. To my Canadian family, thank you for welcoming me into your homes and for supporting us in our various adventures across this beautiful country.

Thank you to my supervisors Lisa and Carolina, for your support and guidance through this busy MSc degree. Thank you for your endless patience, for challenging me, and most of all for helping me to become a scientist. You are both inspirational women in science and amazing role models.

To the members of the Osborne and Tropini labs, without which none of this work would have been possible. Thank you for the laughs, comradery, the softball games and ski days. You are incredible scientists, and I am the luckiest to have had the opportunity to learn from and with you.

I would also like to thank the members of the McCoy and Geuking Labs at the University of Calgary for their ongoing friendship. Some of my happiest memories are hiking around the Rockies with you. Most of all, thank you to Kathy and Markus for taking a chance on me, and for your encouragement and support ever since.

Thank you to my committee members Dr. Kirk Bergstrom, Dr. Marc Horwitz and Dr. Curtis Suttle, for your professional and scientific support and guidance throughout my degree. I really appreciate the time you have contributed to my education and am thankful to have had so much support.

Finally, I would not be where I am today without my fiancé, Joey. Thank you for being my best friend through all times good and bad, for being my biggest supporter in all my exploits, and for loving me unconditionally. You help me daily to be the best version of myself and you advocate for my mental health at times when I cannot. This is your thesis too.

Chapter 1: Introduction

1.1 Bacteriophages in the mammalian microbiome

Bacteriophages, or phages, are viruses that solely infect prokaryotes, with species and strain-level specificity¹. Phages can be detected in almost every biological niche, from marine and soil ecosystems², to hostile environments such as alkaline hot springs, arctic sea ice and even deep subsea floor sediments³. It is therefore no surprise that they are the most abundant and genetically diverse organisms on Earth^{1,2,4}. In marine and soil environments, lytic (virulent) phages typically dominate bacteria at a ratio of ten to one⁵, whereas lysogenic (temperate) phages are less abundant. However, in the mammalian gastrointestinal tract (GIT), the ratio of phages to bacteria is closer to one to one⁵ and lysogenic phages are thought to dominate the mammalian gut virome⁶⁻⁸. Upon infection of a bacterium, the lysogenic phage genome integrates into the bacterial chromosome, or is maintained as a plasmid⁹. The phage genome (prophage) replicates with the bacterial host and can impart virulence factors that contribute to the survival of its host^{1,10}. Environmental changes and stressors can result in prophage induction and reversion to the lytic lifecycle⁹. This ultimately results in the lysis and death of the host bacterium and release of new virions. “Piggyback-the-winner” population dynamics describes a stable coexistence of lysogenic phages and bacteria in the intestinal environment⁷. However, arguments have been made for a lytic phage-dominated gut microbiome^{11,12}, with lysogenic phage abundance having associations with disease¹³.

Obligatory lytic phages infect bacterial cells by injecting their genetic material into the cell, where they hijack the bacterium’s transcriptional machinery to facilitate their own replication¹⁴. Once progeny virions have assembled, the new viruses lyse the cell, killing the bacterium. This cycle is then continued when the progeny virions infect a new bacterium¹⁴. This guarantees continual turnover of bacteria, which drives genetic diversity in microbial ecosystems

and influences bacterial abundance^{4,15}. Obligately lytic phages are the focus of efforts for the development of novel antibacterial therapies (phage therapy), due to their ability to rapidly decimate their target bacteria¹⁶. Lytic phages are preferred over lysogenic phages for treatment of infection, as lysogenic phages have a propensity for enhancing the virulence and lifespan of their target bacteria^{1,10}. *Escherichia* virus T4 is a well characterised lytic phage specifically infecting and replicating within *Escherichia coli* strains¹⁴. T4 phages are double-stranded (ds) DNA, tailed Myoviruses of the class *Caudoviricetes*¹⁴. The T4-*E. coli* phage-bacteria pair and their interactions with the murine GIT in the absence of a complex microbiota is the focus of this thesis research.

1.2 The human gut phageome

The human gut is a complex microbial ecosystem consisting of commensal bacteria, viruses, fungi, archaea and protozoa, referred to collectively as the gut microbiome⁹. The gut microbiota supports homeostasis and promotes health by aiding in the digestion of food, release of nutrients, and the synthesis of metabolites. Alterations in the composition of the microbiota, specifically in the bacteriome, has been associated with multiple diseases in humans, including metabolic disease, diabetes, inflammatory bowel disease (IBD), allergy and colorectal cancer¹⁷. Similarly, recent studies have implicated alterations to the phageome in diseases of the GIT, such as IBD^{18,19}, diabetes²⁰ and metabolic syndrome^{20,21}. Although phages cannot directly infect eukaryotic cells, they may indirectly modify the uptake of bacterial-derived metabolites and nutrients by the metazoan host through their ability to modulate the abundance of gut commensal bacteria^{8,15}. The extent to which phage-bacteria interactions influence disease progression remains unclear. Furthermore, the role of phage-metazoa interactions in gut health and disease is poorly defined and should therefore be considered in future analyses.

The relevance of phages within the human gut microbiome has only been recognised in the wider research community within the past 20 years. It is now accepted that the gut virome is dominated by phages, which make up more than 90% of detected viral genomes²². A keystone study by Reyes et al. (2010) examined the faecal viromes of monozygotic twins and their mothers, finding that faecal viromes are unique between individuals regardless of their relatedness²². This contrasts with bacteriomes, which demonstrate a significant degree of similarity between related individuals. Interestingly, intrapersonal variations in virome composition were low, with more than 95% of virotypes retained in an individual over the period of a year. In this study, the human gut virome was found to be dominated by a few species of lysogenic phages²². However, it is worth noting that 81% of reads from this study were novel and did not match known virus sequences²². The overwhelming abundance of unknown viral reads, known as “viral dark matter”, presents a challenge to the field, but offers great opportunities for exploration into uncharted territory.

A significant hurdle to our exploration of the virome is the lack of universal marker genes akin to 16S and 18S ribosomal subunits of prokaryotes and eukaryotes, respectively^{9,11,23,24}. Most phages in the gut have been identified as dsDNA *Caudoviricetes* (previously *Caudovirales*) or ssDNA *Microviridae*, while RNA phages are relatively rare²³. CrAssphages (class *Caudoviricetes*) were discovered within the last decade and are the most abundant gut phage as of the time of writing^{6,25}. Surprisingly, CrAssphages were found to be six-times more abundant in publicly available databases than all other known phages together²⁵. Representing up to 90% of all reads in viral-like particle (VLP)-derived metagenomes²⁵, the discovery of CrAssphages highlights the wealth of knowledge to be gained from uncovering the “viral dark matter” of the gut.

1.3 Bacteriophage adaptation to the intestinal mucosa

1.3.1 The gut mucosa

The intestinal mucus is a physical barrier that lines the small intestine (SI) and colon, protecting the underlying intestinal epithelium from commensal and pathogenic bacteria alike²⁶. The gut mucosa is composed of mucin glycoproteins that are produced by specialised intestinal epithelial cells called goblet cells. Goblet cells constitutively produce mucin proteins, principally encoded by the *muc2* gene. Mucins are post-translationally O-glycosylated with different combinations of complex carbohydrates, resulting in an extended, stiff “bottle brush”-like structure²⁷. Once secreted into the lumen, mucins become hydrated and expand to form a mesh-like network that lines the small and large intestine. The mucosa protects the underlying intestinal epithelium from physical contact with bacteria while also supporting an ecosystem of gut microbes²⁶.

The intestinal landscape is spatially heterogeneous, with different physical and chemical parameters along its length. Bacterial abundance along the GIT is thought to be dictated by pH, oxygen concentration and antimicrobial peptide production^{28,29}. Beyond changes in physical factors, mucus density, thickness, and composition also vary across different gut regions. There are notable differences in the structure of the mucosa between the SI and colon (**Figure 1.1**). The SI mucosa is composed of a single loose mucus layer that is permeable to microbes, facilitating their colonisation³⁰. However, Paneth cells within intestinal epithelial crypts produce high gradients of antimicrobial peptides which prevents commensal bacteria invasion deeper into the mucus³¹. Additionally, the mucosal immune system aids in the defence of the intestinal epithelium through continual sampling of the gut lumen and secretion of microbe-specific immunoglobulin (Ig) A into the lumen³¹. The colon is defended by a bi-layered mucosa^{29,31,32}.

An outer loose mucosa, similar to that of the SI, contacts the lumen and supports a microbial ecosystem. The inner, dense mucus layer is composed of transmembrane mucin glycoproteins and is, for the most part, devoid of bacteria²⁶. Since the colon has reduced antimicrobial peptide concentrations and fewer gut-associated lymphoid tissues (GALT)²⁶, the inner mucus layer serves to prevent bacterial invasion and contact with the underlying intestinal epithelium³² (**Figure 1.1**). Once thought to be static, it is now appreciated that the mucus layers of the SI and colon move along the intestine with the peristaltic flow of the gut, encasing faecal pellets during their transit³³. Further, the rate of mucus production and organisation of mucus O-linked glycans is responsive to bacterial colonisation and immune system activation³⁴. The dynamic nature of gut mucosa is also relevant to bacterial-phage interaction in the gut. T4 phages display subdiffusive motion in the mucus, increasing chance encounters with their target bacteria in the mucus and providing an additional layer of mucosal immunity³⁵. In the following section, we discuss the interactions between T4 phage and mucus in detail.

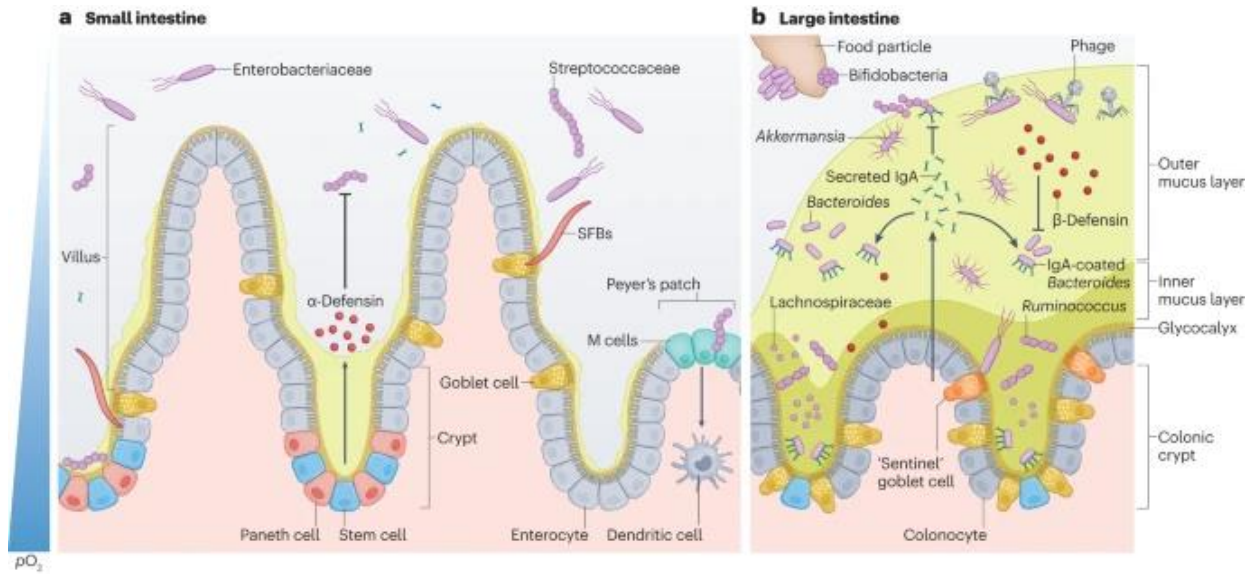


Figure 1.1 Mucus, oxygen, antimicrobial peptides and other immune factors drive bacterial colonization and organization near the epithelium. (A) The SI contains a single mucus layer that protects the underlying intestinal epithelium. Paneth cells produce antimicrobial peptides that prevent colonisation by commensal and pathogenic bacteria. (B) The colon contains a bi-layered mucosa, characterised by a dense inner layer devoid of bacteria, and a loose outer layer which supports a microbial ecosystem. McCallum & Tropini (2023).

1.3.2 T4 phage adherence to mucus

E. coli-targeting T4 phages were recently described to weakly adhere to mucin glycan residues of mucus produced by colonic and lung epithelial cells *in vitro*³⁶. Phage adhesion to mucus is mediated by Ig-like domains located within highly antigenic outer capsid (Hoc) proteins³⁷. Hoc proteins, alongside small outer capsid proteins (Soc) and the major capsid protein gene product 23 (gp23), form the structure of the phage capsid, which contains the phage's genetic material³⁷⁻³⁹. Ig-like domains are common throughout nature and are often involved in cell-cell interactions. Ig-like domains can accommodate large sequence variability^{40,41}, such as that integral to the development of T and B cell receptors (TCR/BCR) and antibodies^{37,42}, which exhibit enormous clonal variability. It has been proposed that the high degree of variability

afforded to T4 phage by its Ig-like domains allows it to adapt its mucin binding specificity in response to host-mediated alterations to mucin glycosylation patterns⁴¹.

It was first demonstrated that Hoc proteins, and their Ig-like domains, are required for T4 phage retention using a gut-on-a-chip system with mucus-producing human colon and lung epithelial cell lines (T84 and A549, respectively)^{35,37}. In this system, a genetically engineered T4 phage strain lacking Hoc proteins (Δ Hoc) was unable to be retained within the gut-on-a-chip, and had reduced *E. coli* killing efficiency^{35,37}. These data support the proposed model of mucus-adherence being essential for T4 phage mobility through mucus by subdiffusion, allowing it to counter the constant outward flow of mucus³⁵. While counter-intuitive, Barr et al. (2015) argue that the decreased rate of motion of phages mediated by mucus-binding is advantageous as it increases the chance encounters between a phage and its host bacterium³⁵. It is estimated that that approximately 25% of known *Caudoviricetes* phages contain Ig-like domains⁴⁰, signifying that mucus-binding domains may be important to phage evolution in the mammalian GIT.

1.4 Phage interactions with eukaryotic cells

The study of phage interactions with their target bacteria *in vitro* has proven useful for understanding how phages and bacteria might interact in the gut. *In vitro*-techniques involving cell culture and transwell assays were used to demonstrate that T4 phages can interact with epithelial cell cultures. As phages are restricted to infecting prokaryotic cells and lack the genes required to replicate in eukaryotic cells, it was initially thought that phages would not interact with the intestinal epithelium. However, T4 phages have been demonstrated to translocate across colon and lung epithelial cell line monolayers by means of macropinocytosis *in vitro*^{43,44}. While indicative of passive interaction between phages and epithelial cells, *in vitro* studies are limited by the absence of other intestinal cell types, such as Paneth, stromal and immune cells.

Additionally, gut physical factors (mucus flow, peristalsis) are absent, which may interfere with a phages ability to encounter the epithelium *in vivo*. Emerging research suggests that phages can be detected as foreign antigen by the mammalian immune system^{18,45–47} (discussed further in **Section 1.6**), suggesting more complex cellular interactions with phages than previously implied.

1.5 Interrogation of the microbiome using gnotobiotic mouse models

Gnotobiotic mouse models are an important tool for investigating bacteria and phages within complex, but controlled, microbial environments. Germ-free (GF) mouse models are devoid of all microorganisms and facilitate the interrogation of microbes and their effects on the host in the environment. GF mice are an excellent tool for separating the genetics from the microbiome, and it is now well established that microbial colonisation of the intestine is required for GIT-, immune- and neurodevelopment⁴⁸. GF mice exhibit gastrointestinal (GI) abnormalities, including an enlarged caecum and reduced mucus thickness⁴⁹, as well as an immature immune system^{48,50}.

Monocolonised mice, while still lacking in GI and immune development compared to specific pathogen-free (SPF) or conventional microbiota mice, are invaluable for unravelling the specific effects of an individual species on the host. Monocolonised mice have been instrumental in understanding the importance of gut bacteria in driving CD4⁺ T cell differentiation. A classic example is the discovery that segmented filamentous bacteria (SFB) are potent inducers of CD4⁺ T helper (Th) 17 cells in mice^{50,51}. Comparatively, fewer studies have utilised GF, mono- and bi-colonised mice in the interrogation of virus-specific effects on GI and immune development. Infection of GF mice with a persistent enteric murine norovirus (MNV strain CR6) was sufficient to restore intestinal morphology and lymphocyte function without causing disease, indicating that enteric viruses support intestinal homeostasis, not unlike their bacterial counterparts⁵².

Similarly, inoculation of GF mice with phages resulted in the increased production of the inflammatory cytokine, IFN γ ¹⁸ (discussed in more detail in **Section 1.6**). Pertinent to this thesis, bi-colonised mice provide opportunities to investigate the impact of one phage-bacteria pair on the mammalian host in a controlled model and without interference by other commensal microbes.

1.6 Phage-specific immune responses

While the historic focus of investigation has been around the relationships between phage and their target bacteria, it is also important to consider potential interactions between phage and the intestinal mucosa, epithelium, and immune system of the metazoan host. These dynamics all likely play an important role in the overall response to intestinal phage colonisation. Most simply, phages have been studied using GF mice to elucidate the impact of phages on the immune system without interference by the microbiota¹⁸. In GF mice, *E. coli* phage dsDNA was detected by pattern-recognition receptors (PRR) within the endosomes of phagocytic immune cells (macrophages and dendritic cells (DCs)). PRRs on innate immune cells play a key role in the activation of the adaptive immune system by detecting pathogen-associated molecular patterns (PAMPs), resulting in downstream cellular signalling. Specifically, the *E. coli* phages examined by Gogokhia et al. (2019) were detected by Toll-like receptor (TLR) 9, a PRR that detects unmethylated CpG dinucleotides – a motif associated with microbial DNA¹⁸. The authors found that this signalling resulting in increased T cell-dependent production of the inflammatory cytokine interferon (IFN)- γ ¹⁸. Sweere et al. (2019) similarly demonstrated interaction of a ssDNA *Pseudomonas aeruginosa* phage with TLR3 (recognising transcribed RNA) in specific pathogen-free (SPF) mice⁴⁵. The resulting signalling induced production of type I IFNs (IFN α and IFN β), which served to benefit the bacterial host by inhibiting phagocytosis of *P. aeruginosa*⁴⁵. Together,

these studies signify that phage DNA can be detected by PRRs and initiate signalling within phagocytic cells at barrier sites such as the gut mucosa¹⁸ and skin⁴⁵. While some phages are capable of manipulating the immune system to prolong the survival of their host⁴⁵, others have demonstrated the ability to aid the immune system, even if inadvertently. Prophage antigens integrated into the genome of *Enterococcus hirae* were detected by DCs, which primed CD8⁺ T cells in an MHC-I dependent manner⁴⁶. This resulted in CD8⁺ T cell cross-reactivity with tumour antigens, production of IFN γ , and improved anti-tumour activity of immunotherapeutic drugs⁴⁶. This study further supports an immunomodulatory role for intestinal phages.

There have been limited efforts to establish the humoral response to intestinal phages – the activation of B cells and production of phage-neutralising antibodies. In the context of phage therapy to treat septic bacterial infections, the production of phage-neutralising antibodies could prove troublesome, particularly if therapeutic phages are neutralised before clearance of the pathogen. Phage therapy has been trialled in humans on the basis of compassionate care^{53–56}. Due to this, the immune responses to phages administered to humans intravenously remains largely unknown. Phage-specific antibody production has been documented in mouse studies involving the continual oral delivery of phages through drinking water^{18,47}. Specifically, phage-specific IgG was detected consistently in the serum^{47,57}, and phage-specific IgA was detected in the faeces^{18,47}. IgA, secreted by B cells of the GALT, plays a protective role within the mucosal surfaces by coating intestinal microbes and controlling their colonisation^{58,59}. However, the effects of IgA on the microbiota are not completely understood⁵⁸, and even less is known about the role of phage-specific IgA in the gut. Taken together, phages can stimulate and prime factions of the mammalian immune system, but the outcome of phage-specific immunity is still unclear.

1.7 Phages in health and disease

1.7.1 The gut phageome is associated with IBD

Numerous sources have described associations between the composition of the gut phageome and the presence of GI disease in humans. IBD is characterised as a group of autoinflammatory disorders of the GIT, namely Crohn's disease (CD) and ulcerative colitis (UC)⁶⁰. IBD has been associated with a "dysbiotic" microbiome, which is generally defined as a maladaptive or sub-normal microbiome with reduced bacterial richness and diversity⁶¹. With the identification of phages as the largest component of the virome^{11,19,22,24}, correlations have now been found between the composition of the phageome and disease. IBD incidence has been associated with increases in *Caudovirectes* phage richness (the number of taxa counted per sample¹⁹), which were not accounted for by IBD-associated decreases in bacterial richness¹⁹. Additionally, shifts from a lytic phage-dominated virome to a lysogenic phage-dominated virome have been previously observed in IBD patients¹¹. During IBD flare-ups, inflammation results in the production of reactive oxygen and nitrogen species, which can trigger the bacterial SOS response and subsequent conversion of lysogenic phages to the lytic cycle¹³. The release of new phage virions into the gut potentially drives further alterations to the gut microbiome, exacerbating disease. Some *E. coli* phages, including T4, have a demonstrated ability to stimulate production of the proinflammatory cytokine IFN γ through their interactions with TLR9 on phagocytic cells¹⁸. Patient-derived, colitis-associated *Caudoviricetes* phages were found to be potent inducers of IFN γ production, and exacerbated the severity of experimental colitis in mouse models^{18,62}. These studies indicate that the inflamed gut may drive changes to the gut phageome, exacerbating disease. In diseases such as IBD it remains unclear whether phages

contribute to disease progression and exacerbation of bacterial “dysbiosis”, or if changes in phage abundance merely reflects changes in the abundance of their bacterial hosts.

1.7.2 Faecal filtrate transplants in the treatment of disease

Faecal microbiota transplants (FMT) have been used with some success to treat patients with recurrent *Clostridioides difficile* infection (rCDI)^{61,63}. CDI causes pseudomembranous colitis and debilitating diarrheal disease in those afflicted⁶⁴. FMTs involve the extraction of bacteria, viruses and other components from the faeces of healthy donors, and transfer to patients with maladapted microbiomes⁶¹. However, FMTs carry a degree of risk as they involve the transfer of undefined live bacteria, which may cause further infection or malignant disease, particularly in immunocompromised individuals^{63,65}. Phages have been implicated in the success of FMTs in studies demonstrating that bacteria-free filtered FMTs, or faecal filtrate transplants (FFT), have similar or greater efficacy for the treatment for recurrent rCDI in humans^{63,66} and necrotizing enterocolitis in pre-term pigs⁶⁵. Following treatment with FFTs, changes to the intestinal phage profile was observed^{63,65}. While it is supposed that the success of FFTs is due to the addition of phages to the diseased gut environment, it is also possible that other components such as microbial metabolites, secreted proteins or enteric viruses could be responsible for these effects⁶⁵. Further pre-clinical trials using purified phages as “phage therapy” in animal models of disease are warranted to determine the mechanism behind FFTs in the treatment of GI disease.

1.8 Phage therapy

The use of phages as antibacterial therapy has been considered by scientists with interest since the initial discoveries of these “invisible anti-microbes” by Twort and d’Hérelle in 1915 and 1917, respectively⁶⁷. D’Hérelle was among the first to use phage therapy to successfully treat a patient with dysentery in 1919⁶⁸, but the success of antibiotics in the 1940’s resulted in a

decline in phage therapy research. However, in Poland and parts of the former Soviet Union, the use of phage therapy continued. The resultant research from this period is often met with scepticism due to “poorly designed trials” and “methodological flaws”^{16,60}, and eventually, antibiotics prevailed in these regions.

Throughout the last decade, there has been renewed interest in phage research owing to the rise of antimicrobial resistant (AMR) pathogens¹⁶. AMR pathogens are predicted to cause 10 million deaths per year by 2050, representing a significant public health burden¹⁶. Strictly lytic phages present an attractive alternative to antibiotics to treat AMR pathogens due to their ability to infect and lyse a specific bacterial host¹⁶. In recent years, lytic phage cocktails have been used intravenously with some success in serious, AMR bacterial septic infections in humans^{16,53}. For example, a life-threatening *Acinetobacter baumannii* infection was cleared by intravenous administration of a cocktail of nine lytic phages⁵³. In another case, a 15 year-old cystic fibrosis patient with *Mycobacterium abscessus* infection was successfully treated with intravenous administration of a phage cocktail consisting of three genetically engineered phages⁵⁶. Lastly, a *P. aeruginosa* infection causing sepsis was successfully treated in an infant organ transplant recipient⁵⁴. In each of these cases, the treatment of patients with phage cocktails was approved for compassionate use, and the success of these trials was gauged by the clearance of the pathogen. In each study, the phage cocktail was noted to be well tolerated by the patient. This is taken to mean that adverse effects, beyond the symptoms present due to disease, were not observed. As highlighted by Van Nieuwenhuysse et al. (2022), guidelines are needed for the use of phage to treat infection, to better characterise what determines therapeutic success or failure⁵⁴.

A key concern for the development of oral phage therapy for the treatment of intestinal infections is the knock-on effects that introduced phages may have on the commensal gut flora.

This is not a concern for intravenous delivery of phage therapy, as the goal is to clear all bacteria. In the intestine, the commensal bacteria are essential for human health, and seemingly small perturbations to the intestinal environment may have drastic effects on the composition of the microbiota⁶⁹. The use of oral phage therapies to treat intestinal infections was thought to avoid the perturbations to the commensal gut flora that are typical of broad-spectrum antibiotics. However, it is not well understood how the addition of a phage cocktail to the GI microbiota to fight infection might impact the abundance of non-targeted gut commensals. Recent work suggests that the introduction of a novel phage into a defined bacteria consortium *in vivo* impacts the abundance of both the phage-targeted and non-targeted bacteria¹⁵. An unintended consequence of this is an altered gut metabolome, which may have downstream effects on the murine host¹⁵. An additional challenge of oral phage therapy is the ability of phages to evolve the ability to “jump” to a related, but untargeted host. De Sordi et al. (2017) demonstrated that a lytic *E. coli* phage was able to evolve the ability to infect a previously resistant *E. coli* strain in a bi-colonised mouse model⁷⁰. However, the benefits of phage-mediated pathogen clearance likely outweigh the risks behind potentially small changes to the bacteriome. The development of phage resistance by bacteria is thought to be occurring constantly between commensal phages and bacteria in the gut. Evolution of phage resistance by bacteria often results in an evolutionary “trade-off” by the bacteria – defined as a coincidental change in bacterial fitness or virulence^{71,72}. This was exploited in a study aiming to re-sensitise AMR *P. aeruginosa* to antibiotics⁷¹. The development of phage resistance by *P. aeruginosa* restored its sensitivity to several antibiotic drugs⁷¹. This study demonstrates an alternative strategy for the use of phage therapy to combat AMR pathogens that readily evolve resistance to phage predation in the gut.

1.9 Hypothesis

Phages are important but underappreciated members of the mammalian gut microbiome. Within the gut mucosa, it is thought that intestinal phages and bacteria participate in a constant “arms-race”, resulting in continual co-evolution^{15,73}. As Ig-like domains are present in ~25% of known *Caudoviricetes* phages^{37,40}, I theorised that the ability of phages to adhere to intestinal mucus is of critical important to their colonisation of the murine GIT. **Therefore, I hypothesised that modification of the T4 phage capsid would alter phage adherence to intestinal mucus *in vivo*, and subsequently reduce the efficiency of phage-bacterial infection and killing.** Additionally, as phages have been shown to translocate across epithelial cell monolayers *in vitro*^{43,44}, and detected by the mammalian immune system *in vivo*^{18,45-47}, **I hypothesised that the inoculation of a gnotobiotic mouse model with wild type (WT) T4 phage facilitates phage translocation to the host lymphoid tissues and interaction with the host immune system.**

I first aimed to investigate the spatial localisation and colonisation ability of T4 phages and their target bacteria, *E. coli*, *in vivo*. To do this, *E. coli* monocolonised mice were inoculated with WT or Δ Hoc T4 phages that lack Hoc proteins and mucus binding abilities. The colonisation potential of both phages and bacteria were measured over time. I next aimed to interrogate the impact of WT T4 phages on the immune system of monocolonised mice by assessing the translocation of T4 phages from the intestinal lumen into the tissue. I aimed to measure phage-induced cytokine production and immune cell activation at the lamina propria, mesenteric lymph nodes (mLN) and spleen. Collectively, the results of this study expands our understanding of phage dynamics within the gut mucosa and the interactions of intestinal phages with the adaptive immune system.

Chapter 2: Methods

2.1 Mouse strains, housing and diets

Mice were housed at the University of British Columbia (UBC) in the Centre for Disease Modelling (CDM), a specific pathogen-free (SPF) animal facility. GF and gnotobiotic (i.e., *E. coli* monocolonized) C57BL/6 mice were bred in the facility within a sterile flexible film isolator (Class Biologically Clean (CBC)) supplied with sterilised mouse diet (PicoLab® Mouse Diet 20 EXT, LabDiet), water, bedding, and nesting material. Experimental mice were both male and female and age-matched within each experiment, with mice being between 6-15 weeks at the onset of experimentation. Experimental mice were transferred from gnotobiotic isolators to sterile, positive pressure, bioexclusion ISO cages (Techniplast) prior to start of each experiment, where mice also received sterilised mouse diet, water, bedding, and nesting. ISO cages were housed on a Digital Ventilated Cage ISO rack (DVC®ISO, Techniplast), which provided cages with a HEPA-filtered air supply. Breeding and experimental mice were kept on a 12-hour day/night cycle. All experiments were performed according to guidelines from UBC Animal Care Committee and Biosafety Committee-approved protocols (A23-0113, A19-0332, A23-0012, B19-0038).

2.2 Bacteria and phage strains

E. coli (K-12, BW25113) was used as the target bacterial strain for T4 phage predation. Wildtype (WT) and Δ Hoc T4 phage stocks were gifted to the project by Dr. Forest Rohwer's laboratory at San Diego State University. The original phage stocks were resuspended in saline magnesium (SM) buffer and stored at 4°C until propagation (see **Table 2.1** for recipes).

Solution	Components
Saline Magnesium buffer	1 L dH ₂ O 50 mM Tris-HCl (pH 7.4) 100 mM NaCl ₂ 8 mM MgSO ₄ ·7H ₂ O
Methacarn	60% Methanol 30% Chloroform 10% acetic acid

Table 2.1 Recipes for commonly used buffers in phage preparation and visualisation

2.3 Phage propagation, cleaning, and purification

WT and Δ Hoc T4 phage were propagated, cleaned and purified as previously described by Bonilla et al. (2016)⁷⁴. Briefly, *E. coli* was amplified from a single colony picked from a streaked agar plate in liquid culture overnight at 37°C and subcultured until in exponential growth phase (optical density at 600 nm (OD₆₀₀) ~0.2). Cultures were supplemented with 0.001M CaCl₂ and MgSO₄, and infected with high titre WT or Δ Hoc T4 phage stocks. Phage-*E. coli* cultures were incubated at 37°C until the culture became clear due to *E. coli* killing by T4 phage. Lysates were centrifuged, passed through a 0.22 μ m filter and treated with chloroform to remove residual bacteria and debris. Phage lysates were then concentrated in a 100 kDa centrifugal filter device (Amicon, Sigma Millipore) and resuspended in SM buffer. Bacterial endotoxins such as lipopolysaccharides (LPS) were removed from the lysate through incubation with 1-octanol. Lastly, residual 1-octanol was removed through evaporation by speed vacuum at room temperature (RT). A vehicle lysate was produced in this same manner, omitting the addition of phages. These protocols have been prepared in detail and submitted for publication to the *Journal of Visualised Experiments* (JoVE).

2.4 *E. coli* monocolonization of germ-free mice and breeding

GF mice, bred in the absence of microorganisms, were monocolonised with *E. coli* (K-12 BW25113). For imaging experiments, mice were transferred to sterile bioexclusion ISO cages and maintained under sterile conditions, with sterile food, bedding and water. Mice were inoculated with 200 µL of an overnight culture of *E. coli* in LB. For the generation and maintenance of *E. coli* monocolonised mice within a sterile flexible film isolator, an overnight culture of *E. coli* in LB was imported into the isolator within a sealed cryovial. The outside of the vial was sterilised by spraying with 5% peracetic acid (PAA). GF mice were monocolonised with *E. coli* through application of the culture to the backs of each mouse within the isolator. *E. coli* colonisation was confirmed by plating faecal pellets onto LB plates 7 days post-colonisation. A colony of *E. coli* monocolonised mice were maintained and bred within the isolator for the duration of their lives. The first generation of monocolonised mice were designated solely as breeders. Their progeny (F1, F2, etc) were confirmed to be colonised with *E. coli* by plating faecal pellets and were used as experimental mice.

2.5 Inoculation of monocolonised mice with phage

To investigate the tripartite interaction between T4 phage, *E. coli* and the metazoan host, *E. coli* monocolonised mice were transferred to sterile bioexclusion ISO cages. Within a disinfected biological safety cabinet (BSC), mice were handled under aseptic conditions. Each mouse was gavaged with 100 µL of autoclaved 1M NaHCO₃ to neutralise stomach acids, followed by gavage 10 mins later with 100 µL of sterile-filtered 2x10⁷ plaque forming units (pfu)/mL T4 phage in SM buffer.

2.6 Quantification of phage and bacteria by spot plating assays

Mouse faecal pellets, caecal contents, livers, mLNs, spleens and serum were collected into sterile microcentrifuge tubes and placed at on ice or at 4 °C. All samples excluding the serum were weighed and homogenised with SM buffer. Faecal and caecal samples were homogenised by vortexing for approximately 5 mins. Solid tissues such as livers, mesenteric lymph nodes and spleens, were homogenised by beating with metal beads using a TissueLyserII (Qiagen) at 20 Hz for 5 min. For each sample, serial dilutions were prepared in factors of 10. For each dilution, 5 µL was spotted onto 1.5 % agar LB plates for *E. coli* quantification, and 0.5% agar LB plates (soft agar) for phage quantification, as previously described^{75,76}. Plates were incubated at 37 °C overnight and colonies/plaques were counted the following day.

2.7 Quantification of phage and bacteria by quantitative PCR (qPCR)

2.7.1 Phage DNA extraction from faeces and caecal contents

T4 phage gene copies were measured using qPCR as an alternative method for phage enumeration. Faecal pellets and caecal contents were harvested, snap frozen, and stored at -80 °C. Prior to DNA extraction, samples were thawed and weighed. DNA was extracted from faecal pellets and caecal contents using the Dneasy PowerSoil Pro Kit (Qiagen) according to the manufacturer instructions.

2.7.2 Generation of T4 phage DNA standards

DNA standards for qPCR were generated from high titre T4 phage lysates. DNA was extracted from phage lysates using the Dneasy Blood & Tissue Kit (Qiagen), with adaptations as previously described by Jakočiūnė and Moodley (2018)⁷⁷. Briefly, concentrated phage lysates were incubated with Dnase I 10x buffer (Qiagen), Dnase I (1 U/µL) (Qiagen), and Rnase A (10 mg/mL) (Qiagen) for 1.5 h at 37°C, to remove residual bacterial DNA and RNA. To inactivate

Dnase I and Rnase A, 0.5 M Ethylenediaminetetraacetic Acid (EDTA) was added to the solution. The phage capsid was digested by incubating phage lysates with Proteinase K (20 mg/mL) (Qiagen) for 1.5 h at 56°C. AL buffer was then added to the phage lysate in a 1:1 ratio and incubated for 10 min at 70°C. An equal volume of 99.9% ethanol was added to the lysate, and the mixture was added to the Dneasy Mini spin column. DNA extraction then proceeded as per the manufacturer instructions. Once extracted, phage DNA was measured using a NanoDrop spectrophotometer (Thermo Fisher Scientific). To calculate the number of genome copies from the DNA concentration, DNA mass (ng/copy) was calculated by multiplying the number of phage genome size (168 903 bp) by a constant for the mass of one bp (1.096×10^{-21} g/bp). Mass of the PCR product was then calculated by multiplying the mass (ng/copy) by the copy number for each standard. The T4 phage DNA stock was diluted in sterile DNase, RNase-free H₂O (Fisher Bioreagents).

2.7.3 Measurement of phage loads by qPCR

T4 Phage genome copies were measured by qPCR using PerfeCTa SYBR® Green Fastmix (QuantaBio) in 12 µL reaction mixture volumes with 3 µL of DNA template. T4 phage DNA was amplified with primers T4phage_F1 (5'- CCA CAC ATA GCG CGA GTA TAA -3') and T4phage_F2 (5'- GAA ACT CGG TCA GGC TAT CAA -3')¹⁵ on a CFX96 Touch Real-Time PCR Detection System (Bio-Rad) with the following amplification settings: 95°C for 2 min, and 40 cycles of 95°C for 30 s, 54°C for 30 s and 72°C for 20 s. All samples were run in triplicate. T4 phage genome copies were extrapolated from a standard curve and normalised to tissue weight.

2.8 Detection of T4 phage DNA by PCR and gel electrophoresis

PCR was used to confirm the presence of wildtype and Δ Hoc T4 phage in faecal and caecal samples. PCR was carried out using GoTaq® Green Master Mix (Promega) in a 24 μ L reaction mixture with 1 μ L of DNA template. T4 phage DNA was amplified in two separate reactions with T4phage_F1 and T4phage_F2 general T4 phage primers (**Section 2.7.3**)¹⁵, or Hoc protein-specific primers Hoc_fd1 (5'- GCA GGA GTT ACG GCT AAG GT -3') and Hoc_rv1 (5'- GAA ACG GCT GAA GCG ACA AC -3'). The PCR was run on a T100 Thermal Cycler (Bio-Rad) under the following amplification settings: 98°C for 3 min, and 35 cycles of 98°C 30 s, 54°C for 30 s and 72°C for 1 min, then 72°C for 10 min. Samples were run on a 2% agarose gel with SYBR™ Safe DNA Gel Stain (ThermoFisher Scientific) added to detect a 96 bp band for WT and Δ Hoc T4 phage (T4phage_F1/F2) and a 74 bp band for Hoc-containing phage (Hoc_fd1/rv1). Gels were imaged with an AlphaImager® EC gel documenter (Alpha Innotech).

2.9 Histology and immunofluorescence

2.9.1 Fixation and processing

To visualise the localisation of T4 phage and *E. coli* within the gut mucosa, small intestines and colons were harvested from phage-inoculated, *E. coli* monocolonised mice. Tissues were fixed and processed as previously described⁷⁸. Briefly, tissues were fixed in methacarn fixative (60% methanol, 30% chloroform, 10% acetic acid)⁷⁸ for 1-2 weeks at room temperature. Tissues were processed by passage through 2 x 30 min in 100% methanol, 2 x 20 min in 100% ethanol and 2 x 15 min in xylene. Tissues were submerged in molten paraffin wax (at 60°C) for 2 h at 60°C. Once processed, tissues were embedded and sectioned by the BC Children's Hospital Research Institute Histology core facility.

2.9.2 Immunostaining

Sectioned tissues were de-waxed with xylene and rehydrated through a series of decreasing concentrations of ethanol (50-100%). Tissues were blocked with SuperBlock™ Blocking Buffer (ThermoFisher Scientific) at RT for 2 h or 4°C overnight. Tissues were then stained with a custom-ordered rabbit anti-gp23 antibody (Boster Bio) (see **Table 2.2**) diluted 1:200 in blocking buffer, to detect T4 phage. Slides were incubated at 4°C overnight with blocking buffer. A goat anti-rabbit antibody conjugated to Rhodamine Red-X (Jackson ImmunoResearch) was diluted to 15 µg/mL in blocking buffer and added to tissue. DAPI was added to stain nucleic acids within bacteria and epithelial cells. Ulex Europaeus Agglutinin (UEA)-1 lectin or Wheatgerm Agglutinin (WGA) conjugated to fluorescein (Vector Laboratories) were added to stain colon and SI mucus, respectively. Secondary antibodies and stains were incubated on slides in the dark at 4°C for 2 h. Slides were washed between steps with PBS. Coverslips were mounted with Prolong™ Gold antifade mountant (Invitrogen) and set at RT overnight.

Antibody	Conjugate	Supplier/cat. #	Working concentration
Immunofluorescence antibodies			
Anti-T4 gp23	n/a	Boster Bio, DZ41238	1:200
Goat Anti-Rabbit IgG (H+L)	Rhodamine Red-X	Jackson ImmunoResearch, 111-295-144	15 ug/mL
Flow cytometry - Block and viability stain			
FcγR block	n/a	AbLab	1:600
LIVE/DEAD™ Fixable Aqua Dead Cell Stain	BV510	Invitrogen/ 19852	1:600
Flow cytometry - Cell surface antibodies			
B220/CD45R (RA3-6B2)	BV421	Biologend/103239	1:300
CD4 (RM4-5)	BV650	BD Bioscience/ 563747	1:300
CD44 (IM7)	APC-Cy7	Biologend/103028	1:300
CD45.2 (104)	Alexa Fluor 700	Biologend/109822	1:300
CD8α (53-6.7)	PE-Cy7	BD Bioscience/552877	1:300
TCRβ (H57-597)	PE Texas Red	Biologend/109240	1:300
Flow cytometry - Intracellular antibodies			
IFNγ (XMG1.2)	APC	Biologend/505810	1:200
TNFα (MP6-XT22)	PE	Biologend/506306	1:200
TBET	PE	Biologend/644810	1:200

Table 2.2 Antibodies

2.9.3 Confocal microscopy

Tissue sections were imaged using a Zeiss LSM 900 confocal microscope equipped with AiryScan 2. Images were collected at 100X magnification with oil immersion. Images were collected using tile scan functions. AiryScan and stitching were applied upon image processing. Images were further processed using FIJI (Image J)⁷⁹.

2.10 Cytokine detection in mouse spleens and mLN

2.10.1 Cytokine bead arrays

Concentrations of cytokines within mouse spleens and mLN were measured using a multi-analyte flow assay kit (BioLegend LEGENDPlex). Spleens and mLN were harvested from mice immediately following euthanasia, snap frozen on dry ice and stored at -80°C. Upon

thawing, samples were weighed and 100 μ L of sterile PBS was added. Tissues were homogenised using a metal bead and the TissueLyser II (Qiagen) at 20-30 Hz for 5-10 min. Samples were centrifuged briefly at 1000 x g to pellet particulates. The LEGENDPlex Mouse Anti-Virus Response Panel (BioLegend) was used to detect 13 cytokines and chemokines in tissues (IFN α , IFN β , IFN γ , IL-1 β , IL-6, IL-10, IL-12, CCL2, CCL5, CXCL1, CXCL10, TNF- α , GM-CSF) (**Table 2.3**) The assay was performed as per manufacturer instructions.

2.10.2 Flow cytometry acquisition and analysis

Samples were acquired using a CytoFLEX equipped with four lasers (Beckman Coulter - blue 488 nm, yellow 561 nm, red 633 nm, violet 405 nm). LegendplexTM Qognit cloud-based analysis software (<https://legendplex.qognit.com>) was used to analyse flow cytometry data as per the manufacturer instructions. Concentrations of each cytokine within tissues were extrapolated from a standard curve generated from recombinant cytokine standards. Concentrations were normalised to tissue weight.

Cytokine	Bead ID
IFN γ	A4
CXCL1	A5
TNF α	A6
CCL2	A7
IL-12	A8
CCL5	A10
IL-1 β	B2
CXCL10	B3
GM-CSF	B4
IL-10	B5
IFN β	B6
IFN α	B7
IL-6	B9

Table 2.3 Cytokines examined in the LEGENDPlex Mouse Anti-Virus Response Panel (BioLegend)

2.11 Immune cell isolation from spleens and mLNs

Spleens and mLNs were harvested from mice immediately after euthanasia and placed into cold wash buffer on ice (see **Table 2.4** for recipes). Spleens and mLNs were mashed through 70 μm nylon mesh filters (Falcon) using the flat end of a syringe to create single cell suspensions. Additional wash buffer was passed through the filters to wash remaining cells through. Cell suspensions were centrifuged at 500 x g for 5 min to pellet cells. Spleens were subjected to Ammonium-Chloride-Potassium (ACK) lysis buffer for 10 min at RT to remove erythrocytes. Spleen and mLN cell suspensions were resuspended in complete tissue culture media (CTCM).

2.12 *Ex vivo* lymphocyte stimulation

To stimulate T cell activation and the corresponding cytokine production, cells isolated from spleens and mLNs of T4 phage-inoculated mice were stimulated with 0.1 $\mu\text{g}/\text{mL}$ phorbol myristate acetate (PMA, Sigma) and 1 $\mu\text{g}/\text{mL}$ ionomycin (Sigma) in CTCM (see **Table 2.4** for recipes) to promote Ca^{2+} signalling and protein kinase C (PKC) activation, respectively, upstream of cytokine transcription. Brefeldin A (BFA) (10 $\mu\text{g}/\text{mL}$) was added to block cytokine transport from the endoplasmic reticulum (ER) to the Golgi complex, resulting in the accumulation of cytokines in the ER. Briefly, two million splenocytes and one million mLN cells were added to each well of a round bottom 96-well plate and centrifuged at 500 x g for 5 min to pellet. Supernatants were removed and cells were resuspended in 200 μL of in stimulation media (PMA/ionomycin/BFA/CTCM). Cells were incubated in stimulation media for 4 h at 37°C, 5% CO_2 . Cells were washed with PBS (Sigma) and resuspended in PBS prior to cell staining.

2.13 Immunostaining of isolated cells for flow cytometry

To detect lymphocyte subsets within spleens and mLNs, cells were added to a 96-well round bottom plate for immunostaining with cell surface and intracellular antibodies (**Table 2.2**). Two million splenocytes and one million mLN cells were added per well. For IELs and LPLs, all isolated cells were added to each well. Plates were centrifuged at 500 x g at 4°C and Fcγ-receptor block (UBC AbLab) and LIVE/DEAD™ Fixable Aqua Dead Cell Stain (Invitrogen) in PBS were added for 20 min at 4°C in the dark. Cell surface antibodies were diluted in BD Horizon™ Brilliant Stain Buffer (BD Biosciences) and added to each well (final dilution 1:300). Cells were incubated for 20 mins at 4°C in the dark. Plates were centrifuged at 500 x g at 4°C and cell pellets were resuspended and fixed in eBioscience™ Foxp3/Transcription Factor Fixation/Permeabilization Concentrate and Diluent (Invitrogen) for 30 mins at RT in the dark. Cells were resuspended in Intracellular antibodies diluted in BD Perm/Wash™ Buffer (BD Biosciences). Intracellular antibodies were diluted in BD Perm/Wash™ Buffer (BD Biosciences) and added to stimulated spleen and lymph node cells. Cells were incubated overnight at 4°C in the dark. Cells were washed the following day twice with BD Perm/Wash™ Buffer (BD Biosciences). All cells were resuspended in FACS buffer (**Table 2.4**) prior to flow cytometry.

2.14 Cell detection by flow cytometry

Immunostained cells were detected and analysed by flow cytometry. Samples were acquired using a CytoFLEX (Beckman Coulter) equipped with four lasers (blue 488 nm, yellow 561 nm, red 633 nm, violet 405 nm). Data was analysed using FlowJo (version 10.9.0 – BD Biosciences). Dead cells, identified by positive staining with the LIVE/DEAD™ Fixable Aqua Dead Cell Stain (Invitrogen), were excluded from all analyses. Examples of gating strategies can be found in **Appendix E**.

Solution	Components
ACK Lysis Buffer	For 1 L: 1 L dH ₂ O 8.29 g NH ₄ Cl 1 g KHCO ₃ 0.0367 g Ethylenediaminetetraacetic Acid (EDTA)
Complete tissue culture media (CTCM)	For 500 mL: 450 mL RPMI-1640 (Sigma) 10% Fetal Bovine Serum (FBS) (Gibco) 2 uM L-Glutamine (Sigma) 50 U/mL Penicillin/Streptomycin (Sigma) 25 mM HEPES (Sigma) 55 uM β-mercaptoethanol (Invitrogen)
FACS buffer	For 500 mL: 500 mL PBS (Sigma) 4% Newborn Calf Serum (NCS) (Sigma) 2 mM (EDTA)
Wash buffer	For 500 mL: 500 mL RPMI-1640 media (Sigma) 2% NCS (Sigma)

Table 2.4 Lymphocyte isolation buffers

2.15 Statistical analysis

Statistical analyses were performed using GraphPad Prism (version 10.0.3). For experiments with comparisons between two or more groups, a Repeated measures (RM) 2way ANOVA or RM Mixed-effects model was fitted with Tukey's or Holm-Šídák's multiple

comparisons, respectively. For the comparison of T4 phage and *E. coli* measurements between two groups within single timepoints, statistics were calculated by multiple unpaired t-tests with Welch's corrections (when sphericity cannot be assumed) and Holm-Šídák's multiple comparisons. For cytokine bead arrays and immunophenotyping, statistical comparisons were completed using an ordinary One-Way ANOVA with Holm-Šídák's multiple comparisons. Error bars represent the standard error of the mean (SEM). * $p < 0.05$, ** $p < 0.01$, *** $p < 0.001$, **** $p < 0.0001$.

Chapter 3: Results

3.1 Wildtype T4 phages are retained in the intestines of bi-colonised mice

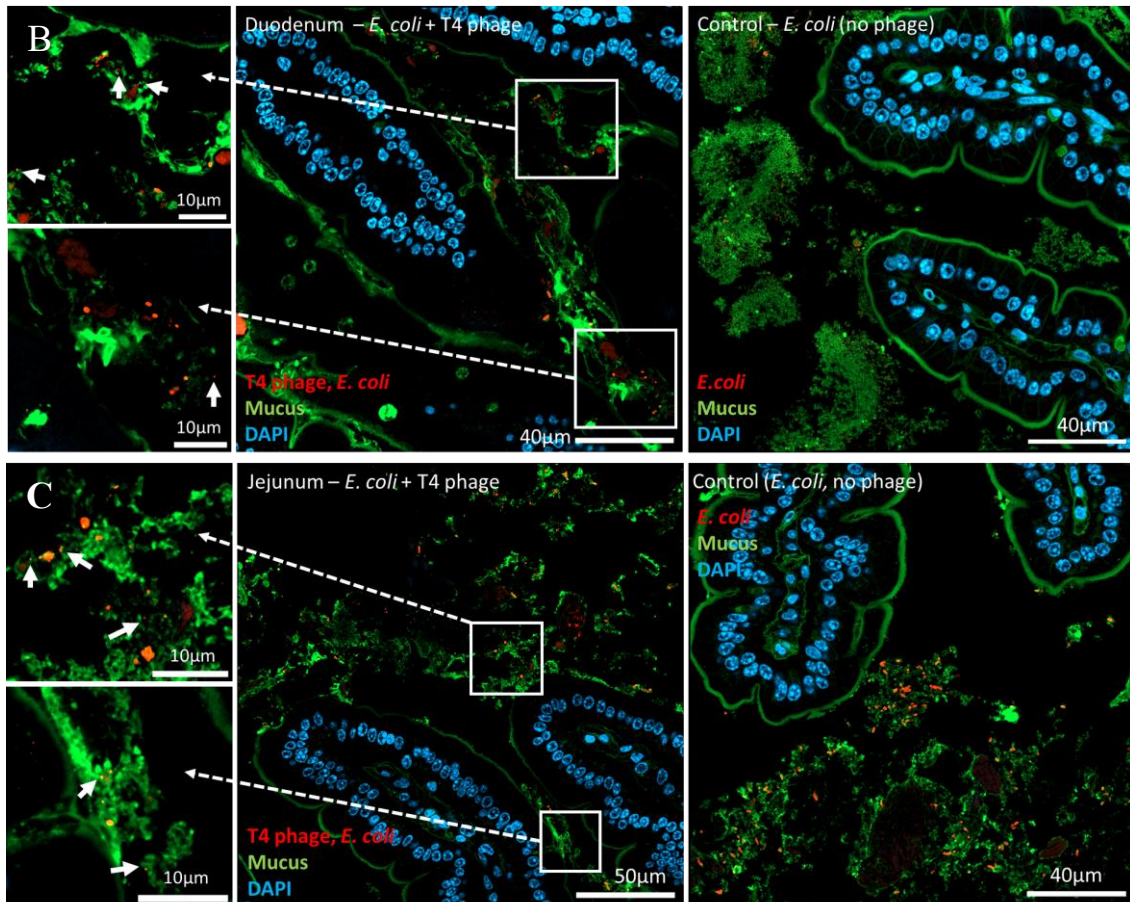
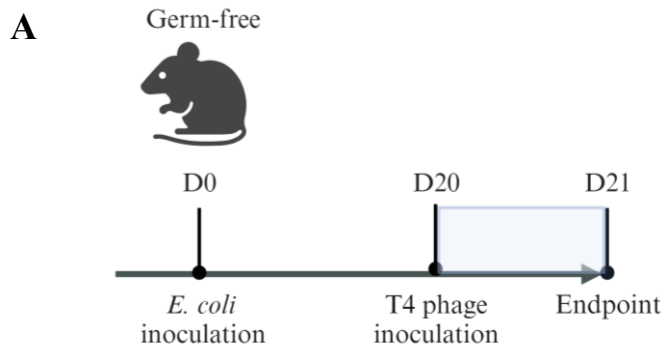
Ig-like domains located within the Hoc capsid proteins of T4 phages are thought to facilitate phage adhesion to intestinal mucus^{35,37}. These domains were determined to be conserved in approximately 25% of known *Caudovirectes* phages^{35,40}, indicating that mucus adhesion may be an evolutionarily conserved function. I aimed to build on previous studies to determine whether T4 phages are better adapted to gut mucosa colonisation, compared to Hoc-deficient (Δ Hoc) T4 phages that lack Ig-like domains.

3.1.1 T4 phage can be visualised by immunofluorescence imaging of mouse intestinal sections and localises within the mucus layer

The gastrointestinal tract of both humans and mice varies along its length in pH, osmolality, oxygen concentration and nutrient availability²⁶. Commensal bacteria localise to different gut regions depending on their metabolic needs and ability to survive within specific physical niches. However, less is known about how gut biogeography impacts phage localisation. Lysogenic phages have been found to reside mainly within the outer (loose) mucus layer and lumen, where the majority of bacteria are located⁶. On the other hand, lytic phages are thought to concentrate within the inner (dense) mucus layer, which is sparsely occupied by bacteria⁶. Since T4 phages adhere to mucus^{35,37} and are able to translocate across epithelial cell layers *in vitro*^{43,44}, I expected that T4 phage would be detected within the intestinal mucus and intestinal epithelial cells of mouse models by immunofluorescence microscopy.

To explore this, GF-born mice were monocolonised with *E. coli* by oral gavage and housed in bio-exclusion cages to maintain sterility (**Chaper 2.1**). After three weeks,

monocolonised mice were orally inoculated with 2×10^6 pfu of WT T4 phage (**Figure 3.1 A**). T4 phage-inoculated bi-colonised mice and control *E. coli* monocolonised mice were euthanised 24 h post-phage inoculation and small and large intestines were fixed in methacarn to preserve mucus structure⁷⁸. Tissue sections were stained with antibodies detecting T4 phage (anti-gp23, red), mucus-binding lectins (WGA or UEA-1, green) and nucleic acids (DAPI, blue). The anti-gp23 antibody demonstrated a degree of cross-reactivity with *E. coli* at high concentrations (**Appendix A**). This cross-reactivity persisted even when specialised, commercial blocking buffers (SuperBlockTM, Thermo Fisher Scientific) were applied (data not shown). Despite this, T4 phages could be distinguished from *E. coli* due to their distinct morphologies (punctate- or rod-shaped, respectively). T4 phage and *E. coli* were detected in both small intestinal (duodenum, jejunum, ileum) and colon sections at 100X magnification (**Figure 3.1 B-E**). Notably, T4 phages were detected visually within intestinal mucus layers throughout the GIT and were not detected in regions of the intestine devoid of mucus (**Figure 3.1 B-E**). T4 phage also appeared to occupy the distal region of the SI (ileum) and the colon most densely (**Figure 3.1 D-E**), where bacteria are also most concentrated²⁸. UEA-1, a mucin-binding lectin, is routinely used to label fucosylated mucus in the colon, but is less effective at labelling SI mucus (data not shown). Therefore, WGA was used instead to stain SI mucus. T4 phages have been suggested by others to adhere specifically to fucosylated glycan residues⁴¹, supporting my postulation that T4 phages colonise the colon most densely. Together, these data suggest that T4 phages localise to the mucus layers of the murine GI tract, supporting *in vitro* findings^{35,37}.



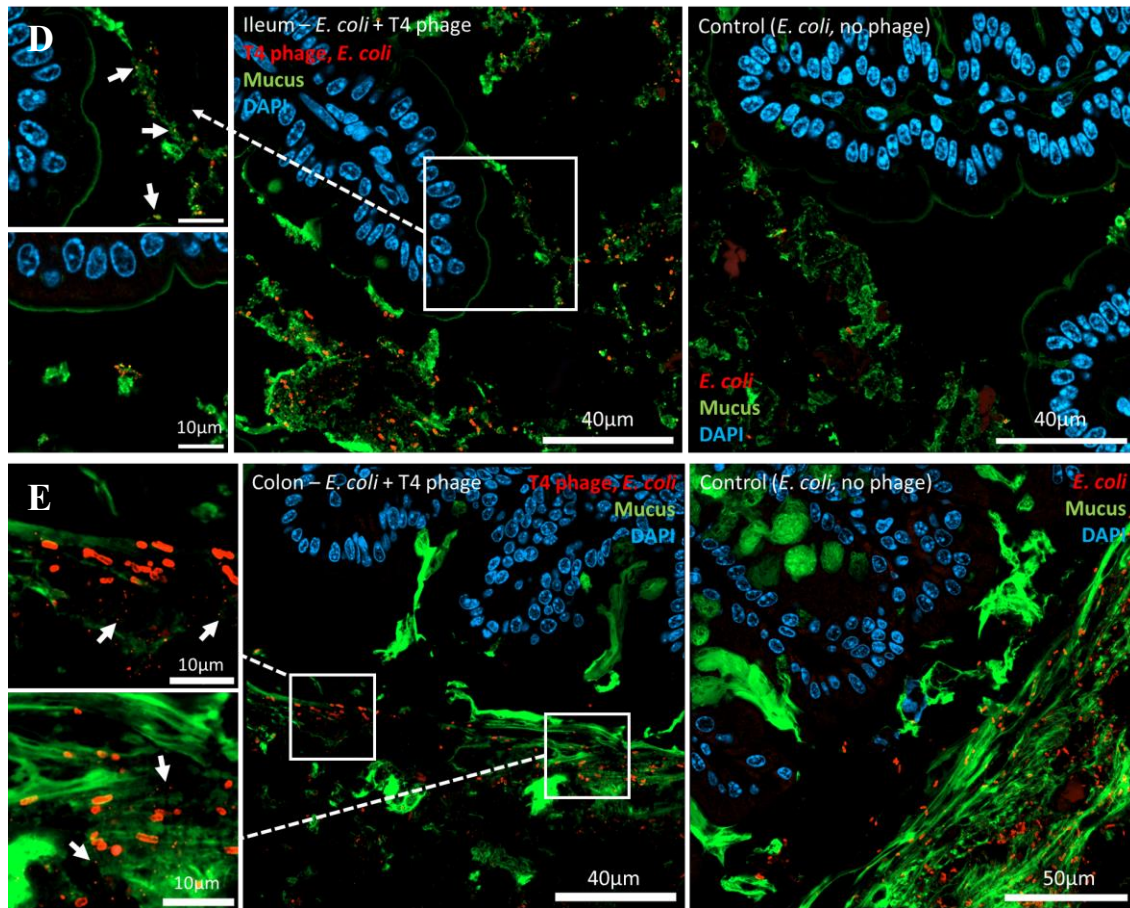


Figure 3.1 T4 phages appear to localise to the ileum (distal SI) and colon more densely than in the duodenum and jejunum. (A) Experimental schematic - GF mice were inoculated with *E. coli* at day 0. At day 20, mice were inoculated with T4 phage. Mice were euthanised on day 21 (24 h post-T4 phage inoculation). Representative images from mice monocolonised with *E. coli* and inoculated with T4 phage for 24 hours. (B) duodenum, (C) jejunum, (D) ileum, (E) colon. Images were taken with a Zeiss 900 LSM confocal microscope at 100X magnification. T4 phage and *E. coli* are labelled by Gp23 antibody (red). SI mucus is labelled with Wheatgerm Agglutinin (WGA) lectin and colonic mucus with *Ulex Europaeus* Agglutinin I (UEA-1), tagged with fluorescein (green). Mouse epithelial cells are labelled with DAPI (blue). Arrows highlight individual phage, which are distinct from the rod-shape of *E. coli* (also red).

3.1.2 T4 phage cohabit with their target bacteria, *E. coli*, in the intestine of bi-colonised mice.

T4 phages infect and lyse the specific strain of *E. coli* used for mouse monocolonisation.

Therefore, I hypothesised that newly introduced intestinal WT T4 phages would outcompete the

resident *E. coli*, reducing its abundance in bi-colonised mice. To test this, monoclonised mice bred under gnotobiotic conditions were inoculated with 2×10^6 pfu of WT T4 phage by oral gavage and maintained under sterile conditions. Faecal pellets were collected every two days for 29 days and the pfu and colony forming units (cfu) of phage and bacteria, respectively, were measured by spot plating assays (**Figure 3.2 A**). In contrast to my expectations, T4 phage and *E. coli* were able to cohabitate within the mouse GI tract, without overall depletion of either organism over the course of the 29-day experiment (**Figure 3.2 B-E**). *E. coli* levels in phage-inoculated mice were maintained stably throughout the experiment, with similar fluctuations observed in both phage- and vehicle-inoculated groups (**Figure 3.2 D-E**). T4 phage levels fluctuated between $\sim 10^2$ and $\sim 10^5$ pfu/mg over the course of the experiment (**Figure 3.2 B-C**), suggesting that there were changes in *E. coli* susceptibility to phage over time, as well as changes in phage infectivity. T4 phage appeared to become extinct in one of five phage-inoculated mice by day 25 (**Figure 3.2 B-C**). This is further discussed in **Chapter 3.1.3 and 3.1.5**. Inter-mouse variation in T4 phage levels appeared unique to each mouse (**Figure 3.2 C**), and appeared to be independent of changes in *E. coli* levels (**Figure 3.2 F**), suggesting that intestinal T4 phage concentrations are not indicative of *E. coli* levels⁶³.

I theorised that decreasing the inoculation dose of T4 phage might result in delayed phage expansion and altered kinetics of both T4 phage and *E. coli* in a bi-colonised gut. To test this, *E. coli* monoclonised mice were inoculated with low T4 phages doses (2×10^2 and 2×10^4 pfu) a standard dose (2×10^6 pfu) or vehicle lysate. Phage and *E. coli* levels were measured in faecal pellets over 25 days. Interestingly, T4 phage levels in all phage-inoculated groups rapidly climbed to $10^7 - 10^8$ pfu/mg of faeces by day one post-inoculation, regardless of the starting inoculation dose (**Figure 3.2 G**). This indicated that in a new gut environment, even as few as

200 pfu of T4 phage can replicate rapidly within their bacterial host. In this setting, T4 phage likely have an upper limit on their population density, that I postulate is dependent on the maximum *E. coli* population density. *E. coli* levels remained mostly unaffected by decreased phage inoculation doses, with no discernable trend between the initial phage inoculation dose and the following *E. coli* abundance in faecal pellets (**Figure 3.2 H**). Overall, these data indicate that WT T4 phage and *E. coli* can coexist within the GIT of bi-colonised mice, without a significant reduction of either population. This also provided a framework for future experiments studying the impact of phage-bacteria dynamics on the murine host.

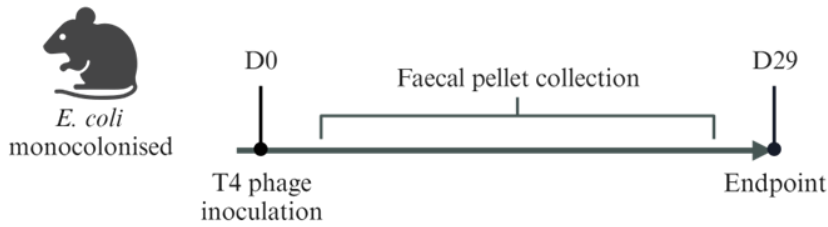
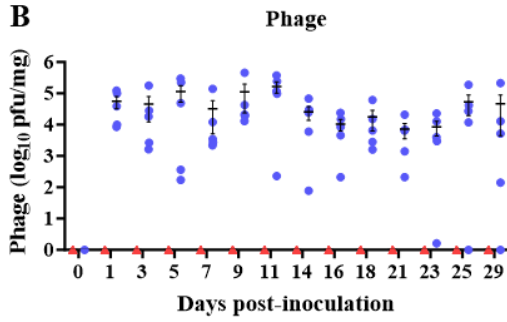
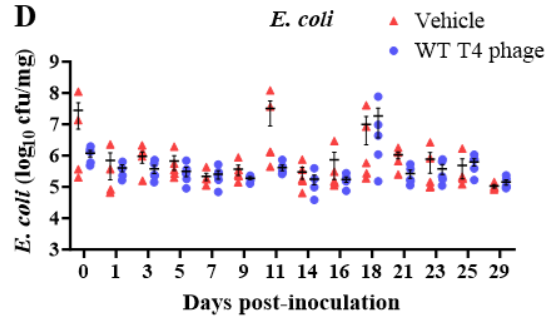
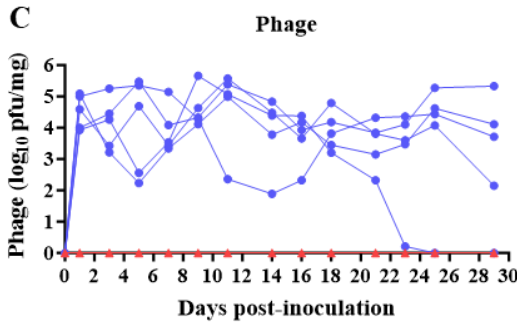
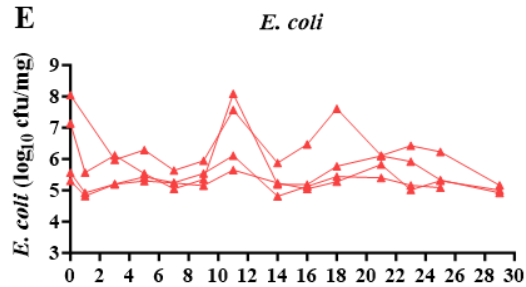
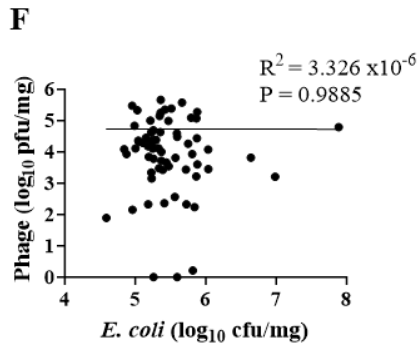
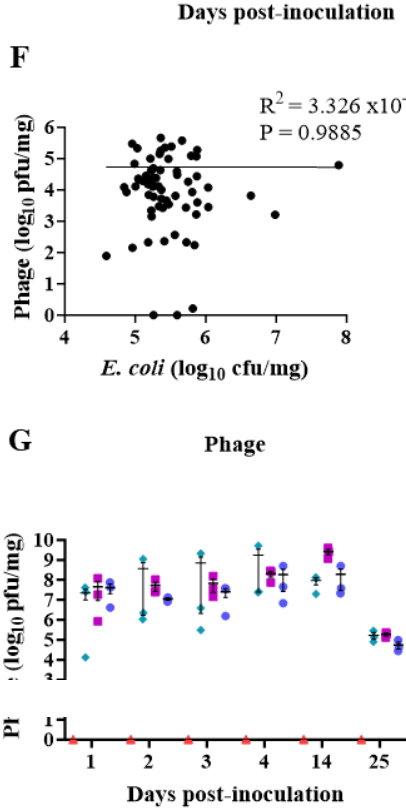
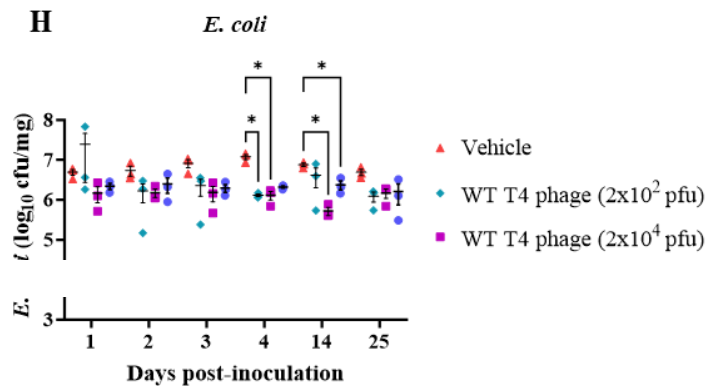
A**B****D****C****E****F****G****H**

Figure 3.2 T4 phage and *E. coli* levels in faecal pellets of C57BL/6 *E. coli* monocolonised mice, over 29 days post- WT T4 phage inoculation by oral gavage. (A) Experimental schematic – *E. coli* monocolonised mice were inoculated with T4 phage at day 0. Faecal pellets were collected every two days up until day 29, when mice were euthanised. (B) T4 phage levels over 29 days post-phage or vehicle inoculation. (C) Phage levels in individual mice inoculated with WT T4 phage. (D) *E. coli* levels up to 29 days-post phage or vehicle inoculation. (E) *E. coli* levels in individual mice inoculated with vehicle or WT T4 phage. (F) Correlation between T4 phage and *E. coli* measured in all mice from all timepoints, excluding day 0. R^2 represents the coefficient of determination (goodness of fit). (G-H) *E. coli* monocolonised C57BL/6 mice were inoculated by oral gavage with different doses of T4 phage (2×10^2 , 2×10^4 , 2×10^6 pfu per mouse) or vehicle. (G) T4 phage levels over 25 days post-phage inoculation. (H) *E. coli* levels over 25 days post-phage inoculation. Statistics calculated by 2way repeated measures ANOVA with Tukey's multiple comparisons. Error bars represent mean \pm standard error of the mean (SEM). * $p < 0.05$, ** $p < 0.01$, *** $p < 0.001$.

3.1.3 Inter-mouse variation in T4 phage colonisation is evident post-inoculation.

Variation in T4 phage and *E. coli* levels were observed between individual mice, representing a unique series of interactions occurring within each mouse GI tract. In the experiments discussed in **Chapter 3.1.2**, one T4 phage inoculated mouse showed decreased levels of viable faecal and caecal T4 phage towards the end of the experiment, as measured by plaque assay. Complete loss of viable phage was observed in this mouse by day 25 post-inoculation (**Figure 3.2 B-C** and **Figure 3.3 A, arrow**). I theorised that phage DNA would not be detected by qPCR if T4 phages were truly lost from this mouse. However, T4 phage was detected in the caecal contents of this mouse, albeit at an order of magnitude lower than measured in the remaining T4 phage-inoculated mice (**Figure 3.3 B, arrow**). To confirm the specific amplification of T4 phage, PCR products were run on a gel and detected at the correct product length (96 bp) (**Figure 3.3 C**). These data indicated that the T4 phages in this mouse, while present, may not have been viable and therefore were unable to infect the ancestral bacterial host used in plaque assays. It is also possible that the phage present in this mouse was viable but had evolved within the murine intestine such that it is no longer capable of infecting

the ancestral strain of *E. coli*. Future studies will be required to determine the genetic diversity between ancestral and evolved *E. coli* in these experiments.

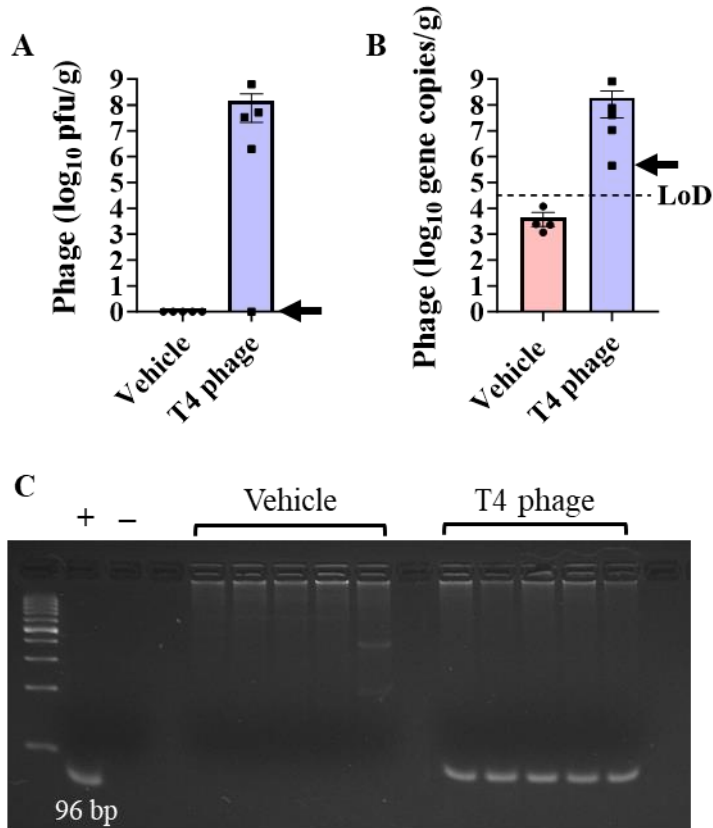


Figure 3.3 T4 phage unable to be detected in mouse caecal contents by plaque assay was detected by qPCR. *E. coli* monoclonised mice orally inoculated with T4 phage or vehicle were euthanised 29 days post-inoculation. (A) T4 phage was measured in caecal contents of mice by spot plating (plaque assay). Viable phage could not be detected in one of five mice. (B) T4 phage gene copies were detected by qPCR in all mice inoculated with T4 phage. (C) DNA gel electrophoresis of caecal contents of qPCR products. T4 phage PCR products (96 bp band) were detected in T4 phage-inoculated caecal contents, and not vehicle-treated caecal contents. Error bars represent mean and SEM. LoD = Limit of detection.

3.1.4 The T4 phage Hoc protein may be required for T4 phage habitation of the bi-colonised mouse intestine.

Δ Hoc T4 phages, lacking Hoc proteins, have decreased ability to be maintained in a gut-on-a-chip system with mucus-producing cell lines, resulting in abrogated *E. coli* killing^{35,37}. Therefore, I predicted that Δ Hoc T4 phages would transiently colonise the mouse GIT before being lost from the microbiota due to their inability to adhere to intestinal mucus. To test this, *E. coli* monocolonised mice were inoculated with 2×10^6 pfu of WT or Δ Hoc T4 phage, or a vehicle control, and phage and *E. coli* abundance were measured daily (**Figure 3.4 A**). In initial experiments, phage levels in Δ Hoc-inoculated mice peaked at $\sim 5 \times 10^3$ pfu/mg of faeces at one day post-inoculation, compared to WT T4 phage levels, which peaked at $\sim 4 \times 10^6$ pfu/mg of faeces at day 5 (**Figure 3.4 B-C**). Over the course of the experiment, Δ Hoc levels decreased gradually, and were significantly lower than WT T4 phage levels by day four post-inoculation (**Figure 3.4 B-C**). By day 9, Δ Hoc phages were no longer able to be detected by plaque assays (**Figure 3.4 B-C**) or by PCR (**Appendix B**) in all mice. *E. coli* levels remained stable across all groups, with no significant differences seen between groups following phage or vehicle inoculation (**Figure 3.4 D-E**). Together, these experiments indicated that Δ Hoc phages were unable to colonise the gut of *E. coli* monocolonised mice long-term, which supports *in vitro* data indicating that Hoc proteins are necessary for intestinal mucus adhesion and resistance to peristalsis.

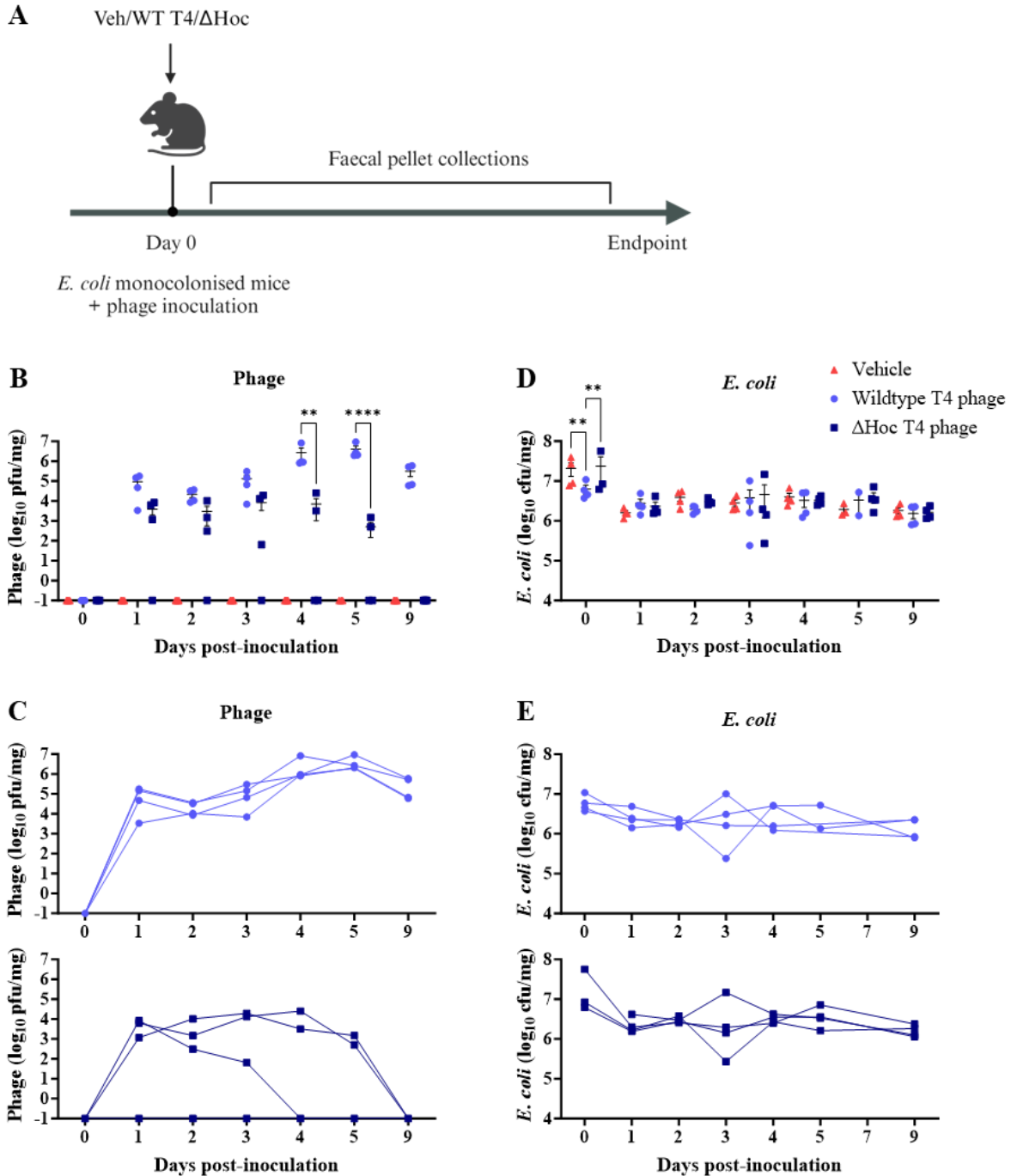


Figure 3.4 First trial – Δ Hoc T4 phage and *E. coli* levels in bi-colonised mice following inoculation with WT or Δ Hoc T4 phage. (A) Experimental schematic: *E. coli* monocolonised mice were inoculated with 2×10^6 pfu of WT or Δ Hoc T4 phage. Phage and *E. coli* levels in faecal pellets were measured daily. (B) T4 phage levels in faecal pellets over the course of the first nine-day experiment. Each point represents one mouse. (C) Phage levels in individual mice. (D) *E. coli* levels in faecal pellets over the course of the first experiment. Each point represents one mouse. (E) *E. coli* levels in individual mice. Statistics calculated by RM Mixed-effects

model with Holm-Šídák's multiple comparisons. * $p < 0.05$, ** $p < 0.01$, *** $p < 0.001$, **** $p < 0.0001$. Error bars represent mean \pm SEM.

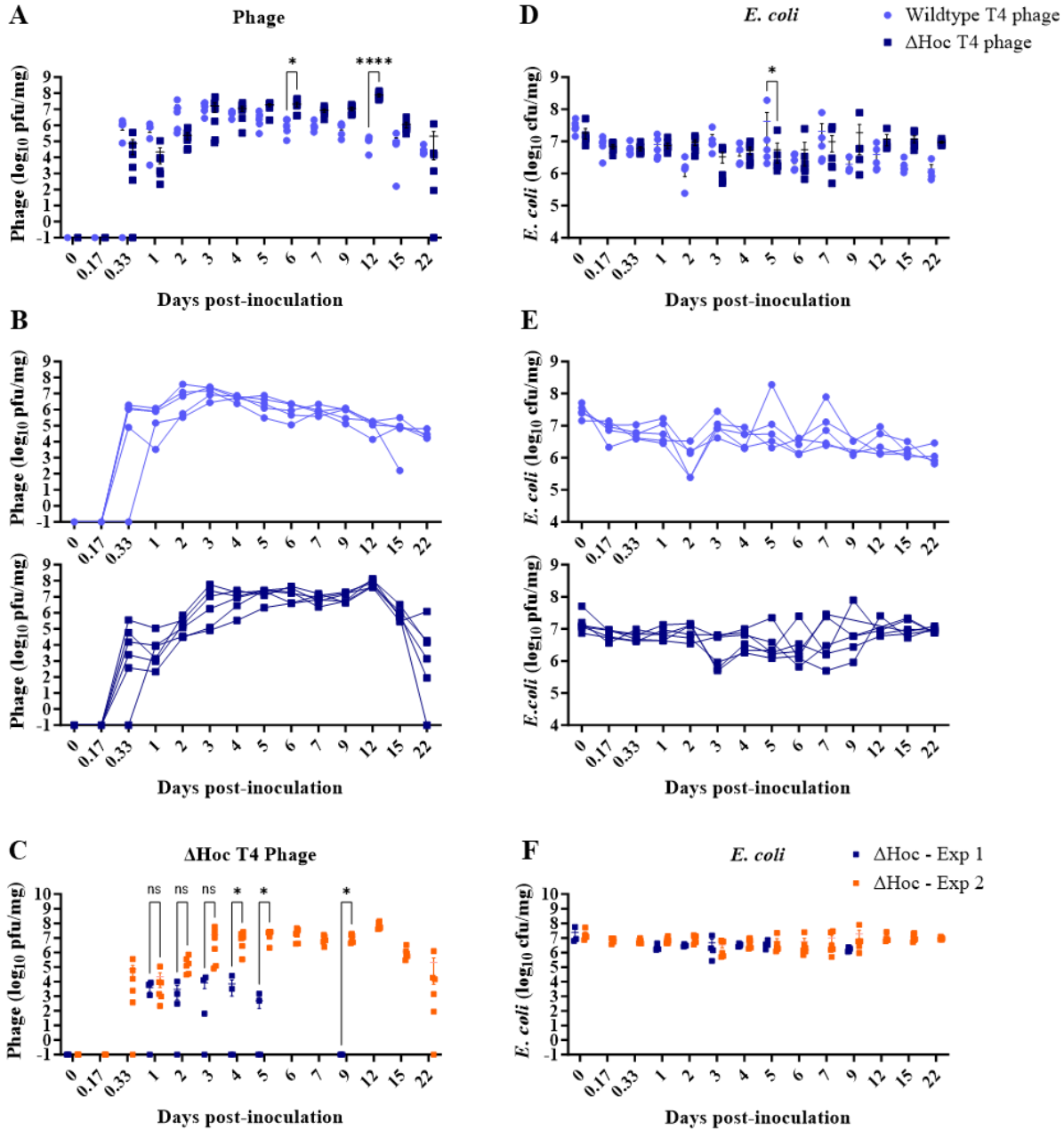


Figure 3.5 Second trial - ΔHoc T4 phage and *E. coli* levels in bi-colonised mice following inoculation with WT or ΔHoc T4 phage. (A) T4 phage levels in faecal pellets over the course of 22 days in the second experiment. Each point represents one mouse. (B) Phage levels in individual mice. (C) *E. coli* levels in faecal pellets over the course of the first experiment. Each point represents one mouse. (D) *E. coli* levels in individual mice. (E) Comparison of ΔHoc T4

phage levels in mice inoculated with Δ Hoc phage in both experimental trials. (F) Comparison of *E. coli* levels in mice inoculated with Δ Hoc phage in both experimental trials. (A-B, D-E) Statistics calculated using a RM Mixed-effects model with Šídák's multiple comparisons. (C & F) Statistics calculated by multiple unpaired t-tests with Welch correction and Holm-Šídák's multiple comparisons. Ns $p > 0.05$, * $p < 0.05$, ** $p < 0.01$, *** $p < 0.001$, **** $p < 0.0001$. Error bars represent mean \pm SEM.

The conclusions of this first experiment need to be interpreted with caution. In a repeat experiment, a notable difference in the kinetics of Δ Hoc T4 phage within *E. coli* monocolonised mice was apparent. This experiment was repeated with WT T4 phage inoculated mice serving as the control. In contrast to the first iteration of this experiment, Δ Hoc T4 phages were detected at similar or greater levels as WT T4 phage until day 22 post-inoculation (**Figure 3.5 A**). At day 22, Δ Hoc T4 phage levels appeared to decrease and were undetectable by plaque assay in one of six mice (**Figure 3.5 A-B**). Importantly, Δ Hoc T4 phage levels were significantly different between the first and second experiments from day 4 onwards (**Figure 3.5 C**), indicating that Δ Hoc T4 phage kinetics significantly differed between trials. Additionally, *E. coli* levels in Δ Hoc phage-inoculated mice were stable over the duration of both experiments (**Figure 3.5 D-F**), indicating that differences in phage kinetics does not drastically alter *E. coli* levels in faecal pellets.

Altogether, these results indicated that phage colonization may be sensitive to initial intestinal conditions and stochasticity. While the results of the first experiment suggested that Δ Hoc T4 phages are not maintained in the GIT of *E. coli* monocolonised mice (**Figure 3.4 A-B**), the second experiment demonstrated long-term Δ Hoc T4 phage colonization. These data would then indicate that mucus adherence is not essential for phage retention in the gut. It is possible that the stochastic coevolution between T4 phage and *E. coli* lead to differing results between

trials. To clarify this, future studies should investigate the metagenomic differences between Δ Hoc phages in each trial. In addition, studies should aim to determine whether the differences in colonisation ability by Δ Hoc can be accounted for by differences in animal cage changing schedules, due to coprophagia: the tendency of mice to consume faeces.

3.1.5 T4 phage can be transferred between mice by co-housing

The observation that Δ Hoc T4 phage was not maintained stably in the guts of bi-colonised mice in the first trial (**Chapter 3.1.4 – Figure 3.4 C-D**) suggested that mice were not able to be re-colonised by coprophagia. To test this, *E. coli* monocolonised, phage-naïve mice (never colonised with phage) were co-housed with WT T4 phage and *E. coli* bi-colonised (donor) mice inoculated with phage 21 days prior. After 7 days of co-housing, faecal pellets were collected from mice and T4 phage and *E. coli* levels were measured (**Figure 3.6 A**). After 7 days, T4 phages were detected in co-housed mice, and colonised to similar levels (within an order of magnitude) as T4 phage-inoculated (donor) mice (**Figure 3.6 B**). This indicated that WT T4 phages were able to be transferred from inoculated to co-housed mice by coprophagia (**Figure 3.6 B**). *E. coli* levels were unchanged in T4 phage inoculated mice over 7 days but decreased in co-housed mice from baseline levels four-fold (within an order of magnitude), which was likely due to initial fluctuations in *E. coli* abundance by T4 phage introduction (**Figure 3.6 C**). Together, these data suggest that T4 phages can be transferred between co-housed mice by coprophagy or other means. With regards to the experiments in **Chapter 3.1.4**,

these data suggest that the Δ Hoc T4 phage lost from orally inoculated mice were no longer viable and had degraded, as Δ Hoc T4 phage could be detected neither by plaque assay nor qPCR.

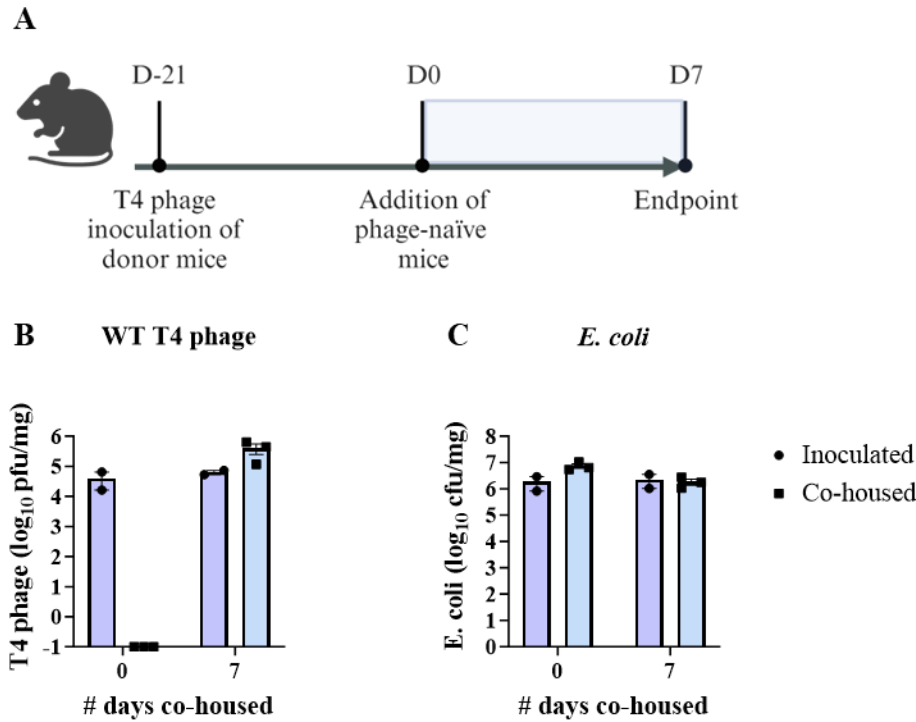


Figure 3.6 Co-housing of *E. coli* monocolonised, phage-naïve mice with WT T4 phage-inoculated mice. (A) Experimental Schematic: Phage-naïve female mice ($n = 3$) were co-housed with WT T4 phage-inoculated mice ($n = 2$). Phage and *E. coli* levels were measured after 7 days of co-housing. (B) WT T4 phage levels measured in faecal pellets at days 0 and 7 of co-housing. (C) *E. coli* levels measured in faecal pellets at days 0 and 7 of co-housing. Each point represents one mouse. Bars represent mean \pm SEM.

Collectively, the results presented in this section indicate that WT T4 phage can stably colonise the intestines of *E. coli* monocolonised mice with minimal impact on bacterial abundance.

Although WT T4 phage appeared visually to localise within mucus layers in the SI and colon, T4 phage colonisation could not be conclusively attributed to the presence of a functional Hoc protein and mucus-adhesion properties. Differing results between experimental repeats indicate

that evolutionary pressures in the gut environment leads to stochastic behaviour of T4 phage.

However, further studies are needed to fully elucidate the behaviour of Δ Hoc T4 phage *in vivo*.

3.2 T4 Phages introduced to the intestine of *E. coli* monocolonised mice induce a weak, Th1 skewing immune response

Gut microbes are essential for the process of digestion, allowing for the extraction of nutrients and metabolites, which in turn play a role in gut health and homeostasis¹⁷. Our gut commensal bacteria are also important for GIT and immune development, as exemplified by numerous studies in GF and gnotobiotic mouse models⁴⁸. It has been previously demonstrated that phages can be detected by PRRs within the endocytic vesicles of DCs and macrophages, resulting in downstream signalling, cytokine production and T cell activation^{18,45,46}. However, little is known about where these interactions occur. Here, I aimed to characterise the immune response to gut colonising T4 phage in bi-colonised mice, in the absence of other microorganisms.

3.2.1 T4 phage do not translocate across the intestinal epithelium of bi-colonised mice *in vivo*.

Previous studies have indicated that T4 phages are able to translocate across intestinal epithelial cells by macropinocytosis *in vitro*^{43,44}. However, it is unknown whether T4 phages interact with intestinal epithelial cells *in vivo*, or whether phages interact with the immune system in the intestinal lumen or in the mucosal tissues. Therefore, I sought to determine whether T4 phages translocate across the intestinal epithelium *in vivo*. To test this, *E. coli* monocolonised mice were orally inoculated with WT T4 phage and were euthanised after 1, 3, 7, 14 or 29 days. T4 Phage and *E. coli* levels were measured in homogenised mLN, spleens and livers, and in serum (**Figure 3.7 A**). In contrast to *in vitro* findings, viable T4 phages were not detected consistently in the liver, spleen, mLN or serum of T4 phage-inoculated mice (**Figure 3.7 B-E**). T4 phages were detected in one of four mice in the liver and spleen, at 27 pfu/mg and 264

pfu/mg, respectively (**Figure 3.7 B-C**). However, in the livers and spleens, no viable phage was detected in three out of four mice. Viable T4 phage was not detected in the mLNs or sera of any mice across all time points (**Figure 3.7 D-E**). Together this suggests that if viable phages interact with the murine immune system, it likely occurs within the intestinal lumen. *E. coli* levels were also measured in the tissues (**Appendix C**) however, a consistent phenotype could not be established. To further explore the mechanism behind phage interaction with the metazoan host, qPCR should be performed to detect DNA of inactivated T4 phages in the mLNs, spleen and liver, as engulfed phages may be degraded by phagocytic cells.

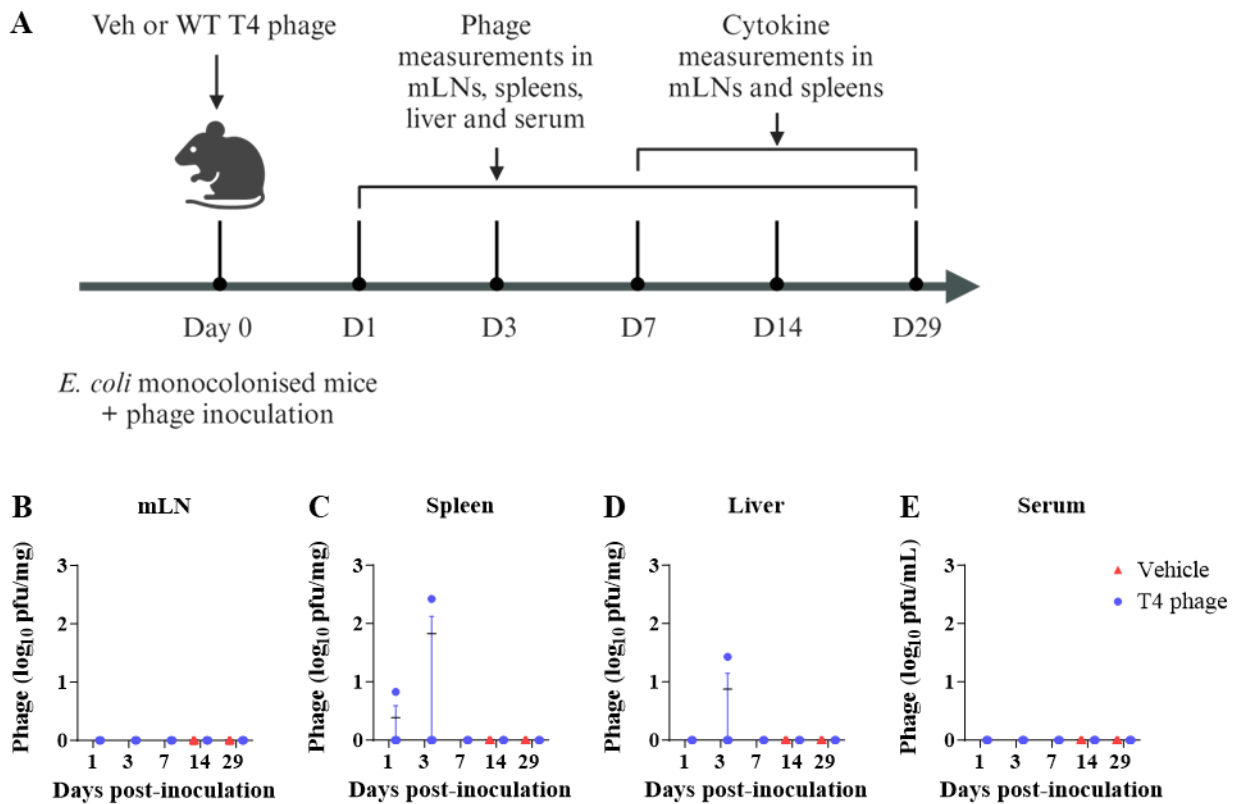


Figure 3.7 T4 phage were unable to translocate across the intestinal epithelium after inoculation into *E. coli* monoclonised mice. (A) Experimental schematic - *E. coli* monoclonised mice were inoculated with T4 phage or vehicle at day 0. Mice were euthanised at each time point and viable phage were measured in tissues and serum. (B) Phage levels in liver

tissue. (C) Phage levels in spleen tissue. (D) Phage levels in MLN tissue. (E) Phage levels in Serum. Error bars represent mean \pm SEM.

3.2.2 T4 phage inoculation of *E. coli* monocolonised mice leads to local increases in pro-inflammatory cytokine production

Since viable T4 phages did not appear to translocate across the intestinal epithelium in bi-colonised mice, I investigated whether luminal T4 phage impacted the production of antiviral cytokines locally in the gut-draining mLNs or in the spleen, the site of systemic immune surveillance. Previous work has shown that phages are capable of signalling via TLRs^{18,45}, similarly to eukaryotic viruses. Therefore, to investigate the changes in cytokine production, *E. coli* monocolonised mice were orally inoculated with T4 phage or vehicle, and mLNs and spleens were harvested at days 7, 14 and 29 post-inoculation (**Figure 3.7 A**). Cytokines were measured using a multianalyte flow assay kit (BioLegend), which assayed for a panel of 13 mouse antiviral cytokines (**Table 2.4**). Compared with vehicle controls, a significant increase in interleukin (IL)-12 levels was observed locally in the mLNs of T4 phage-inoculated mice at day 29, but not in the spleen (**Figure 3.8 A**). IL-12 is an immunoregulatory cytokine produced mainly by antigen presenting cells (APCs) and epithelial cells during the early stages of viral infection. IL-12 signalling can result in the activation of natural killer (NK) cells and differentiation of CD4⁺ Th1 cells⁸⁰. A local increase in Th1 cells represents a type-I inflammatory immune response, that is typically associated with viral infections⁸¹. The observed IL-12 increase at a late time point indicates either an intestinal event at late stages of this experiment, resulting in immune activation, or that IL-12 levels were increased in the gut-associated tissues but not the mLN at early time points. Indicative of early innate immune

activation, increases in the proinflammatory cytokine IL-1 β were detected in the mLNs at day 7 post-inoculation (**Figure 3.8 B**). Increased levels of IL-1 β suggests priming of phagocytic cells and potential inflammasome activation and subsequent promotion of inflammation leading to viral/bacterial clearance⁸². IL-1 β supports leukocyte migration to infection sites, and therefore may be detected at higher levels in the GALT and lamina propria than I observed in the mLN. In support of previous findings, I observed increases in the proinflammatory cytokines Tumour Necrosis Factor α (TNF α)⁴⁵ (**Figure 3.8 C**) and IFN γ ¹⁸ (**Figure 3.8 D**) locally in the mLNs of bi-colonised mice at days 7 and 29. IFN γ production supports my assertion of NK and Th1 cell activation due to elevated IL-12 levels in response to T4 phage colonisation of the gut. Both NK and Th1 cells produce IFN γ , and in turn promote macrophage activation and pathogen clearance⁸⁰.

A small but significant increase in the levels of the anti-inflammatory cytokine IL-10 was observed in the mLN at day 29 (**Figure 3.8 E**). Among other cells, IL-10 can be produced by regulatory T cells (Tregs), which may indicate induction of an immunotolerant response to mitigate phage-induced inflammation in these mice. Notably, IL-10 levels were elevated in only two of five phage-inoculated mice, but were elevated in concert with IL-12, signifying dampening of type-1 inflammation. Finally, increases in IFN α were observed in the mLN at 29 days post-inoculation with T4 phage (**Figure 3.8 F**). This was unexpected, as typically type I IFNs are produced by phagocytes at the early stages of infection. However, Sweere et al. (2019) determined that type I IFN production by dendritic cells (DCs) can be induced by TLR3 signalling by an ssDNA phage⁴⁵. Although a significant increase in IFN α levels were detected in the spleen at day 7, a ~0.25 (pg/mL)/mg increase from vehicle controls was determined not to be biologically relevant (**Figure 3.8 F**). No other significant differences were detected in the other

cytokines and chemokines investigated (**Appendix D**). Taken together, these results point towards type-1 immune response to the continual presence of T4 phage within the intestine and indicate elevation of pro-inflammatory cytokines. Although Th1-skewing cytokines were detected at late experimental time points, we cannot rule out phage-induced innate immune responses and Th1 cell activation. It is worth mentioning that in this experiment, T4 phage inoculation was well tolerated by mice and no clinical signs of disease were observed. Therefore, it is uncertain whether an “infection” event occurs early on in phage colonisation. Together this suggests that phages may play roles in immune system priming and development, similar to gut commensal bacteria. Additionally, these results indicate that phages are likely inactivated upon interaction with phagocytic cells, which may explain our inability to detect viable phage in the mLNs, spleen, liver, and serum. It remains to be determined whether Th1 cell responses are caused directly by phage, or indirectly through phage lysis of their target bacteria in the gut.

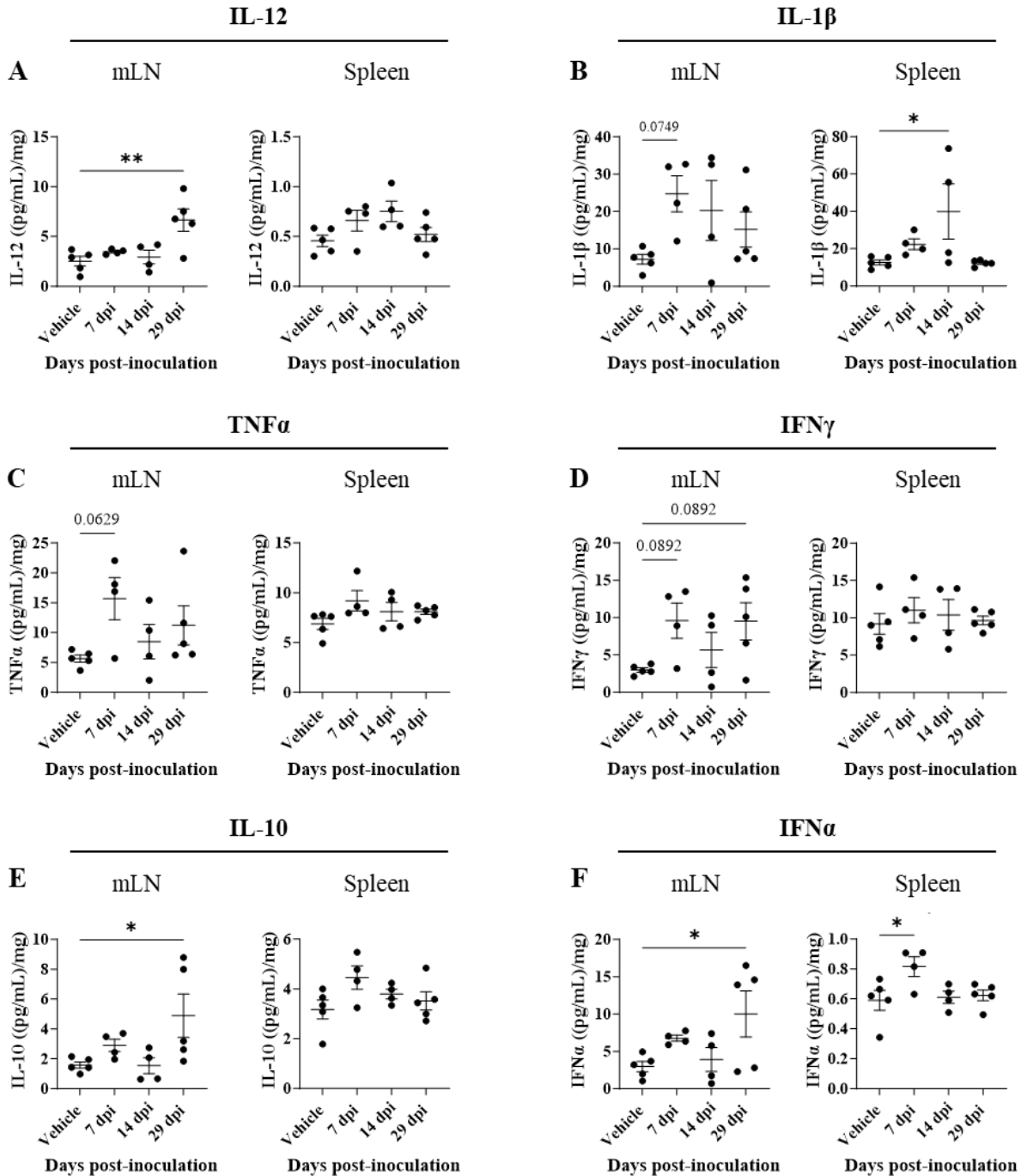


Figure 3.8 Oral inoculation of T4 phage into *E. coli* monocolonised mice resulted in modest but significant increases in cytokine levels in the MLN and spleen. T4 phage-inoculated mice were euthanised at days 7, 14 and 29 and a panel of 13 cytokines were measured in the MLN and spleen by cytokine bead array. Vehicle mice were euthanised at day 29. For each mouse, cytokine levels were measured in the MLN and spleen and concentrations were calculated by extrapolation to a standard curve. Concentrations were normalised to the tissue weight. (A) IL-12. (B) IL-1 β . (C) TNF α . (D) IFN γ . (E) IL-10. (F) IFN α . Each point represents an individual

mouse. Statistics were calculated by ordinary one-way ANOVA with Holm-Šidák's multiple comparisons between each time point and the vehicle control. Error bars represent the mean and SEM. Ns $p > 0.05$, * $p < 0.05$, ** $p < 0.01$.

3.2.3 T4 phage inoculation of *E. coli* monocolonised mice leads to elevated numbers of activated CD4+ Th1 cells and CD8+ T cells in the mLN

To further explore the role of the adaptive immune system in response to intestinal T4 phage, I investigated the adaptive immune cell subsets present in secondary lymphoid organs, namely the mLN and spleen. Briefly, *E. coli* monocolonised mice were inoculated with T4 phage, Murine Norovirus (MNV) CW3 or vehicle control. MNV CW3 was used as a positive control for an intestinal infection⁸³⁻⁸⁵. Eight days following inoculation mice were euthanised and cells were isolated from the mLN and spleen. Isolated cells were permeabilized and immunostained (see **Table 2.2** for antibody panels). Cell markers of interest were detected by flow cytometry and specific populations were gated using the strategy shown in **Appendix E**. Since an increase in the levels of pro-inflammatory cytokines (namely IL-12, TNF α and IFN γ) were detected in the mLNs of T4 phage-inoculated mice (**Figure 3.8 A, C, D**), I aimed to determine whether this was related to an expansion of lymphocytes in secondary lymphoid organs. Compared with the vehicle group, T4 phage inoculation resulted in a non-significant but trending increase in the number of B cells in the mLNs, but not the spleens (**Figure 3.9 A-D**). While also not significant, an increase in the number of CD4+ T cells was observed in the mLN (**Figure 3.9 E-F**). These increases were not observed in the spleens (**Figure 3.9 G-H**). A similar increase in the number of CD8+ T cells was also observed in the mLNs (**Figure 3.9 I-L**). There was no apparent difference in the total number of CD45.2+ leukocytes in the mLNs and spleens between groups, confirming that observed increases in B and T cell numbers in the mLNs were

not due to overall increases in total leukocytes analysed (**Appendix F**). The observed expansion of B cells in the mLN, while small, suggests potential production of T4-phage specific antibodies. Phage-specific antibody production has been reported previously by others^{18,47,57}, and therefore should be further investigated in our models by serum and faecal Ig enzyme-linked immunosorbent assay (ELISA).

To establish whether mLN and splenic T cells were activated in response to intestinal T4 phage or MNV inoculation, levels of activated (CD44-high) CD4+ and CD8+ T cells were measured (**Figure 3.10 A-B**). A trending increase in the number of activated CD4+ T cells (**Figure 3.10 C-F**) and CD8+ T cells (hereby referred to as cytotoxic T lymphocytes, CTLs) (**Figure 3.10 G-J**) was observed in the mLNs but not the spleens of T4 phage-inoculated mice, compared with vehicle-inoculated mice. This suggested that the small increases in TNF α and IFN γ previously detected in mLNs (**Figure 3.8 C-D**) could be related to T cell activation, as effector CD4+ Th1 cells and CTLs produce these cytokines following activation. To determine whether T4 phage inoculation resulted in increased Th1 differentiation and activation, cells expressing the transcription factor Tbet, a critical regulator of Th1 fate, were detected by flow cytometry (**Figure 3.10 A**). There was a small increase in the number of activated Th1 cells in the mLNs of T4 phage and MNV-inoculated mice compared to vehicle-inoculated controls (**Figure 3.10 K-N**), suggesting that Th1 cells may be weakly activated in response to phage inoculation *in vivo*. In summary, these results indicate that T4 phage-inoculation of *E. coli* monoclonised mice facilitates modest T cell activation and expansion and promotes Th1 differentiation in mLNs.

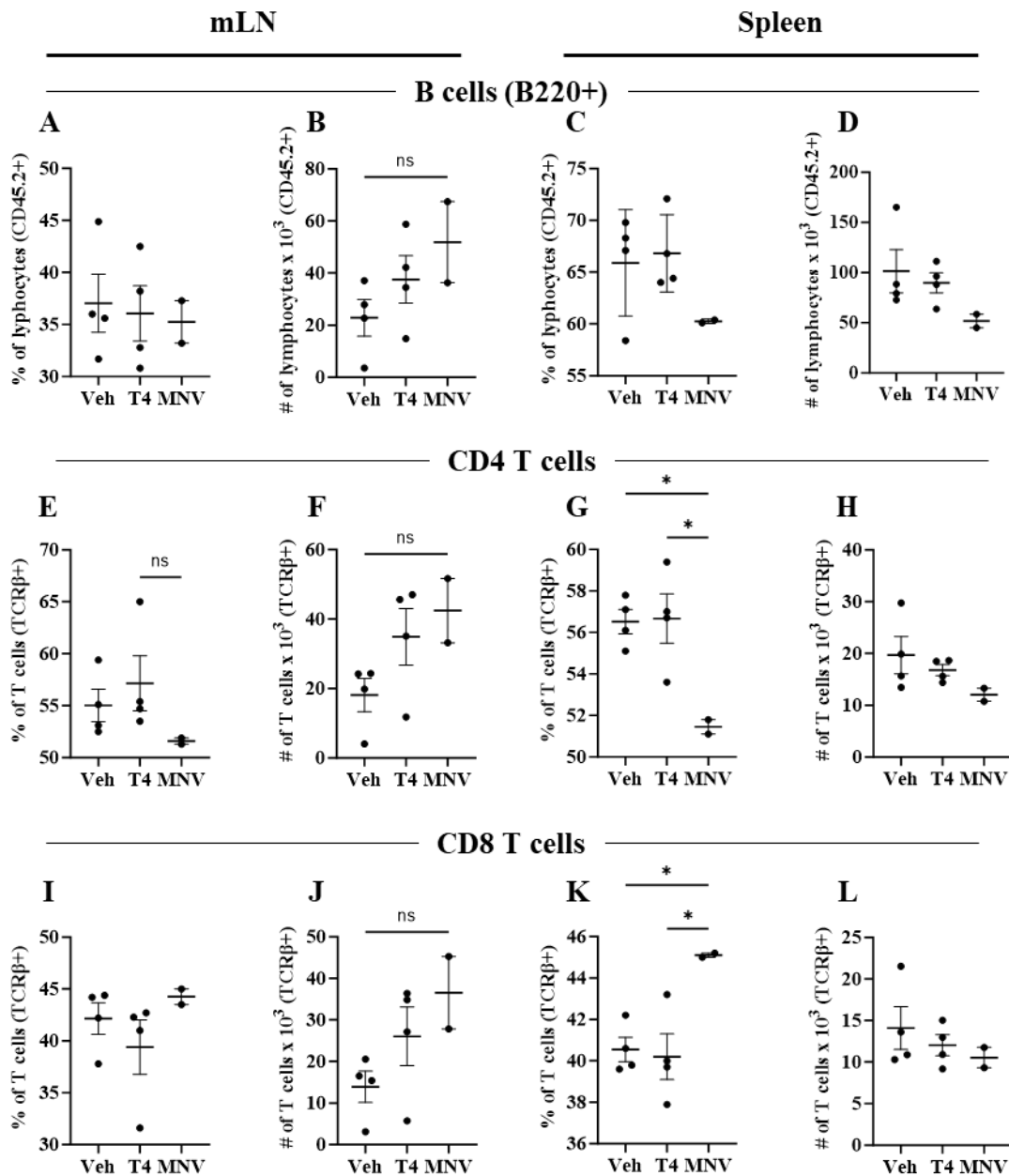


Figure 3.9 T4 phage inoculation of *E. coli* monocolonised mice leads to elevated numbers of B cells, CD4+ and CD8+ T cells in the mLN. *E. coli* monocolonised mice were inoculated by oral gavage with vehicle, T4 phage or MNV (CW3). Spleens and mLNs were harvested on day 8 post-inoculation. Cells were isolated, immunostained and detected by flow cytometry. (A-D) B cells, gated on CD45.2+ lymphocytes: (A) Proportion in mLNs. (B) Count in mLNs. (C) Proportion in spleens. (D) Count in spleens. (E-H) CD4+ T cells, gated on TCRβ+ T cells. (E) Proportion in mLNs. (F) Count in mLNs. (G) Proportion in spleens. (H) Count in spleens. (I-L) CD8+ T cells, gated on TCRβ+ T cells. (I) Proportion in mLNs. (J) Count in mLNs. (K) Proportion in spleens. (L) Count in spleens. Each point represents an individual mouse. Statistics were calculated by ordinary one-way ANOVA with Holm-Šidák's multiple. Error bars represent the mean and SEM. Ns $p > 0.05$, * $p < 0.05$.

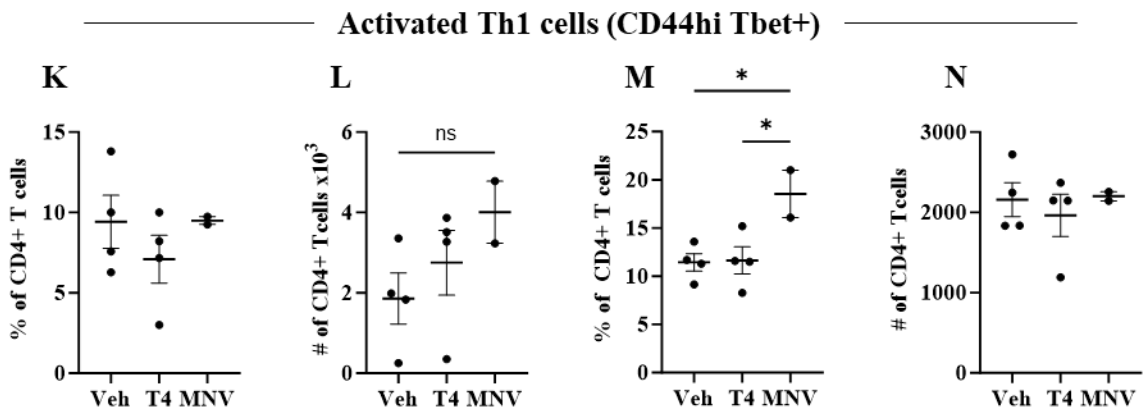
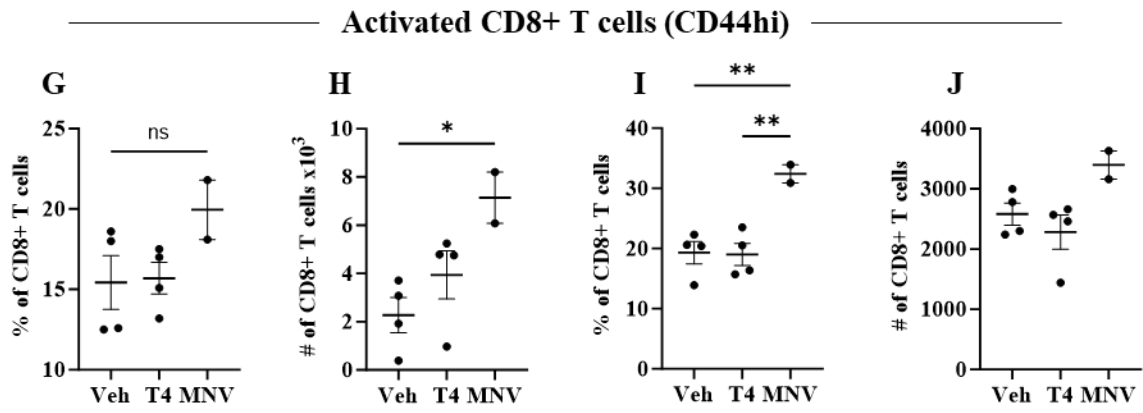
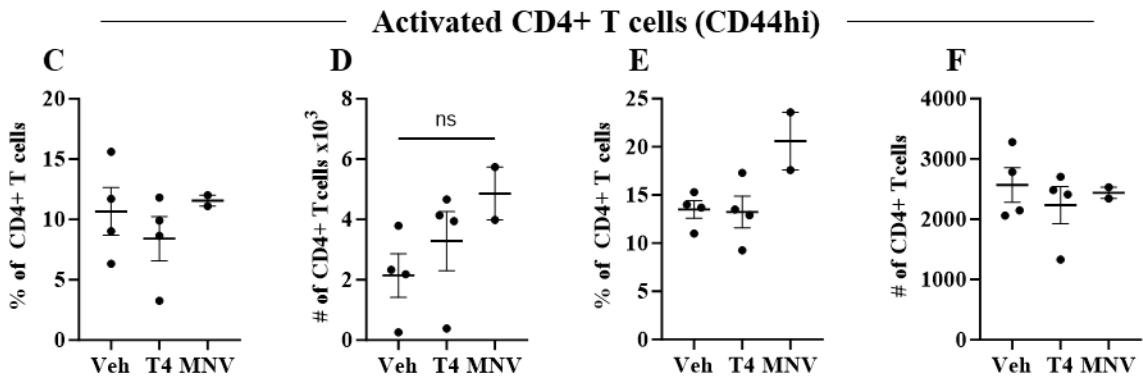
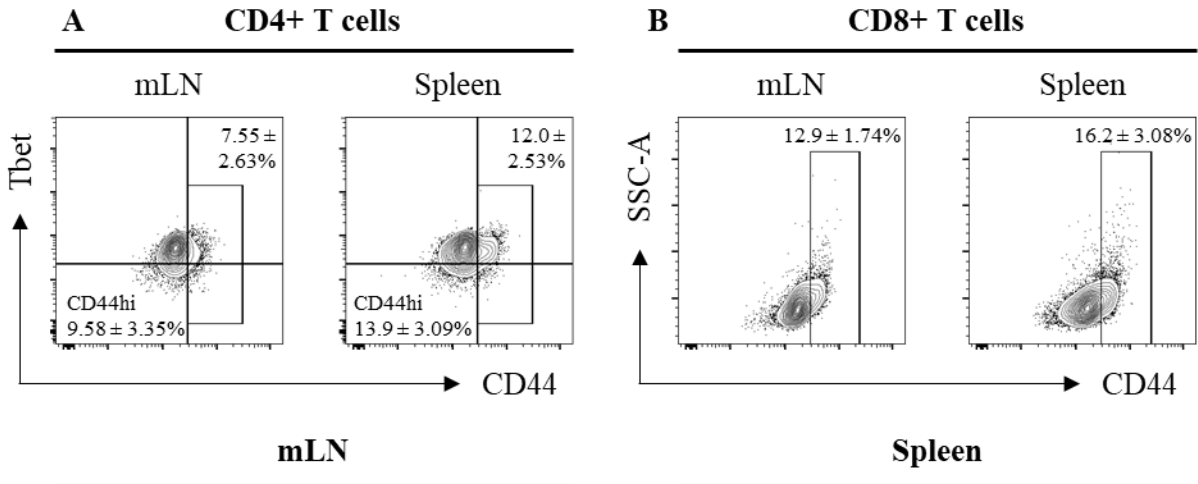


Figure 3.10 T4 phage inoculation of *E. coli* monoclonised mice leads to elevated numbers of CD4+, CD8+ and CD4+ Tbet+ Th1 cells in mLNs. *E. coli* monoclonised mice were inoculated by oral gavage with vehicle, T4 phage or MNV (CW3). Spleens and mLNs were harvested on day 8 post-inoculation. Cells were isolated, immunostained and detected by flow cytometry. (A-B) Representative gating strategies from a T4 phage inoculated mouse: (A) CD44-high, activated CD4+ T cells and CD44-high, Tbet+ Th1 cells in mLNs and spleens. (B) CD44-high, activated CD8+ T cells in mLNs and spleens. Annotations describe gated proportions \pm the standard deviation (SD). (C-F) CD44-high, activated CD4+ T cells, gated on CD4+ TCR β + T cells. (C) Proportion in mLNs. (D) Counts in mLNs. (E) Proportion in spleens. (F) Counts in spleens. (G-J) CD44-high, activated CD8+ T cells, gated on CD4+ TCR β + T cells. (G) Proportion in mLNs. (H) Counts in mLNs. (I) Proportion in spleens. (J) Counts in spleens. (K-N) CD44-high, activated, Tbet+ Th1 cells, gated on CD4+ TCR β + T cells. (K) Proportion in mLNs. (L) Counts in mLNs. (M) Proportion in spleens. (N) Counts in spleens. Each point represents an individual mouse. Statistics were calculated by ordinary one-way ANOVA with Holm-Šídák's multiple comparisons. Error bars represent the mean and SEM. Ns $p > 0.05$, * $p < 0.05$, ** $p < 0.01$.

3.2.4 T4 phage inoculation of *E. coli* monoclonised mice does not significantly increase the cytokine-production capacity of T cells within mLNs and spleens

To determine the capacity of T cells to be activated and produce proinflammatory cytokines in response to oral inoculation with T4 phage, I stimulated cells isolated from spleens and mLNs *ex vivo*. Cells isolated from mice inoculated with vehicle, T4 phage or MNV CW3 were stimulated with PMA/ionomycin/BFA to induce the production and accumulation of cytokines within lymphocytes⁸⁶. Highly activated cells were identified as CD44-high and double positive for IFN γ and TNF α (**Figure 3.11 A-B; Appendix G**). Following stimulation, neither significant nor biologically relevant differences in the proportion or number of activated, cytokine-producing CD4+ T cells were observed in the mLNs and spleens of T4 phage-inoculated mice, compared with vehicle controls (**Figure 3.11 C-F**). Similarly, activated, cytokine-producing CD8 T cells did not appear to be expanded in the mLNs or spleens of T4 phage-inoculated mice (**Figure 3.11 G-J**). These data indicate that the increased levels of TNF α and IFN γ in mLNs previously observed in this thesis (**Figure 3.8 C-D**) may not be biologically

relevant. That was observed in this thesis This is supported by my observations that, like MNV CW3 infection⁵², T4 phage inoculation of WT mice is asymptomatic and does not cause adverse events. Additionally, visible signs of inflammation such as diarrhea, intestinal shortening and secondary lymphoid organ enlargement were absent in inoculated mice. Therefore, I theorise that phages may play a role in T cell priming due to the observed expansion of activated T and B cells, but absence of inflammatory cytokines⁵². These data also support my assertions that increases in the levels of IL-12 in the mLN in response to T4 phage inoculation (**Figure 3.8 A**) supports Th1 differentiation (**Figure 3.10 L**). However, it remains to be determined whether phage-inoculation results in effector T cell homing to the intestine.

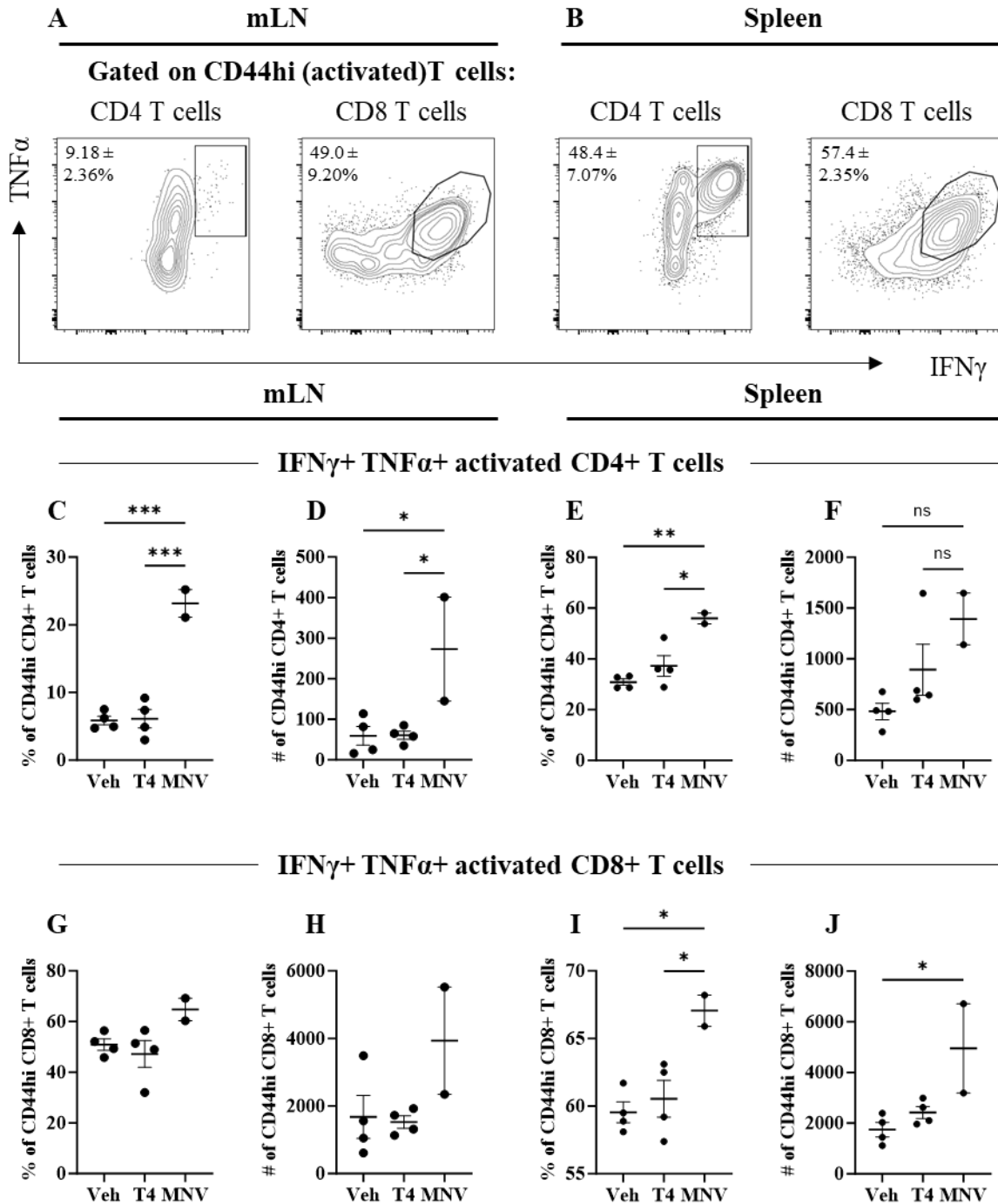


Figure 3.11 T4 phage inoculation of *E. coli* monocolonised mice leads to small, non-significant increases in proportions and numbers of IFN γ and TNF α producing CD4+ T cells upon *in vitro* stimulation. *E. coli* monocolonised mice were inoculated with vehicle, T4 phage or MNV (CW3) and spleens and mLNs were harvested on day 8 post-inoculation. Cells were isolated and stimulated with PMA/ionomycin for four hours at 37°C, 5% CO₂. Export of

cytokines from the Golgi was blocked with Brefeldin A (BFA). Cells were permeabilised, immunostained and detected by flow cytometry. Annotations describe gated proportions \pm SD. (A-B) Representative gating strategies from a T4 phage inoculated mouse, gated on CD44-high, activated CD4⁺ and CD8⁺ T cells. (A) IFN γ ⁺ TNF α ⁺ T cells in mLNs. (B) IFN γ ⁺ TNF α ⁺ T cells in spleens. (C-F) Activated IFN γ ⁺ TNF α ⁺ CD4⁺ T cells, gated on CD44⁺, CD4⁺, TCR β ⁺ T cells. (C) Proportion in mLNs. (D) Counts in mLNs. (E) Proportion in spleens. (F) Counts in spleens. (G-J) Activated IFN γ ⁺ TNF α ⁺ CD8⁺ T cells, gated on CD44⁺, CD8⁺, TCR β ⁺ T cells. (G) Proportion in mLNs. (H) Counts in mLNs. (I) Proportion in spleens. (J) Counts in spleens. Each point represents an individual mouse. Statistics were calculated by ordinary one-way ANOVA with Holm-Šídák's multiple comparisons. Error bars represent the mean and SEM. Ns $p > 0.05$, * $p < 0.05$, ** $p < 0.01$, *** $p < 0.001$.

Chapter 4: Discussion

4.1 Discussion

In this study, I aimed to understand the influence of T4 phage on its target bacterium, *E. coli*, and the murine immune system in a bi-colonised gnotobiotic mouse model. The use of bi-colonised mice was crucial to this work as it allowed for the isolation of T4 phage-specific effects in the absence of noise from other phage-bacteria interactions. Using this model, I learned that T4 phage can stably colonise the murine GIT without depleting the *E. coli* population. These effects occurred independently of the phage inoculation dose, indicating that T4 phages replicate rapidly upon introduction to the gut, reaching their maximum abundance within 24 hours. Together, these findings suggest the development of a heterogeneous population of *E. coli* within this model, likely with both phage-susceptible and -resistant populations present. In direct contrast, previous studies using T4 phage-*E. coli* (K-12) bi-colonised mice observed that T4 phage could not be detected in the faeces of mice one day following inoculation⁸⁷. *E. coli* monocolonisation by gavage at the onset of phage inoculation may be responsible for the observed differences in phage colonisation, since the intestinal mucosa of GF mice is not fully formed^{29,49}. Interestingly, Weiss et al. (2009) found that T7 phage could co-exist with *E. coli* in this model and reported that the majority of *E. coli* (80%) remained susceptible to T7 infection⁸⁷. It was speculated that *E. coli* were protected from T7 predation by spatial niches in the gut⁸⁷. However, in my study I was unable to determine discrete niches occupied by *E. coli* or T4 phage sub-populations. Future studies using a combination of fluorescence imaging of mouse intestinal sections and cell-quantification tools will be important for further our understanding of phage-bacterial spatial localisation within the gut.

Importantly, fluctuations of approximately three orders of magnitude in phage and bacteria levels were observed throughout experiments (**Figure 3.2 B-E**). I expected that phage levels would correspond to the abundance of their target bacteria; however, changes in T4 phage and *E. coli* abundance seemed to occur independently of each other (**Figure 3.2 F**). In one phage-inoculated mouse, T4 phage DNA was detected despite the absence of viable phage plaques (**Figure 3.3 A-B**). I speculated that the phage in this mouse had evolved to the extent that it was no longer able to infect the ancestral strain of *E. coli* used for plaque assays. I have also considered that these phages may have become pseudolysogenic: a phenomenon in which lytic phage replication stalls within a host cell⁸⁸. Although not well understood, pseudolysogeny is thought to occur when bacteria are starved in low nutrient environments or are undergoing periods of slow growth in environments such as the gut microbiome^{88,89}. T4 phages have proven ability to undergo pseudolysogeny in culture, due to the activity of the *rI* gene^{89,90}. However, T4 phages quickly return to the lytic cycle upon incubation in fresh, nutrient rich media⁹⁰, demonstrating that pseudolysogeny is an unlikely possibility for the “loss” of phage seen in the aforementioned animal. Metagenomics and targeted transcriptomics analyses (i.e., transcription of the *rI* gene) of intestinal and ancestral phages may identify the genetic determinants behind T4 phage evolution in bi-colonised mice.

Beyond the characterization of wildtype T4 in an *E. coli* monocolonised mouse, I also investigated the effects of loss of the phage mucus binding protein Hoc on phage viability *in vivo*. Similar to the WT, variation in phage-bacteria abundance of approximately two orders of magnitude ($SEM_{\Delta Hoc} = 1.27 \times 10^3$ pfu/mg) were also observed upon investigation of the ΔHoc T4 phages in the murine gut. ΔHoc T4 phage levels were lower than WT phage by at least one order of magnitude (**Figure 3.4 B-E**). In line with my hypothesis, initial experiments suggested that T4

phages lacking Hoc proteins were unable to be retained in murine gut long-term, hinting at the importance of mucus binding abilities for maintenance. However, upon repetition of these experiments, Δ Hoc T4 phages were detected at similar levels as WT T4 phage, with possible decreases detected from 15 days-post inoculation (**Figure 3.5 A-B**). Together, these results indicated that the Ig-like domains within T4 phage Hoc proteins may not be crucial for T4 phage colonisation of a simple microbiota mouse gut. I propose that Δ Hoc T4 phages might be capable of evolving, to promote their retention within mucus. Alternatively, it is possible that T4 phages possess additional Ig-like domain-bearing proteins that offer some redundancy in mucus-adhesion. Metagenomics studies may elucidate the genetic differences in Δ Hoc T4 phages between experimental trials, allowing us to understand if a genetic variation is responsible for the differences in Δ Hoc T4 phage colonisation seen between trials. As discussed previously, Ig-like domains are predicted to be conserved in approximately 25% of known *Caudoviricetes* phages⁴⁰, implicating mucus adhesion as an evolutionarily conserved function of phages³⁷. Since the publication of these numbers in 2006, advancements in sequencing technologies have shed light on the composition of our intestinal “viral dark matter”^{11,22,25,91}. Of significance, CrAssphages (class *Caudoviricetes*) were found to represent up to 90% of all reads in VLP-derived metagenomes in the human gut²⁵. Studies investigating the proportion of Ig-like domain containing proteins in intestinal phages have not since been published. Therefore, future bioinformatics studies should also assess the importance of Ig-like domains using current intestinal phage databases.

T4 phage Ig-like domains and mucus adhesion was previously associated with transcytosis of phage across epithelial cells *in vitro*^{43,44}. In this present study, viable T4 phages did not appear to translocate across the intestinal epithelium in bi-colonised mice, in direct

contrast to *in vitro* studies (**Figure 3.7**). The reasons for this are likely due to the inherent complexities of the gut environment, such as the integrity of the intestinal barrier, infiltration of immune cells to the gut tissue, the secretion of antibodies and antimicrobial peptides, and mucus efflux and gut peristalsis. These characteristics are difficult to replicate *in vitro*, even with more complex culture systems such as gut-on-a-chip and organoid cultures. Despite the inability of viable phage to translocate in our studies, T4 phages appeared to stimulate a small but significant inflammatory response involving the production of IL-12, IL-1 β and IFN γ (**Figure 3.8 A, B, D**), which may suggest innate immune cell activation, inflammasome induction and Th1 cell differentiation and activation¹⁸. These results were interpreted with caution as significant increases in IL-12 were detected at late stages of phage intestinal “infection”, whereas it is typically associated with early responses to infection. I speculate that a spike in IL-12 levels later time points could be due to an intestinal event, such as an overgrowth of phage/bacteria. Th1 cells typically respond to intracellular viral or bacterial infections, and previous studies by others have demonstrated that phages are capable of interacting with PRRs (TLR3⁴⁵ and TLR9¹⁸) within the endocytic vesicles of phagocytic cells^{18,45}. While it was determined that T4 phage-inoculation resulted in a trending increase in activated Th1 cells and CTLs in the mLN (**Figure 3.10 C-N**), neither CD4⁺ or CD8⁺ T cells had a significantly increased capacity to produce inflammatory cytokines during *ex vivo* stimulation (**Figure 3.11 C-J**) compared to vehicle controls. This suggested that, like commensal bacteria, intestinal phages may be involved in immune system priming. It is also possible that the small increases in IFN γ levels observed (**Figure 3.8 D**) were related to the activation of other cell types, such as natural killer (NK) cells and type I innate lymphoid cells (ILC1s). Like MNV infection, intestinal T4 phage seemingly resulted in Th1 differentiation (**Figure 3.10 L**). Further interrogation of the T4 phage-specific

immune response would be beneficial, particularly in determining the immune cell subsets within the GALT (lamina propria and Peyer's patches), and T cell activation and migration to intestinal tissues. A limitation to the present study is that we were unable to attribute the observed immune responses solely to T4 phage as phage-induced bacterial lysis results in the release of bacterial compounds that may result in the activation of T cells and cytokine production. Therefore, future studies will be geared toward determining T cell specificity to phage in these preclinical models and also in conventional microbiota mice, with better adapted immune systems.

Simplified microbiome mouse models, such as mono- and bi-colonised mice are excellent tools for examining the interactions between phage and bacteria in the GIT. However, a limitation of these models is that they do not recapitulate the physiology of their conventional microbiota counterparts. More similar to GF mice, *E. coli* monocolonized mice have reduced mucus production⁴⁹, and an immature immune system^{48,92}. Abt et al. (2012) and Ichinohe et al. (2011) demonstrated that mice treated with a broad spectrum cocktail of antibiotics to deplete their endogenous microbiome have impaired antiviral immunity, resulting in reduced innate and adaptive immune activation, and reduced expression of genes related to virus detection (PRRs) and inflammatory cytokine signalling^{83,93}. Therefore, it is possible that the phage-associated increases in inflammatory cytokines and the T cell activation observed in this study are dampened by the inherent immaturity of the immune system in gnotobiotic mice. Therefore, these experiments should be repeated using conventional microbiota mouse models to better understand the immune response to intestinal phage.

Of some interest, I report that levels of IL-1 β were raised in the mLN and spleen in T4 phage colonised mice compared with vehicle-treated controls (**Figure 3.8 B**). IL-1 β is an

inflammatory cytokine that mediates a wide variety of immune responses to infection⁹⁴.

Importantly, secretion of its active form results from induction of the inflammasome: a cytosolic multiprotein complex that forms upon cytosolic invasion of DCs and macrophages by bacteria or viruses^{93,94}. Similar to the TLRs previously discussed, a cytosolic PRR, absent in melanoma 2 (AIM2), may also be able to detect phage dsDNA, resulting in the induction of the AIM2 inflammasome⁹⁴. Further investigation of immune cell populations within the GALT, mLNs and spleen will assist in our identification of the immune pathways activated by intestinal phages.

4.2 Applications

The work presented here contributes to the field of phageome research, as I have elucidated that the T4 phage-*E. coli* dyad can stably co-exist within the GIT of a simplified microbiome mouse model. Phage therapy is a desirable application for lytic phages such as T4, as their host-specificity may allow for the targeting of invading intestinal pathogens, such as adherent invasive *E. coli* (AIEC). While the focus of phage therapy development tends to be geared towards treating septic bacterial infections, it is important to understand how the addition of a phage cocktail to the GIT may alter the intestinal ecosystem. Possible consequences of phage addition to a complex GI community include disruption of bacterial abundances and subsequent changes to the metabolome¹⁵. These changes, along with the presence of the introduced phage itself, may promote disease progression through bacteriome imbalance^{18,19,60}. However, our study implies that the coexistence of lytic phages with their target bacteria may result in poor efficacy of phage therapies in clinical trials^{87,95,96}. As commensal bacteria compete amongst themselves for space and nutrients along the GIT^{26,28}, bacteria within spatial niches experience reduced growth rates. In our study, this may account for the inhibited phage lysis efficiency *in vivo* and coexistence between bacteria and phage. Therefore, therapeutic lytic

phages may be more suitably applied as a cocktail of phages targeting a single infectious bacterium¹⁶. Theoretically, this could circumvent the emergence of phage-resistant clones, however this remains to be seen¹⁶.

4.3 Future directions

Given the co-existence of T4 phage and *E. coli* observed in this study, future experiments will evaluate the genetic determinants driving T4 phage colonisation in the gut of bi-colonised mice. Specifically, metagenomics will shed light on the coevolution of both organisms. I am interested to learn the degree of genetic separation between intestinally evolved phage/*E. coli* and their ancestral counterparts. Similarly, transcriptomics approaches can be used to decipher the functional changes in phages and bacteria over time. Targeted approaches may be able to identify the expression of phage-resistance genes in *E. coli*, as well as the associated expression of phage-encoded genes promoting their virulence, or potentially, pseudolysogeny⁸⁸⁻⁹⁰. Given that Hoc proteins may not be required for mucus-binding *in vivo*, I would like to explore the possibilities that i) T4 phage contain additional Ig-like domains within other structural proteins that may offer redundancy in mucus binding, and ii) that Hoc proteins are not essential for phage colonisation in the gut. To investigate the latter, I would like to investigate the colonisation ability of WT T4 phages in *muc2* knock-out mice, lacking the predominant gut mucin, Muc2. *Muc2*^{-/-} mice are characterised by defective mucosal layers and a leaky gut barrier⁹⁷. Colonisation of T4 phage in Muc2 deficient mice may indicate that T4 phage do not rely on mucus adhesion for intestinal colonisation.

To further investigate my second aim, future directions should focus on immune responses to phage within the GALT (Peyer's patches, lamina propria (LP)). Given that I characterised the T4 phage-specific immune response by a low-level expansion of activated Th1

cells and CTLs and by the limited production of IL-12, IL-1 β and IFN γ within the mLN, I would like to determine the extent of Th1 cell and CTL activation and migration to the GALT. Therefore, I would like to isolate immune cells from the Peyer's patches, LP and intestinal epithelium, and investigate the presence of cell types involved in antiviral responses, such as DCs, macrophages, NK cells and ILC1s. Additionally, I would like to investigate the presence of activated, gut homing T cells by examining the repertoire of cell surface integrins associated with tissue infiltration, such as CD11a, CD49d and CD103⁸³. Together, these studies will provide a more detailed picture of phage-specific immune activation in the gut than that achieved currently in this thesis.

4.4 Conclusion

In conclusion, I determined that T4 phage colonise the murine gut following inoculation, without major perturbation to the resident *E. coli* population. T4 phage colonisation appeared to be independent of both phage dose and mucus-adhering Ig-like domains within Hoc proteins. A small but significant increase in the production of Th1-skewing, proinflammatory cytokines was detected locally in response to a single inoculation dose of T4 phage, with the caveat that GF and bi-colonised mice have an immature immune system. Taken together, this work indicates that phages can co-exist alongside their target bacteria in the GIT of mice and may play roles in the priming and development of the innate and adaptive immune systems.

References

1. Rohwer, F., and Segall, A.M. (2015). A century of phage lessons. *Nature* 528, 46–47. 10.1038/528046a.
2. Suttle, C.A. (2005). Viruses in the sea. *Nature* 437, 356–361. 10.1038/nature04160.
3. Gil, J.F., Mesa, V., Estrada-Ortiz, N., Lopez-Obando, M., Gómez, A., and Plácido, J. (2021). Viruses in Extreme Environments, Current Overview, and Biotechnological Potential. *Viruses* 13, 81. 10.3390/v13010081.
4. Wommack, K.E., and Colwell, R.R. (2000). Virioplankton: viruses in aquatic ecosystems. *Microbiol Mol Biol Rev* 64, 69–114. 10.1128/MMBR.64.1.69-114.2000.
5. Shkoporov, A.N., Turkington, C.J., and Hill, C. (2022). Mutualistic interplay between bacteriophages and bacteria in the human gut. *Nature reviews. Microbiology*. 10.1038/s41579-022-00755-4.
6. Townsend, E.M., Kelly, L., Muscatt, G., Box, J.D., Hargraves, N., Lilley, D., and Jameson, E. (2021). The Human Gut Phageome: Origins and Roles in the Human Gut Microbiome. *Frontiers in Cellular and Infection Microbiology* 11. 10.3389/fcimb.2021.643214.
7. Silveira, C.B., and Rohwer, F.L. (2016). Piggyback-the-Winner in host-associated microbial communities. *NPJ Biofilms Microbiomes* 2, 16010. 10.1038/npjbiofilms.2016.10.
8. Reyes, A., Wu, M., McNulty, N.P., Rohwer, F.L., and Gordon, J.I. (2013). Gnotobiotic mouse model of phage-bacterial host dynamics in the human gut. *Proceedings of the National Academy of Sciences of the United States of America* 110, 20236–20241. 10.1073/pnas.1319470110.
9. Mirzaei, M.K., and Maurice, C.F. (2017). Ménage à trois in the human gut: interactions between host, bacteria and phages. *Nat Rev Microbiol* 15, 397–408. 10.1038/nrmicro.2017.30.
10. Wahida, A., Tang, F., and Barr, J.J. (2021). Rethinking phage-bacteria-eukaryotic relationships and their influence on human health. *Cell host & microbe* 29, 681–688. 10.1016/j.chom.2021.02.007.
11. Clooney, A.G., Sutton, T.D.S., Shkoporov, A.N., Holohan, R.K., Daly, K.M., O’Regan, O., Ryan, F.J., Draper, L.A., Plevy, S.E., Ross, R.P., et al. (2019). Whole-Virome Analysis Sheds Light on Viral Dark Matter in Inflammatory Bowel Disease. *Cell Host & Microbe* 26, 764-778.e5. 10.1016/J.CHOM.2019.10.009.

12. Gregory, A.C., Zablocki, O., Zayed, A.A., Howell, A., Bolduc, B., and Sullivan, M.B. (2020). The Gut Virome Database Reveals Age-Dependent Patterns of Virome Diversity in the Human Gut. *Cell host & microbe* 28, 724-740.e8. 10.1016/j.chom.2020.08.003.
13. Diard, M., Bakkeren, E., Cornuault, J.K., Moor, K., Hausmann, A., Sellin, M.E., Loverdo, C., Aertsen, A., Ackermann, M., De Paepe, M., et al. (2017). Inflammation boosts bacteriophage transfer between *Salmonella* spp. *Science* 355, 1211–1215. 10.1126/science.aaf8451.
14. Rohwer, F.Y., Merry; Hisakawa, Nao; Maughan, Heather (2014). *Life in Our Phage World: A Centennial Field Guide to the Earth's Most Diverse Inhabitants (Wholon)*.
15. Hsu, B.B., Gibson, T.E., Yeliseyev, V., Liu, Q., Lyon, L., Bry, L., Silver, P.A., and Gerber, G.K. (2019). Dynamic Modulation of the Gut Microbiota and Metabolome by Bacteriophages in a Mouse Model. *Cell host & microbe* 25, 803-814.e5. 10.1016/j.chom.2019.05.001.
16. Gordillo Altamirano, F.L., and Barr, J.J. (2019). Phage Therapy in the Postantibiotic Era. *Clinical Microbiology Reviews* 32. 10.1128/CMR.00066-18.
17. Brestoff, J.R., and Artis, D. (2013). Commensal bacteria at the interface of host metabolism and the immune system. *Nat Immunol* 14, 676–684. 10.1038/ni.2640.
18. Gogokhia, L., Buhrke, K., Bell, R., Hoffman, B., Brown, D.G., Hanke-Gogokhia, C., Ajami, N.J., Wong, M.C., Ghazaryan, A., Valentine, J.F., et al. (2019). Expansion of Bacteriophages Is Linked to Aggravated Intestinal Inflammation and Colitis. *Cell host & microbe* 25, 285-299.e8. 10.1016/j.chom.2019.01.008.
19. Norman, J.M., Handley, S.A., Baldridge, M.T., Droit, L., Liu, C.Y., Keller, B.C., Kambal, A., Monaco, C.L., Zhao, G., Fleshner, P., et al. (2015). Disease-Specific Alterations in the Enteric Virome in Inflammatory Bowel Disease. *Cell* 160, 447–460. 10.1016/j.cell.2015.01.002.
20. Rasmussen, T.S., Mentzel, C.M.J., Kot, W., Castro-Mejía, J.L., Zuffa, S., Swann, J.R., Hansen, L.H., Vogensen, F.K., Hansen, A.K., and Nielsen, D.S. (2020). Faecal virome transplantation decreases symptoms of type 2 diabetes and obesity in a murine model. *Gut* 69, 2122–2130. 10.1136/gutjnl-2019-320005.
21. Borin, J.M., Liu, R., Wang, Y., Wu, T.-C., Chopyk, J., Huang, L., Kuo, P., Ghose, C., Meyer, J.R., Tu, X.M., et al. (2023). Fecal virome transplantation is sufficient to alter fecal microbiota and drive lean and obese body phenotypes in mice. *Gut Microbes* 15, 2236750. 10.1080/19490976.2023.2236750.
22. Reyes, A., Haynes, M., Hanson, N., Angly, F.E., Heath, A.C., Rohwer, F., and Gordon, J.I. (2010). Viruses in the faecal microbiota of monozygotic twins and their mothers. *Nature* 466, 334–338. 10.1038/nature09199.

23. Sausset, R., Petit, M.A., Gaboriau-Routhiau, V., and De Paepe, M. (2020). New insights into intestinal phages. *Mucosal immunology* 13, 205–215. 10.1038/s41385-019-0250-5.
24. Shkoporov, A.N., and Hill, C. (2019). Bacteriophages of the Human Gut: The “Known Unknown” of the Microbiome. *Cell host & microbe* 25, 195–209. 10.1016/j.chom.2019.01.017.
25. Dutilh, B.E., Cassman, N., McNair, K., Sanchez, S.E., Silva, G.G.Z., Boling, L., Barr, J.J., Speth, D.R., Seguritan, V., Aziz, R.K., et al. (2014). A highly abundant bacteriophage discovered in the unknown sequences of human faecal metagenomes. *Nat Commun* 5, 4498. 10.1038/ncomms5498.
26. Nguyen, J., Pepin, D.M., and Tropini, C. (2021). Cause or effect? The spatial organization of pathogens and the gut microbiota in disease. *Microbes and Infection* 23, 104815. 10.1016/j.micinf.2021.104815.
27. Pelaseyed, T., Bergström, J.H., Gustafsson, J.K., Ermund, A., Birchenough, G.M.H., Schütte, A., van der Post, S., Svensson, F., Rodríguez-Piñeiro, A.M., Nyström, E.E.L., et al. (2014). The mucus and mucins of the goblet cells and enterocytes provide the first defense line of the gastrointestinal tract and interact with the immune system. *Immunol Rev* 260, 8–20. 10.1111/imr.12182.
28. McCallum, G., and Tropini, C. (2023). The gut microbiota and its biogeography. *Nat Rev Microbiol.* 10.1038/s41579-023-00969-0.
29. Bergstrom, K., and Xia, L. (2022). The barrier and beyond: Roles of intestinal mucus and mucin-type O-glycosylation in resistance and tolerance defense strategies guiding host-microbe symbiosis. *Gut microbes* 14, 2052699. 10.1080/19490976.2022.2052699.
30. Johansson, M.E.V., Ambort, D., Pelaseyed, T., Schütte, A., Gustafsson, J.K., Ermund, A., Subramani, D.B., Holmén-Larsson, J.M., Thomsson, K.A., Bergström, J.H., et al. (2011). Composition and functional role of the mucus layers in the intestine. *Cell. Mol. Life Sci.* 68, 3635–3641. 10.1007/s00018-011-0822-3.
31. Schroeder, B.O. (2019). Fight them or feed them: how the intestinal mucus layer manages the gut microbiota. *Gastroenterol Rep (Oxf)* 7, 3–12. 10.1093/gastro/goy052.
32. Johansson, M.E.V., Phillipson, M., Petersson, J., Velcich, A., Holm, L., and Hansson, G.C. (2008). The inner of the two Muc2 mucin-dependent mucus layers in colon is devoid of bacteria. *Proc Natl Acad Sci U S A* 105, 15064–15069. 10.1073/pnas.0803124105.
33. Bergstrom, K., Shan, X., Casero, D., Batushansky, A., Lagishetty, V., Jacobs, J.P., Hoover, C., Kondo, Y., Shao, B., Gao, L., et al. (2020). Proximal colon-derived O-glycosylated mucus encapsulates and modulates the microbiota. *Science* 370, 467–472. 10.1126/science.aay7367.

34. McGuckin, M.A., Lindén, S.K., Sutton, P., and Florin, T.H. (2011). Mucin dynamics and enteric pathogens. *Nat Rev Microbiol* 9, 265–278. 10.1038/nrmicro2538.
35. Barr, J.J., Auro, R., Sam-Soon, N., Kassegne, S., Peters, G., Bonilla, N., Hatay, M., Mourtada, S., Bailey, B., Youle, M., et al. (2015). Subdiffusive motion of bacteriophage in mucosal surfaces increases the frequency of bacterial encounters. *Proceedings of the National Academy of Sciences of the United States of America* 112, 13675–13680. 10.1073/pnas.1508355112.
36. Hansson, G.C. (2020). Mucins and the Microbiome. *Annual review of biochemistry* 89, 769–793. 10.1146/annurev-biochem-011520-105053.
37. Barr, J.J., Auro, R., Furlan, M., Whiteson, K.L., Erb, M.L., Pogliano, J., Stotland, A., Wolkowicz, R., Cutting, A.S., Doran, K.S., et al. (2013). Bacteriophage adhering to mucus provide a non-host-derived immunity. *Proceedings of the National Academy of Sciences of the United States of America* 110, 10771–10776. 10.1073/pnas.1305923110.
38. Barr, J.J., Youle, M., and Rohwer, F. (2013). Innate and acquired bacteriophage-mediated immunity. *Bacteriophage* 3, e25857. 10.4161/bact.25857.
39. Yap, M.L., and Rossmann, M.G. (2014). Structure and function of bacteriophage T4. *Future Microbiol* 9, 1319–1327. 10.2217/fmb.14.91.
40. Fraser, J.S., Yu, Z., Maxwell, K.L., and Davidson, A.R. (2006). Ig-like domains on bacteriophages: a tale of promiscuity and deceit. *Journal of molecular biology* 359, 496–507. 10.1016/j.jmb.2006.03.043.
41. Chin, W.H., Kett, C., Cooper, O., Müseler, D., Zhang, Y., Bamert, R.S., Patwa, R., Woods, L.C., Devendran, C., Korneev, D., et al. (2022). Bacteriophages evolve enhanced persistence to a mucosal surface. *Proceedings of the National Academy of Sciences* 119. 10.1073/pnas.2116197119.
42. Halaby, D.M., and Mornon, J.P. (1998). The immunoglobulin superfamily: an insight on its tissular, species, and functional diversity. *J Mol Evol* 46, 389–400. 10.1007/pl00006318.
43. Nguyen, S., Baker, K., Padman, B.S., Patwa, R., Dunstan, R.A., Weston, T.A., Schlosser, K., Bailey, B., Lithgow, T., Lazarou, M., et al. (2017). Bacteriophage Transcytosis Provides a Mechanism To Cross Epithelial Cell Layers. *mBio* 8. 10.1128/mBio.01874-17.
44. Bichet, M.C., Chin, W.H., Richards, W., Lin, Y.-W., Avellaneda-Franco, L., Hernandez, C.A., Oddo, A., Chernyavskiy, O., Hilsenstein, V., Neild, A., et al. (2021). Bacteriophage uptake by mammalian cell layers represents a potential sink that may impact phage therapy. *iScience* 24, 102287. 10.1016/j.isci.2021.102287.
45. Sweere, J.M., Van Belleghem, J.D., Ishak, H., Bach, M.S., Popescu, M., Sunkari, V., Kaber, G., Manasherob, R., Suh, G.A., Cao, X., et al. (2019). Bacteriophage trigger antiviral

- immunity and prevent clearance of bacterial infection. *Science (New York, N.Y.)* 363. 10.1126/science.aat9691.
46. Fluckiger, A., Daillère, R., Sassi, M., Sixt, B.S., Liu, P., Loos, F., Richard, C., Rabu, C., Alou, M.T., Goubet, A.-G., et al. (2020). Cross-reactivity between tumor MHC class I-restricted antigens and an enterococcal bacteriophage. *Science (New York, N.Y.)* 369, 936–942. 10.1126/science.aax0701.
 47. Majewska, J., Kaźmierczak, Z., Lahutta, K., Lecion, D., Szymczak, A., Miernikiewicz, P., Drapała, J., Harhala, M., Marek-Bukowiec, K., Jędruchiewicz, N., et al. (2019). Induction of Phage-Specific Antibodies by Two Therapeutic Staphylococcal Bacteriophages Administered per os. *Frontiers in immunology* 10, 2607. 10.3389/fimmu.2019.02607.
 48. Thomson, C.A., Morgan, S.C., Ohland, C., and McCoy, K.D. (2022). From germ-free to wild: modulating microbiome complexity to understand mucosal immunology. *Mucosal Immunology* 15, 1085–1094. 10.1038/s41385-022-00562-3.
 49. Li, H., Limenitakis, J.P., Fuhrer, T., Geuking, M.B., Lawson, M.A., Wyss, M., Brugiroux, S., Keller, I., Macpherson, J.A., Rupp, S., et al. (2015). The outer mucus layer hosts a distinct intestinal microbial niche. *Nat Commun* 6, 8292. 10.1038/ncomms9292.
 50. Geuking, M.B., and Burkhard, R. (2020). Microbial modulation of intestinal T helper cell responses and implications for disease and therapy. *Mucosal Immunology* 13, 855–866. 10.1038/s41385-020-00335-w.
 51. Ivanov, I.I., Atarashi, K., Manel, N., Brodie, E.L., Shima, T., Karaoz, U., Wei, D., Goldfarb, K.C., Santee, C.A., Lynch, S.V., et al. (2009). Induction of Intestinal Th17 Cells by Segmented Filamentous Bacteria. *Cell* 139, 485–498. 10.1016/j.cell.2009.09.033.
 52. Kernbauer, E., Ding, Y., and Cadwell, K. (2014). An enteric virus can replace the beneficial function of commensal bacteria. *Nature* 516, 94–98. 10.1038/nature13960.
 53. Schooley, R.T., Biswas, B., Gill, J.J., Hernandez-Morales, A., Lancaster, J., Lessor, L., Barr, J.J., Reed, S.L., Rohwer, F., Benler, S., et al. (2017). Development and Use of Personalized Bacteriophage-Based Therapeutic Cocktails To Treat a Patient with a Disseminated Resistant *Acinetobacter baumannii* Infection. *Antimicrobial agents and chemotherapy* 61. 10.1128/AAC.00954-17.
 54. Van Nieuwenhuysse, B., Van der Linden, D., Chatzis, O., Lood, C., Wagemans, J., Lavigne, R., Schroyen, K., Paeshuysse, J., de Magnée, C., Sokal, E., et al. (2022). Bacteriophage-antibiotic combination therapy against extensively drug-resistant *Pseudomonas aeruginosa* infection to allow liver transplantation in a toddler. *Nat Commun* 13, 5725. 10.1038/s41467-022-33294-w.

55. Petrovic Fabijan, A., Lin, R.C.Y., Ho, J., Maddocks, S., Ben Zakour, N.L., Iredell, J.R., and Westmead Bacteriophage Therapy Team (2020). Safety of bacteriophage therapy in severe *Staphylococcus aureus* infection. *Nat Microbiol* 5, 465–472. 10.1038/s41564-019-0634-z.
56. Dedrick, R.M., Guerrero-Bustamante, C.A., Garlena, R.A., Russell, D.A., Ford, K., Harris, K., Gilmour, K.C., Soothill, J., Jacobs-Sera, D., Schooley, R.T., et al. (2019). Engineered bacteriophages for treatment of a patient with a disseminated drug-resistant *Mycobacterium abscessus*. *Nat Med* 25, 730–733. 10.1038/s41591-019-0437-z.
57. Majewska, J., Beta, W., Lecion, D., Hodyra-Stefaniak, K., Kłopot, A., Kaźmierczak, Z., Miernikiewicz, P., Piotrowicz, A., Ciekot, J., Owczarek, B., et al. (2015). Oral Application of T4 Phage Induces Weak Antibody Production in the Gut and in the Blood. *Viruses* 7, 4783–4799. 10.3390/v7082845.
58. Pabst, O., and Slack, E. (2020). IgA and the intestinal microbiota: the importance of being specific. *Mucosal Immunol* 13, 12–21. 10.1038/s41385-019-0227-4.
59. McCoy, K.D., Ronchi, F., and Geuking, M.B. (2017). Host-microbiota interactions and adaptive immunity. *Immunological Reviews* 279, 63–69. 10.1111/imr.12575.
60. Federici, S., Kviatcovsky, D., Valdés-Mas, R., and Elinav, E. (2023). Microbiome-phage interactions in inflammatory bowel disease. *Clin Microbiol Infect* 29, 682–688. 10.1016/j.cmi.2022.08.027.
61. Baaziz, H., Baker, Z.R., Franklin, H.C., and Hsu, B.B. (2022). Rehabilitation of a misbehaving microbiome: phages for the remodeling of bacterial composition and function. *iScience* 25, 104146. 10.1016/J.ISCI.2022.104146.
62. Sinha, A., Li, Y., Mirzaei, M.K., Shamash, M., Samadfam, R., King, I.L., and Maurice, C.F. (2022). Transplantation of bacteriophages from ulcerative colitis patients shifts the gut bacteriome and exacerbates the severity of DSS colitis. *Microbiome* 10, 105. 10.1186/s40168-022-01275-2.
63. Ott, S.J., Waetzig, G.H., Rehman, A., Moltzau-Anderson, J., Bharti, R., Grasis, J.A., Cassidy, L., Tholey, A., Fickenscher, H., Seegert, D., et al. (2017). Efficacy of Sterile Fecal Filtrate Transfer for Treating Patients With *Clostridium difficile* Infection. *Gastroenterology* 152, 799-811.e7. 10.1053/J.GASTRO.2016.11.010.
64. Guery, B., Galperine, T., and Barbut, F. (2019). *Clostridioides difficile* : diagnosis and treatments. *BMJ*, l4609. 10.1136/bmj.l4609.
65. Brunse, A., Deng, L., Pan, X., Hui, Y., Castro-Mejía, J.L., Kot, W., Nguyen, D.N., Secher, J.B.-M., Nielsen, D.S., and Thymann, T. (2022). Fecal filtrate transplantation protects against necrotizing enterocolitis. *The ISME journal* 16, 686–694. 10.1038/s41396-021-01107-5.

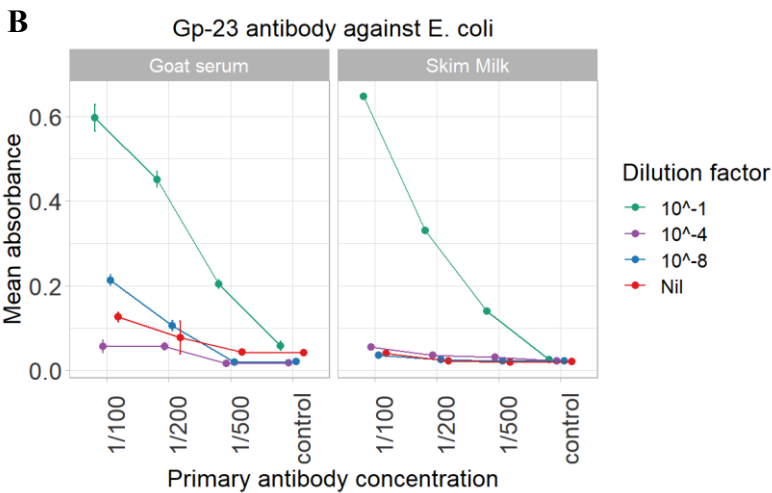
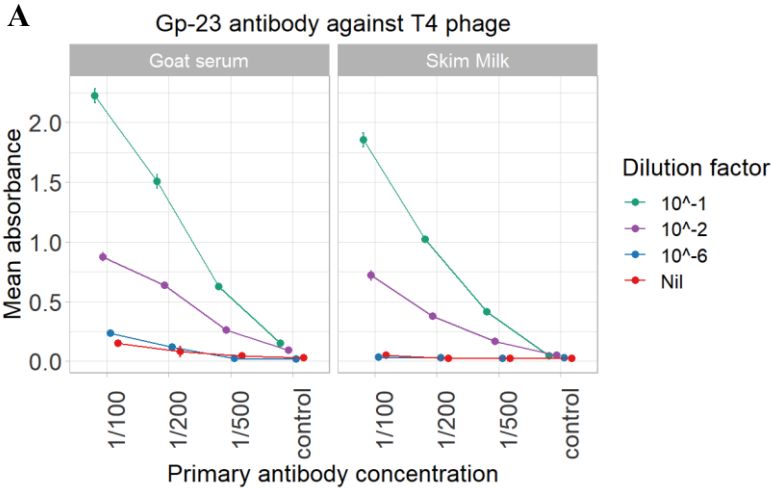
66. Zuo, T., Wong, S.H., Lam, K., Lui, R., Cheung, K., Tang, W., Ching, J.Y.L., Chan, P.K.S., Chan, M.C.W., Wu, J.C.Y., et al. (2018). Bacteriophage transfer during faecal microbiota transplantation in *Clostridium difficile* infection is associated with treatment outcome. *Gut* 67, 634–643. 10.1136/gutjnl-2017-313952.
67. Publications service (2007). On an invisible microbe antagonistic toward dysenteric bacilli: brief note by Mr. F. D'Herelle, presented by Mr. Roux. *Research in Microbiology* 158, 553–554. 10.1016/j.resmic.2007.07.005.
68. Chanishvili, N., and Alavidze, Z. (2020). Early Therapeutic and Prophylactic Uses of Bacteriophages. In *Bacteriophages: Biology, Technology, Therapy*, D. R. Harper, S. T. Abedon, B. H. Burrowes, and M. L. McConville, eds. (Springer International Publishing), pp. 1–30. 10.1007/978-3-319-40598-8_12-1.
69. Tropini, C., Moss, E.L., Merrill, B.D., Ng, K.M., Higginbottom, S.K., Casavant, E.P., Gonzalez, C.G., Fremin, B., Bouley, D.M., Elias, J.E., et al. (2018). Transient Osmotic Perturbation Causes Long-Term Alteration to the Gut Microbiota. *Cell* 173, 1742-1754.e17. 10.1016/j.cell.2018.05.008.
70. De Sordi, L., Khanna, V., and Debarbieux, L. (2017). The Gut Microbiota Facilitates Drifts in the Genetic Diversity and Infectivity of Bacterial Viruses. *Cell Host & Microbe* 22, 801-808.e3. 10.1016/j.chom.2017.10.010.
71. Chan, B.K., Siström, M., Wertz, J.E., Kortright, K.E., Narayan, D., and Turner, P.E. (2016). Phage selection restores antibiotic sensitivity in MDR *Pseudomonas aeruginosa*. *Scientific reports* 6, 26717. 10.1038/srep26717.
72. Hasan, M., and Ahn, J. (2022). Evolutionary Dynamics between Phages and Bacteria as a Possible Approach for Designing Effective Phage Therapies against Antibiotic-Resistant Bacteria. *Antibiotics (Basel)* 11, 915. 10.3390/antibiotics11070915.
73. Duerkop, B.A., Clements, C.V., Rollins, D., Rodrigues, J.L.M., and Hooper, L.V. (2012). A composite bacteriophage alters colonization by an intestinal commensal bacterium. *Proceedings of the National Academy of Sciences of the United States of America* 109, 17621–17626. 10.1073/pnas.1206136109.
74. Bonilla, N., Rojas, M.I., Netto Flores Cruz, G., Hung, S.-H., Rohwer, F., and Barr, J.J. (2016). Phage on tap—a quick and efficient protocol for the preparation of bacteriophage laboratory stocks. *PeerJ* 4, e2261. 10.7717/peerj.2261.
75. Zucoloto, A.Z., Yu, I.-L., McCoy, K.D., and McDonald, B. (2021). Generation, maintenance, and monitoring of gnotobiotic mice. *STAR Protocols* 2, 100536. 10.1016/j.xpro.2021.100536.

76. Baer, A., and Kehn-Hall, K. (2014). Viral concentration determination through plaque assays: using traditional and novel overlay systems. *Journal of visualized experiments : JoVE*, e52065. 10.3791/52065.
77. Jakočiūnė, D., and Moodley, A. (2018). A Rapid Bacteriophage DNA Extraction Method. *Methods and Protocols 1*, 27. 10.3390/mps1030027.
78. Ng, K.M., and Tropini, C. (2021). Visualization of Gut Microbiota-host Interactions via Fluorescence In Situ Hybridization, Lectin Staining, and Imaging. *Journal of visualized experiments : JoVE*. 10.3791/62646.
79. Schindelin, J., Arganda-Carreras, I., Frise, E., Kaynig, V., Longair, M., Pietzsch, T., Preibisch, S., Rueden, C., Saalfeld, S., Schmid, B., et al. (2012). Fiji: an open-source platform for biological-image analysis. *Nat Methods 9*, 676–682. 10.1038/nmeth.2019.
80. Murphy, K., and Weaver, C. (2016). *Janeway's immunobiology 9th edition*. (Garland Science/Taylor & Francis Group, LLC).
81. Filyk, H.A., and Osborne, L.C. (2016). The Multibiome: The Intestinal Ecosystem's Influence on Immune Homeostasis, Health, and Disease. *EBioMedicine 13*, 46–54. 10.1016/j.ebiom.2016.10.007.
82. de Zoete, M.R., Palm, N.W., Zhu, S., and Flavell, R.A. (2014). Inflammasomes. *Cold Spring Harb Perspect Biol 6*, a016287. 10.1101/cshperspect.a016287.
83. Abt, M.C., Osborne, L.C., Monticelli, L.A., Doering, T.A., Alenghat, T., Sonnenberg, G.F., Paley, M.A., Antenus, M., Williams, K.L., Erikson, J., et al. (2012). Commensal Bacteria Calibrate the Activation Threshold of Innate Antiviral Immunity. *Immunity 37*, 158–170. 10.1016/j.immuni.2012.04.011.
84. Tomov, V.T., Osborne, L.C., Dolfi, D.V., Sonnenberg, G.F., Monticelli, L.A., Mansfield, K., Virgin, H.W., Artis, D., and Wherry, E.J. (2013). Persistent enteric murine norovirus infection is associated with functionally suboptimal virus-specific CD8 T cell responses. *J Virol 87*, 7015–7031. 10.1128/JVI.03389-12.
85. Sharon, A.J., Filyk, H.A., Fonseca, N.M., Simister, R.L., Filler, R.B., Yuen, W., Hardman, B.K., Robinson, H.G., Seo, J.H., Rocha-Pereira, J., et al. (2022). Restriction of Viral Replication, Rather than T Cell Immunopathology, Drives Lethality in Murine Norovirus CR6-Infected STAT1-Deficient Mice. *J Virol 96*, e0206521. 10.1128/jvi.02065-21.
86. Fujiwara, T., Oda, K., Yokota, S., Takatsuki, A., and Ikehara, Y. (1988). Brefeldin A causes disassembly of the Golgi complex and accumulation of secretory proteins in the endoplasmic reticulum. *J Biol Chem 263*, 18545–18552.
87. Weiss, M., Denou, E., Bruttin, A., Serra-Moreno, R., Dillmann, M.-L., and Brüßow, H. (2009). In vivo replication of T4 and T7 bacteriophages in germ-free mice colonized with *Escherichia coli*. *Virology 393*, 16–23. 10.1016/j.virol.2009.07.020.

88. Łoś, M., and Węgrzyn, G. (2012). Pseudolysogeny. *Adv Virus Res* 82, 339–349. 10.1016/B978-0-12-394621-8.00019-4.
89. Los, M., Węgrzyn, G., and Neubauer, P. (2003). A role for bacteriophage T4 rI gene function in the control of phage development during pseudolysogeny and in slowly growing host cells. *Research in Microbiology* 154, 547–552. [https://doi.org/10.1016/S0923-2508\(03\)00151-7](https://doi.org/10.1016/S0923-2508(03)00151-7).
90. Bryan, D., El-Shibiny, A., Hobbs, Z., Porter, J., and Kutter, E.M. (2016). Bacteriophage T4 Infection of Stationary Phase *E. coli*: Life after Log from a Phage Perspective. *Front. Microbiol.* 7. 10.3389/fmicb.2016.01391.
91. Reyes, A., Semenkovich, N.P., Whiteson, K., Rohwer, F., and Gordon, J.I. (2012). Going viral: next-generation sequencing applied to phage populations in the human gut. *Nat Rev Microbiol* 10, 607–617. 10.1038/nrmicro2853.
92. Al-Asmakh, M., and Zadjali, F. (2015). Use of Germ-Free Animal Models in Microbiota-Related Research. *Journal of microbiology and biotechnology* 25, 1583–1588. 10.4014/jmb.1501.01039.
93. Ichinohe, T., Pang, I.K., Kumamoto, Y., Peaper, D.R., Ho, J.H., Murray, T.S., and Iwasaki, A. (2011). Microbiota regulates immune defense against respiratory tract influenza A virus infection. *Proc Natl Acad Sci U S A* 108, 5354–5359. 10.1073/pnas.1019378108.
94. Lamkanfi, M., and Dixit, V.M. (2011). Modulation of Inflammasome Pathways by Bacterial and Viral Pathogens. *The Journal of Immunology* 187, 597–602. 10.4049/jimmunol.1100229.
95. Buttimer, C., Sutton, T., Colom, J., Murray, E., Bettio, P.H., Smith, L., Bolocan, A.S., Shkorporov, A., Oka, A., Liu, B., et al. (2022). Impact of a phage cocktail targeting *Escherichia coli* and *Enterococcus faecalis* as members of a gut bacterial consortium in vitro and in vivo. *Front Microbiol* 13, 936083. 10.3389/fmicb.2022.936083.
96. Lourenço, M., Chaffringeon, L., Lamy-Besnier, Q., Pédrón, T., Campagne, P., Eberl, C., Bérard, M., Stecher, B., Debarbieux, L., and De Sordi, L. (2020). The Spatial Heterogeneity of the Gut Limits Predation and Fosters Coexistence of Bacteria and Bacteriophages. *Cell Host & Microbe* 28, 390-401.e5. 10.1016/j.chom.2020.06.002.
97. Mager, L.F., Burkhard, R., Pett, N., Cooke, N.C.A., Brown, K., Ramay, H., Paik, S., Stagg, J., Groves, R.A., Gallo, M., et al. (2020). Microbiome-derived inosine modulates response to checkpoint inhibitor immunotherapy. *Science (New York, N.Y.)* 369, 1481–1489. 10.1126/science.abc3421.

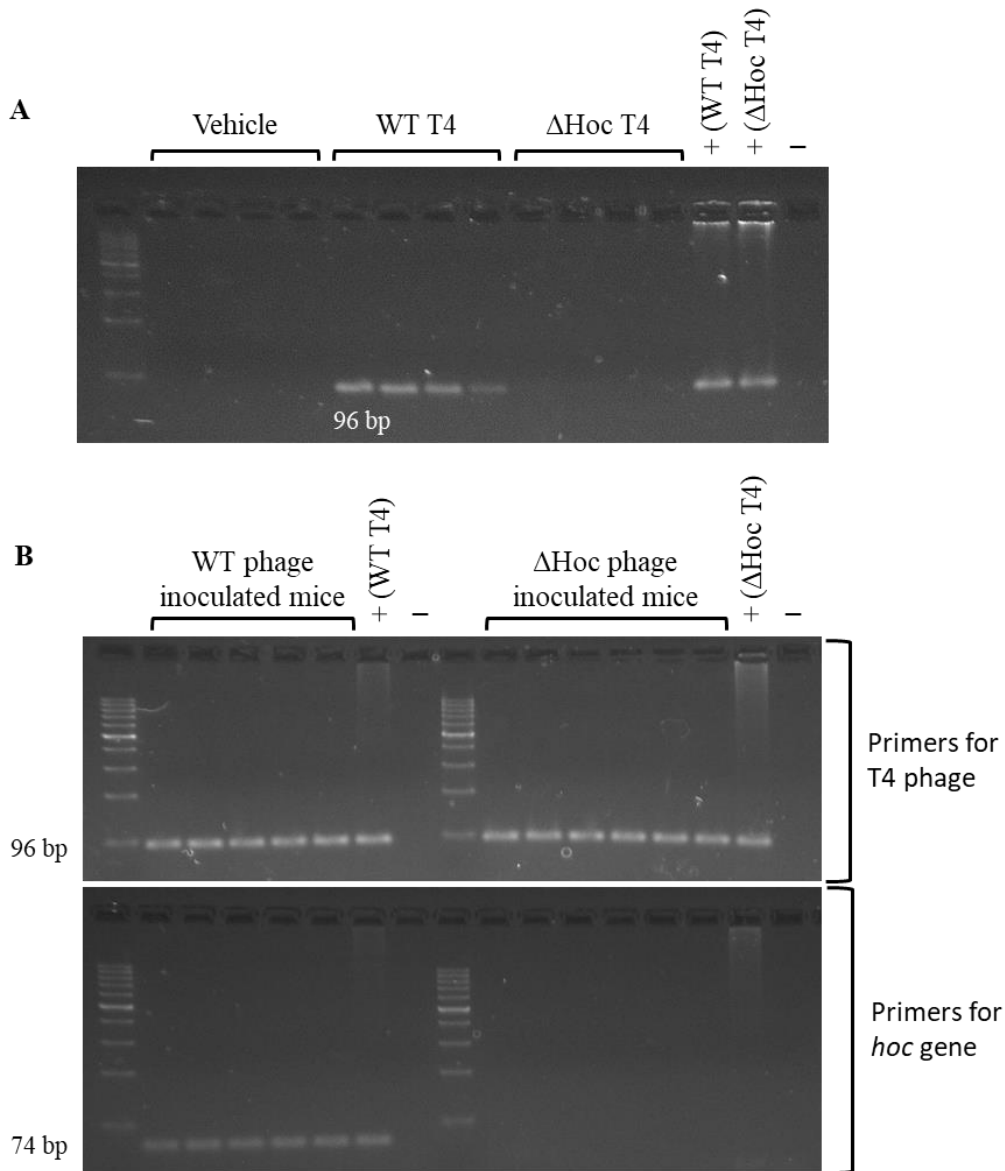
Appendices

Appendix A Cross-reactivity of T4 phage anti-Gp23 antibody with *E. coli*



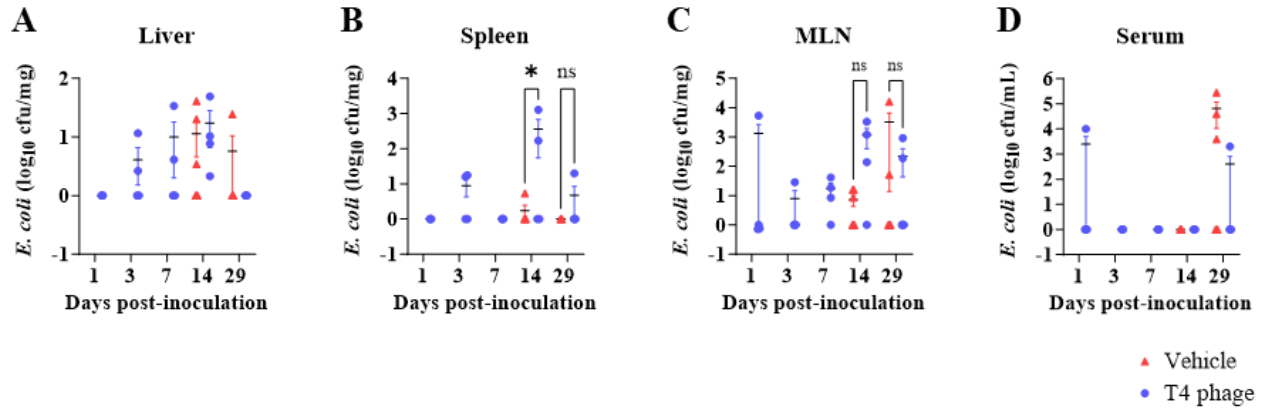
Appendix A Cross-reactivity of T4 phage anti-Gp23 antibody with *E. coli*. Whole virus/bacteria ELISAs were used to determine the specificity of the anti-gp23 antibody (Boster Bio) to T4 phage. (A) Using goat-serum and skim milk blocking solutions, anti-gp-23 was able to detect T4 phage in a concentration-specific manner. (B) Anti-gp23 detected *E. coli* non-specifically.

Appendix B DNA gel of extracted phage DNA from faecal pellets from the experiments discussed in Chapter 3.1.4



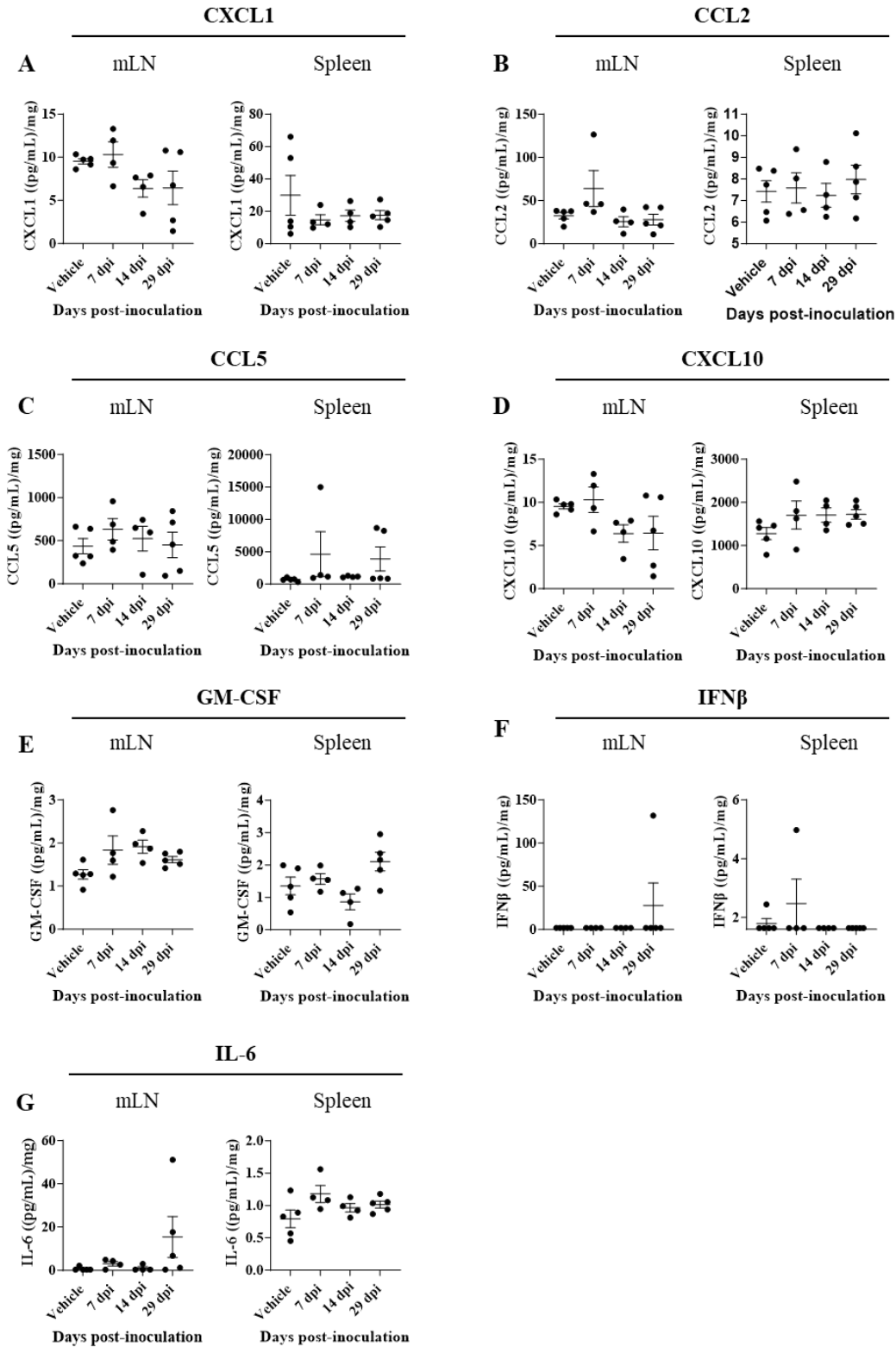
Appendix B DNA gel of extracted phage DNA from faecal pellets from the experiments discussed in Chapter 3.1.4. Samples were collected from WT and Δ Hoc T4 phage (A) **Figure 3.4** and (B) **Figure 3.5**, at day 9 and day 12 post-phage inoculation, respectively. (A) T4 phage gene copies were detected in WT T4 phage-inoculated mice, but not vehicle or Δ Hoc-inoculated mice. (B) Phage gene copies were detected WT and Δ Hoc-inoculated mice. *Hoc* genes could only be amplified in WT inoculated, but not Δ Hoc-inoculated mice.

Appendix C *E. coli* appeared to translocate across the intestinal epithelium both with and without T4 phage inoculation



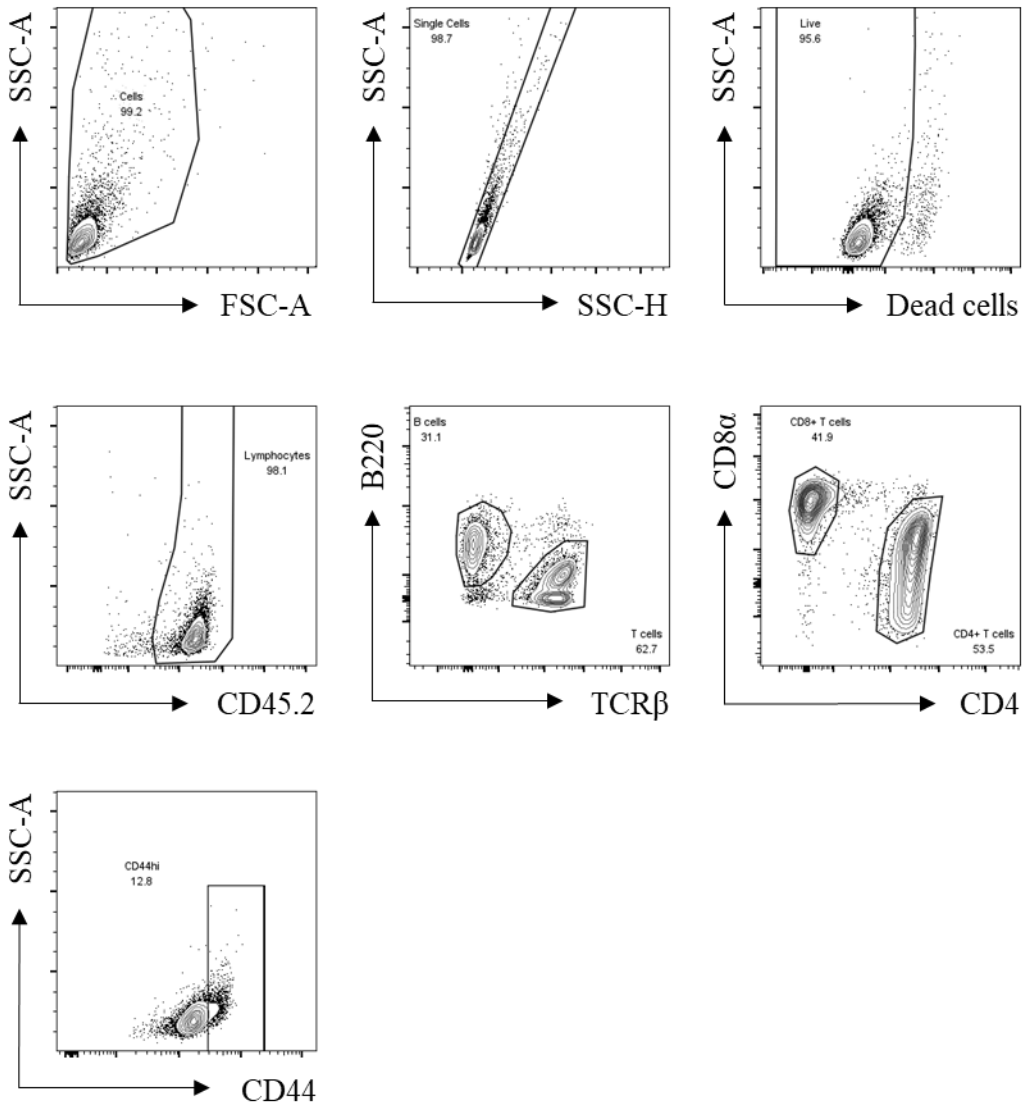
Appendix C *E. coli* appeared to translocate across the intestinal epithelium both with and without T4 phage inoculation. *E. coli* monoclonised mice were inoculated with T4 phage or vehicle at day 0. Mice were euthanised at each time point and *E. coli* were measured in tissues and serum by spot plating. (A) *E. coli* levels in liver tissue. (B) *E. coli* levels in spleen tissue. (C) *E. coli* levels in MLN tissue. (D) *E. coli* levels in Serum. Statistics calculated by multiple unpaired T-tests with Holm-Šídák's multiple comparisons. Ns p > 0.05, * p < 0.05. Error bars represent mean ± SEM.

Appendix D Oral inoculation of T4 phage into *E. coli* monocolonised mice did not stimulate chemokine production or increase levels of IFN β or IL-6



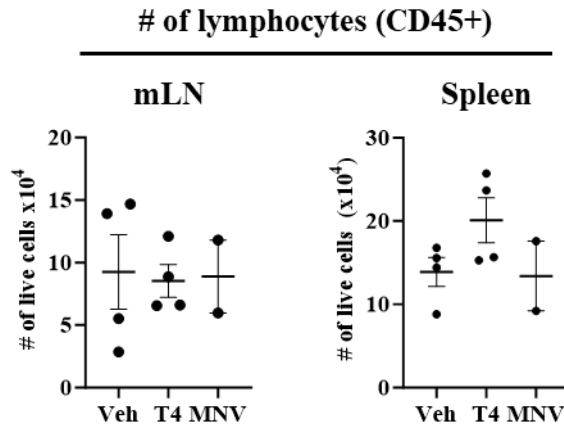
Appendix D Oral inoculation of T4 phage into *E. coli* monoclonised mice did not stimulate chemokine production or increase levels of IFN β or IL-6. T4 phage-inoculated mice were euthanised at days 7, 14 and 29 and a panel of 13 cytokines were measured in the MLN and spleen by cytokine bead array. Vehicle mice were euthanised at day 29. For each mouse, cytokine levels were measured in the MLN and spleen and concentrations were calculated by extrapolation to a standard curve. Concentrations were normalised to the tissue weight. (A) CXCL1. (B) CCL2. (C) CCL5. (D) CXCL10. (E) GM-CSF. (F) IFN β . (G) IL-6. Each point represents an individual mouse. Statistics were calculated by ordinary one-way ANOVA with Holm-Šídák's multiple comparisons between each time point and the vehicle control. Error bars represent the mean and SEM. All differences were not significant: ns $p > 0.05$.

Appendix E Representative flow cytometry gating strategy for immunophenotyping of cells isolated from T4 phage-inoculated mouse mLN and spleens



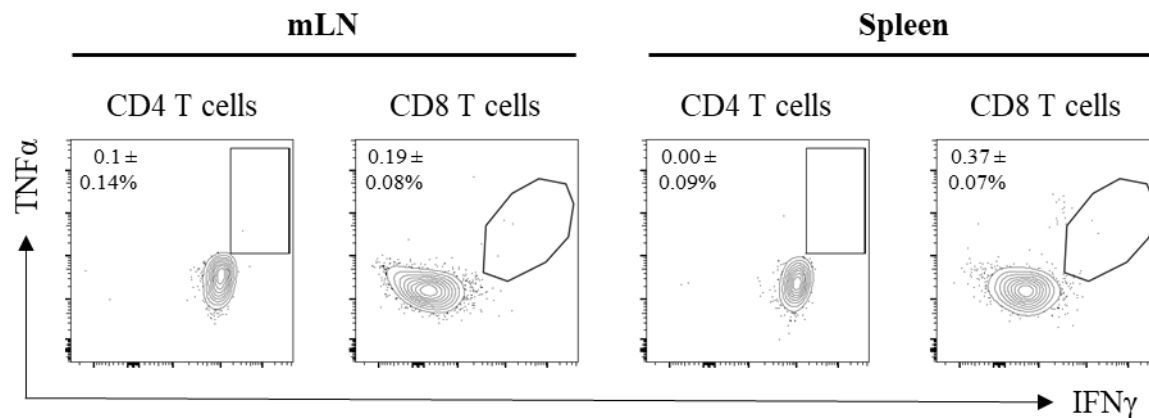
Appendix E Representative flow cytometry gating strategy for immunophenotyping of cells isolated from T4 phage-inoculated mouse mLN and spleens. The data shown are representative results from one T4 phage inoculated mouse that was euthanised at 8 days post-inoculation. Flow cytometry plots demonstrate that cells were gated for experiments based on this strategy.

Appendix F Total lymphocyte numbers in mLNs and spleens were not significantly different between vehicle, T4 phage and MNV-inoculated mice



Appendix F Total lymphocyte numbers in mLNs and spleens were not significantly different between vehicle, T4 phage and MNV-inoculated mice. Each point represents an individual mouse. Statistics were calculated by ordinary one-way ANOVA with Holm-Šídák's multiple comparisons. Error bars represent the mean and SEM. Ns $p > 0.05$, * $p < 0.05$, ** $p < 0.01$.

Appendix G Representative flow cytometry gating strategy for PMA/ionomycin stimulation controls



Appendix G Representative flow cytometry gating strategy for PMA/ionomycin stimulation controls. Cells were isolated from T4 phage-inoculated mouse mLN and spleens and were incubated for four hours at 37°C, 5% CO₂, without PMA/ionomycin and with BFA to block cytokine exocytosis. Cells were gated on CD44-high, CD4+ and CD8+ TCRβ+ T cells. Annotations describe gated proportions ± SD.